Biosynthesis of (2E)-hexenal and its physiological roles in plants under stress conditions

Kunishima, Mikiko

(Degree)
博士（農学）

(Date of Degree)
2017-03-25

(Date of Publication)
2018-03-01

(Resource Type)
doctoral thesis

(Report Number)
甲第6946号

(URL)
https://hdl.handle.net/20.500.14094/D1006946

Doctoral Dissertation

Biosynthesis of (2*E*)-hexenal and its physiological roles in plants under stress conditions

植物における(2*E*)-hexenal の生合成と
ストレス条件下での生理機能の解析

Mikiko KUNISHIMA

國嶋　幹子

January, 2017

Graduate School of Agricultural Science

Kobe University

Contents

Chapter I

General introduction

Life on the earth depends ultimately on the photosynthesis performed by green plants. Through the process, oxygen and carbohydrates are generated from atmospheric carbon dioxide and water using energy provided from the sun. In other words, photosynthesis converts light energy to chemical energy and avails oxygen, both of which are essential for continuity of life. Plant roots gather and stems distribute sparse water and leaves absorb carbon dioxide through stomata and capture solar radiation. Higher plants are non-mobile and have to adapt to their environment. Accordingly, most plants, growing in natural environments that are, to a considerable degree, unfavorable for their growth, are often prevented from expressing their full potential for production and are considered "stressed". Plant productivity usually falls far short of the potential under stressed conditions (Boyer, 1982).

Unfavorable factors to which plants are exposed can be divided into two, biotic and abiotic stresses. Biotic stresses include pests, pathogens, fungi, bacteria, viruses, and nematodes (Bahmani, 2015). Abiotic stresses such as heat, cold, drought, and salinity are the most common factors that have huge adverse effects on plant growth, development and productivity. These stresses reduce the average yield by less than half of the potential (Boyer, 1982; Wang, 2010) and have a great impact on agricultural production and quality of the products (Chen, 2012). Accordingly, much attention has been paid to these abiotic factors in relation to plant growth, development and productivity.

Plants under abiotic stress conditions

Various abiotic stresses lead to production of reactive oxygen species (ROS), including H_2O_2, $O_2^{\cdot}$ and $^1O_2$. ROS are major determinants of the regulation of stress responses as well as phytohormones in plants (Oracz, 2016). For example, ROS enhanced under stress conditions functions as an alarm signal that triggers acclamatory /defense responses by specific signal transduction pathways that involve H_2O_2 as a secondary messenger (MHC de Carvalho, 2008).

ROS are generated by non-enzymatic or enzymatic pathways under stress. Under environmental stress, disturbance of the metabolic balance in oxidative organelles often results

in enhanced production of ROS (Mittler, 2002). The chloroplast in stressed plants is one of the major site of ROS production. Disturbance of the photochemical reactions leads to ROS production, which is enhanced by conditions limiting CO_2 fixation such as drought and salt stresses and their combination with high light intensity (Mittler, 2002; Foyer, 2003).

In enzymatic pathway, NADPH oxidases catalyze the production of superoxides (Sagi, 2006). Superoxides is dismutated to H_2O_2 either spontaneously or by SOD activity (Sharma, 2012).The *Respiratory burst oxidase homolog* (*Rboh*) gene family encodes the key enzymatic subunit of the plant NADPH oxidase (Ogasawara, 2008). Analyses of Rboh mutants and antisense lines provided genetic proof of the function of rboh in the pathogen-induced oxidative burst.

ROS play two divergent roles in plants; at low concentrations they act as signaling molecules that mediate stress responses in plant cells, whereas at high concentrations they cause exacerbating damage to cellular components. When ROS reache above threshold level, they cause oxidative damage to lipids, proteins and DNA leading to altered intrinsic membrane properties like fluidity, ion transport and loss of enzyme activity, ultimately resulting in cell death. In order to avoid the oxidative damage, higher plants possess a complex anti-oxidative defense system comprising of non-enzymatic like ascorbic acid and enzymatic like superoxide reductase components (Sharma, 2012).

Lipid peroxidation

Two common sites of ROS attack on the membrane lipid molecules are the unsaturated (double) bond between two carbon atoms and the ester linkage between glycerol and the fatty acid. The polyunsaturated fatty acids present in membrane lipids are particularly sensitive to attack by ROS (Sharma, 2012). Lipid peroxidation aggravates the oxidative stress through production of lipid-derived radicals (LOOH) that increase in a chain-reaction manner and damage proteins and DNA. The level of lipid peroxidation has been widely used as an indicator of ROS mediated damage to cell membranes under stressful conditions. Increased peroxidation and degradation products of lipids have been reported in plants growing under environmental stresses (Sharma, 2005; Han, 2009; Tanou, 2009; Mishra, 2011), accompanied by increased production of ROS.

Oxylipins, Reactive carbonyl species and RSLVs

Oxidized fatty acids, termed oxylipins (Fig. 1-1), are an important class of signaling molecules in plants, especially related to plant stress responses and innate immunity. Oxylipins include the phytohormone, jasmonic acid, and a number of other molecules including hydroxy-, oxo- or keto-fatty acids or volatile aldehydes. The best-characterized oxylipins are jasmonic acid (JA) and its immediate precursor 12-oxo-phytodienoic acid (OPDA), which are formed enzymatically and accumulate in response to various stresses, in particular wounding and pathogen infection (Eckardt, 2008; Block et al., 2005). The structural diversity of oxylipins is further increased by esterification of the compounds in plastidial glycolipids, for instance the Arabidopsides, or by conjugation of oxylipins to amino acids. The biosynthesis of oxylipins is highly dynamic and occurs in both a constitutive mode and as a consequence of various stresses (Mosblech, 2009).

Among the oxylipins, α, β-unsaturated aldehydes and ketones including OPDA, 2-hexenal, phytoprostane and malondialdehyde, derived from LOOH, are designated as reactive carbonyl species (RCS) (Mano, 2012). Being reactive species like ROS, RCS have two biological aspects; toxicity and signaling function. Saturated carbonyls can react with amino group to form Schiff-bases. In addition to this reactivity, RCS have high electrophilicity due to the α, β-unsaturated bond and hence form Michael adducts with nucleophilic targets such as thiol and amino groups. Acrolein and methyl vinyl ketone negatively affect photosynthetic activity as determined by chlorophyll fluorescence (Almeras et al., 2003; Berger et al., 2007). Yamauchi et al. (2008), using antibodies against malondialdehyde (MDA), acrolein and crotonaldehyde, found that the OEC33 protein in photosystem II (PSII) and light-harvesting chlorophyll-binding proteins were preferentially modified by RCS in heat-stressed leaves. They further showed that the modification of OEC33, CP47 and CP43 was associated with the inactivation of water-oxidizing complex under strong light at high temperature (Yamauchi, 2010). MDA is one of the final products of peroxidation of unsaturated fatty acids in membrane lipids and is responsible for cell membrane damage (Hegedüs, 2004).

Compounds containing α, β-unsaturated carbonyl groups are increasingly implicated as potent regulators of gene expression; some are powerful cytotoxins known to accumulate at the site of lesion formation in host–pathogen interaction (Alméras, 2003). Activities of octadecanoids (Howe and Schilmiller, 2002) and small and highly reactive compounds derived

from oxygenated lipid derivatives have also received much attention (Alméras, 2003).Small and highly reactive compounds, such as acrolein, crotonaldehyde, (2*E*)-pentenal and (2*E*)-hexenal accumulated in plants under abiotic stress conditions, such as high light intensity and heat (Mano, 2010; Loreto, 2006; Yamauchi, 2008). Based on reported biological activity of chemicals with an α,β-unsaturated carbonyl group, short-chain leaf volatiles having an α,β-unsaturated carbonyl bond in their structure, collectively named reactive short chain leaf volatiles(RSLVs), are presumed, despite lack of literature records, to act as signal molecules that induce expression of abiotic stress-related genes (Vokkenweider, 2000; Almeras, 2003).

Biosynthesis and functions of green leaf volatiles

The green odor of plants is characterized by green leaf volatiles (GLVs), which are composed of eight volatile compounds comprised of C_6-aldehydes including 2-hexenal and C_6-alcohols and their esters. GLVs are produced from thylakoid membrane-bound polyunsaturated fatty acids in chloroplasts by a series of enzymes as summarized in Fig. 1-2. Briefly, linolenic acid released by lipase from thylakoid membranes is peroxidized by 13-lipoxygenase (LOX, Chen, 2004) and then cleaved by hydroperoxide lyase (HPL) to produce (3*Z*)-hexenal in the chloroplasts (Hatanaka, 1987, Howe, 2000). Branching from (3*Z*)-hexenal to (2*E*)-hexenal then forms unsaturated GLVs in two series, i.e., (3*Z*)- and (2*E*)-, based on the position of the unsaturated bond in their structures. (3*Z*)-Hexenal and (2*E*)-hexenal are subsequently reduced to alcohols by aldehyde reductases, aldo/keto reductases (Yamauchi, 2011), and alcohol dehydrogenases (Bate, 1998). Alcohol forms of GLVs are further converted to ester forms by a BADH acyltransferase (D'Auria, 2007). A saturated form of GLV, *n*-hexanal, is produced through the oxidation of linoleic acid mediated by 13-lipoxygenase and hydroperoxide lyase along with the hydrogenation of the C–C double bond in (2*E*)-hexenal by alkenal reductase (Mano, 2002). Among GLV species, (2*E*)-hexenal was identified by Curtius and Franzen (1912) at an early stage in GLV research history and named the leaf aldehyde (originally named Blätteraldehyd in German). Despite this early discovery, biosynthetic pathway of (2*E*)-hexenal has remained unknown, although it has been assumed to be converted from (3*Z*)-hexenal by an isomerase (Phillips, 1979; Noordermeer, 1999).

GLVs have recently emerged as key players in plant defense, plant–plant interactions and plant–insect interactions. Some GLVs inhibit the growth and propagation of plant pathogens,

including bacteria, viruses and fungi. In certain cases, GLVs released from plants under herbivore attack can serve as airborne messengers to neighbouring plants and to attract parasitic or parasitoid enemies of the herbivores. The plants that perceive these volatile signals are primed and can then adapt in preparation for the oncoming challenges (HMN Ul, 2015).

Outline of the Dissertation

This study was designed to elucidate functions of RSLVs in stress responses in plants. First, a comprehensive microarray analysis was conducted using *Arabidopsis thaliana.* Exposure of the plant to the RSLVs (2*E*)-hexenal, (2*E*)-butenal and heptane-2-one, resulted in efficient induction of abiotic stress-related genes. Among the RSLVs (2*E*)-hexenal, a widely distributed GLV in plants, was selected for further studies. Then, hexenal isomerase (HI) responsible for the conversion of (3*Z*)-hexenal to (2*E*)-hexenal was purified and the corresponding HI gene was isolated. Tomato, which produces abundant (3*Z*)-hexenal with limited (2*E*)-hexenal, was transformed with the HI gene to verify the latter function in the plant and to modify RSLVs profile of tomato. Furthermore, physiological responses of the transgenic tomato plants to biological stresses were recorded.

This dissertation is composed of four chapters. Following Chapter I reviewing background of the study, Chapter II describes functions and signal transduction of RSLVs through studies using microarray and mutant analyses. As a result, aldehyde molecules with 4 to 10 carbons exhibited no inhibitory effect on PSII activity, a pivotal function of plants related to photosynthesis, but induced expression of abiotic stress-related genes, especially those induced by heat and oxidative stresses. Drastic reduction of heat stress-responses in Arabidopsis *hsfa1* mutant indicated partial involvement of HSFA1 in RSLVs signal transduction. However, no obvious changes were observed in induction of oxidative stress-responsive genes, suggesting the involvement of another pathway(s) than that associated with HSFA1 in the RSLVs signal transduction. In chapter III, hexenal isomerase responsible for the conversion of (3*Z*)-hexenal to (2*E*)-hexenal was isolated from Paprika fruit, the highest producer of (2*E*)-hexenal among the screened leaves and fruits of several plants. Based on the partial amino acid sequences, full length DNA encoding the protein was obtained. The protein was heterologously expressed in *Escherichia coli* and the purified enzyme was characterized. Tomato, which produces (3*Z*)-hexenal as a major volatile with a negligible amount of (2*E*)-hexenal, was transformed by

the HI gene to alter its RSLVs profile. (3*Z*)-Hexenal decreased to a negligible level and (2*E*)-hexenal increased in some transgenic tomato lines, thus establishing the *in vivo* function of HI in (3*Z*)-hexenal biological conversion to (2*E*)-hexenal in tomato. In Chapter IV, the results obtained in Chapter II and Chapter III are collectively discussed to get insight into the physiological importance of (2*E*)-hexenal.

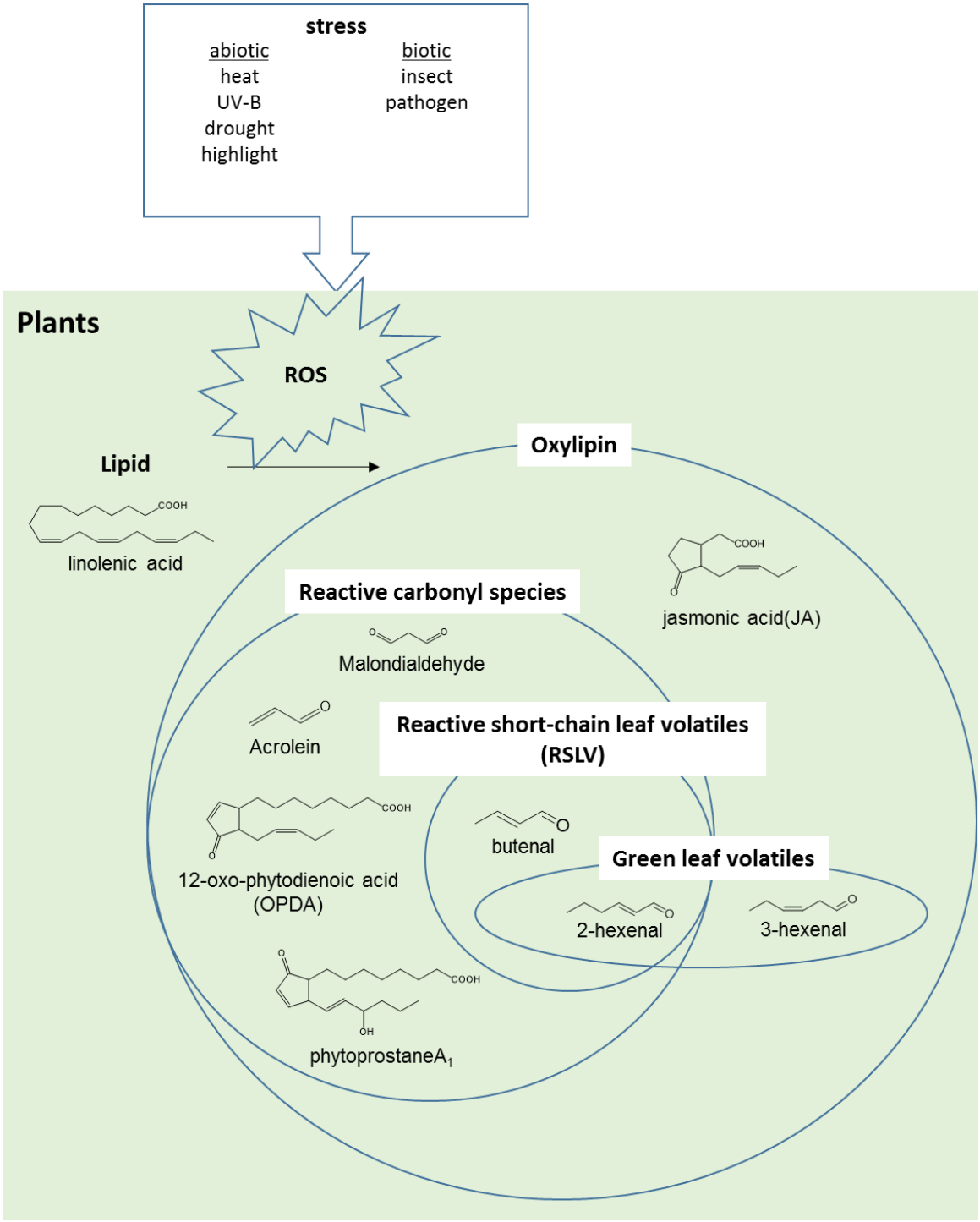

Figure 1-1. Classification of oxylipins

Oxylipin is a group of oxygenated lipid-derived compounds. RCS are compounds having α, β -unsaturated bonds. RSLVs are short chain leaf volatiles having α, β -unsaturated bonds. Green leaf volatiles are C6 compounds derived from linolenic acid or linoleic acid.

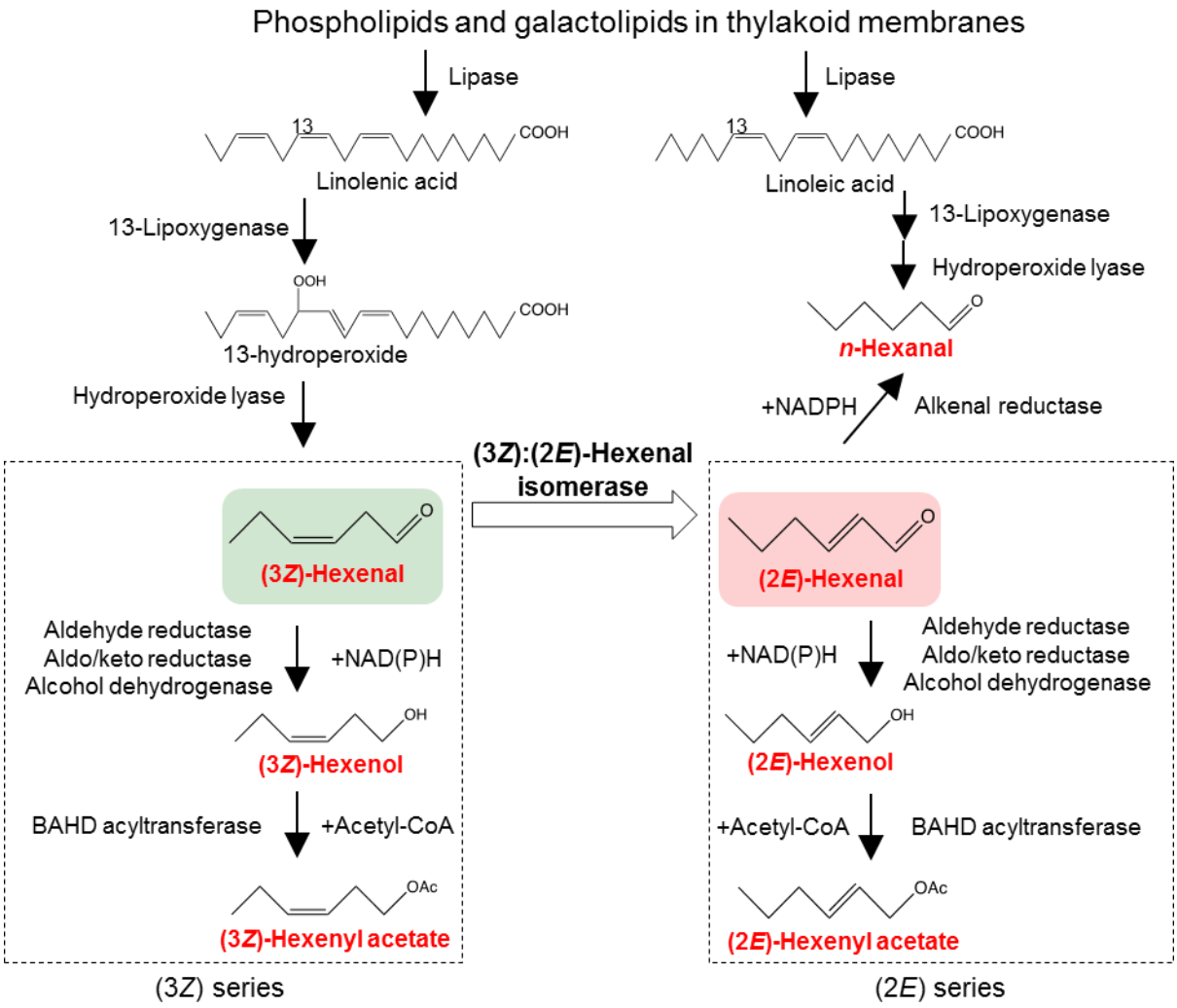

Figure 1-2. Biosynthetic pathway of GLVs.

Major GLV species are enclosed by round-shaped squares. Enzymes catalyzing each reaction are underlined. Isomerization step catalyzed by HI is shown by white arrow. Enzymatic reactions for alcohol- and acetate-forms formation need cofactors. The enzyme responsible for conversion of (*3Z*)-hexenal to (*2E*)-hexenal was unidentified when this work was started.

Chapter II

Functional analysis of reactive short chain leaf volatiles

Abiotic stresses cause serious damage to plants. Accordingly, plants undergo complicated stress responses through transduction of signals the production of which is triggered by environmental stimuli. In this chapter, activities of a series of short-chain leaf volatiles with an α, β-unsaturated carbonyl bond in their structures (reactive short-chain leaf volatiles, RSLVs) as candidate signal molecules were studied by performing a comprehensive microarray analysis using *Arabidopsis thaliana*. (2*E*)-Hexenal and (2*E*)-butenal strongly induced the gene expression of abiotic stress-related transcription factors including, *HSFA2*, *MBF1c*, *DREB2A* and *ZAT*s. Expression of *HSFA2* and *MBF1c* induced by the RSLVs was significantly decreased in the HSFA1-knockout mutants, whereas that of *DREB2A* and *ZAT*s was kept at a high level. Considering that HSFA1s are well known master regulators of heat stress response, the results suggest that the RSLV signaling comprises of HSFA1-dependent and independent pathways. RSLV treatment of Arabidopsis plants induced production of chaperon, necessary for repairing impaired proteins, and alleviated delayed growth under heat stress, demonstrating enhanced abiotic stress tolerance.

Material and methods

Chemicals

2-Propenal, (2*E*)-butenal, (2*E*)-pentenal, (2*E*)-heptenal, (2*E*)-octenal,(2*E*)-nonenal, (2*E*)-decenal, (3*E*)-hepten-2-one, (3*E*)-octen-2-one, (3*E*)-nonen-2-one, (3*E*)-decen-2-one, (2*E*)-hexenol, 2-hexanal, and 2-heptanone were purchased from Tokyo Chemical Industry (Tokyo, Japan). 1-Penten-3-one and 3- penten-2-one were purchased from Sigma-Aldrich (St. Louis, MO, USA). (3*Z*)- Hexenal was obtained from Bedoukian Research Inc. (Danbury, CT, USA). (2*E*)- Hexenal, (*E*, *Z*)-4-hexen-3-one, and other reagents were purchased from Wako Pure Chemicals (Osaka, Japan).

Plant materials

Seeds of *Arabidopsis thaliana* (ecotype Columbia-0: Col-0; Wassilewskija: Ws-0) and tomato

(*Solanum lycopersicum* 'Micro-Tom') were sown on Jiffy-7 peat pellets (Sakata Seed Co., Yokohama, Japan) and kept at 4°C for 3 days in the dark. Then plants were transferred to the conditions of a 14-h–light (80 mmol photons m^{-2} s^{-1})/10-h–dark cycle at 23°C. The AOR-deficient Arabidopsis mutant *aor*, which was previously identified as a T-DNA knockout line of AOR (Yamauchi et al. 2008), was obtained from the Arabidopsis Biological Resource Center (ABRC, Columbus, OH, USA). HSFA1s quadruple knock-out mutant (QK) was generously gifted by Dr Y.-Y. Charng, National Taiwan University, Taiwan. Seeds of rice (*Oryza sativa* L., cv. Nipponbare) were immersed in water for a day at 4°C, and the transferred to the conditions of a 14-h–light (80 mmol photons m^{-2} s^{-1})/10-h–dark cycle at 25°C. Oxidative treatment was performed by immersing the aerial parts of plants in 10 mM methylviologen (MP Biomedicals, Solon, OH, USA) under illumination (80 mmol photons m^{-2} s^{-1}). UV-B treatment was performed by irradiation of UV light (VL- 6MC, 312 nm tube, VilberLourmat, France) with 1 mW cm^{-2}. Heat treatment was performed by exposing at 40°C in the presence of light (80 mmol photons m^{-2} s^{-1}).

Volatile treatment

Plants were placed in a transparent plastic box (340 cm^3, NipponGenetics, Tokyo, Japan). Volatiles were diluted with MeCN, which does not induce *HSFA2* mRNA. Each volatile tested (total volume of 3 ml) was absorbed into a piece of paper towel attached to the inside of the cover. The cover was immediately set on the box (Fig. 2-1A), and the plants were incubated at 25°C under illumination (80 mmol photonsm^{-2} s^{-1}). MeCN-treated plants were used as controls.

Quantitative real-time RT-PCR (qRT-PCR)

Total RNA was purified by using an RNeasy Plant Mini Kit (Qiagen, Hilden, Germany), and then cDNA was synthesized by using a RevaTra Ace kit (Toyobo, Osaka, Japan). Gene-specific primers were chosen with the use of the Primer3 program (http://frodo.wi.mit.edu/). Primer sequences are shown in Table 2-2. Quantitative real-time RT-PCR (qRT-PCR) was performed with the use of Thunderbird SYBR Green qPCR Mix (Toyobo) and a LineGene Real-time PCR Detection System (FQD-33A, BioFlux, Tokyo, Japan). For analysis of relative transcript levels, *ACTIN2* mRNA was used as an internal standard in all qRT-PCR experiments; the expression levels of genes of interest were normalized to that of *ACTIN2* by subtracting the cycle threshold

(CT) value of *ACTIN2* from the CT value of the gene of interest. The expression level of MeCN treated controls was set to 1. For determination of absolute copy number of HSFA2, samples including equal amount of *ACTIN2* determined by qRT-PCR and the pMD20 plasmid (Takarabio Inc., Otsu, Japan) containing the *HSFA2* (3.6 kbp, 254 copies/fg) as a reference matrix was used.

Microarray RNA sample preparation and hybridizations

Total RNA was purified by using an RNeasy Plant Mini Kit (Qiagen) from at least 6 plants. The double-strand (ds) cDNA was generated with a modified procedure of the Superscript Choice System (Life Technologies, Carlsbad, CA). Briefly, the 1st strand cDNA was synthesized from 10.0 mg total RNA, by 1.0 unit SuperScript II reverse transcriptase (Life Technologies) in the presence of 100 pmoles Oligo dT(20) primer. After 2nd strand synthesis, the template RNA was digested with RNase A, then the synthesized DNA was purified with phenol: chloroform: isoamyl alcohol. The purified DNA was precipitated in ethanol, and the pellet was washed, dried, reconstituted and quantified. cDNA samples were labeled using the random priming method with Cy3- labeled random nonamer as primers and Klenow DNA polymerase at 37^{o}C for 2 h (NimbleGen One-color Labeling Kit, NimbleGen Roche, Madison, WI). The labeled DNA was precipitated in isopropanol, and the pellet was washed, dried, reconstituted and quantified. For each hybridizations, 4 mg of labeled DNA was diluted by NimbleGen sample tracking control kit buffers respectively, and be added with NimbleGen hybridization buffers according to the manufacturer's protocols. The arrays (ATH6_60mer_expr X4) were hybridized with labeled DNA on a NimbleGen Hybridization System at 42^{o}C for 16 h. Arrays were washed by NimbleGen wash buffer kit according to the manufacturer's protocols and scanned using an Axon GenePix 4000B scanner at 5 mm resolution. The microarray experiments using the Agilent Arabidopsis ver4.0 (44 k) microarray (Agilent Technologies) with a onecolor method were performed according to the manufacturer's instructions. Data extraction, normalization and production of heat map by UPGMA clustering were performed by Subio Platform software (Subio, Kagoshima, Japan), and Microsoft Excel was used to organize and interpret the data. ''Ratio'' values are the mean of 3 independent experiments, and genes showing a value above 2.0 or below 0.5 (99.8%confidence) were considered as up- or down-regulated, respectively. Datasets of gene expression under each stressed condition were obtained from AtGenExpress

database (The Arabidopsis Information Resource, The Ohio State University, OH, USA). Expression data used in this figure are data of shoot in time course (0.25, 0.5, 1, 3, 6 h of heat, UV-B, drought or wound stresses) and (0.5, 1, 3, 6, 12 h of oxidative, salt, osmotic or cold stresses)

Identification of RSLVs

Harvested plants were immersed in MeCN (2 ml), and 1 ml of 10 mM 2-ethylhexanal was added as an internal standard. After incubation for 30 min at 60°C, 1 ml of the solution was transferred to another glass tube, and 38 ml of HCOOH and 50 ml of 20 mM dinitrophenyl hydrazine dissolved in MeCN were added. After incubation for 60 min at room temperature, 1 ml of saturated NaCl solution and 0.1 g of $NaHCO_3$ were added and well mixed. After incubation for 20 min, 0.5 ml of the MeCN layer was transferred to a plastic tube and evaporated. The resultant residue was dissolved in 200 ml of MeCN, and the solution was filtered through a Cosmonice filter (pore size 0.45 mm, NacalaiTesque, Kyoto, Japan). The resultant cleared solution was used as the DNP-carbonyl preparation for HPLC analysis. HPLC analysis was performed by the method described previously（Yamauchi et al. 2008; Matsui et al. 2009; Yin et al. 2009）. Data were analyzed by using PowerChrom software (eDAQ Pty Ltd., Denistone East, NSW, Australia). For accurate identification of DNP-RSLVs, DNP-RSLVs were subsequently analyzed by liquid chromatography-mass spectrometry (LC/MS/MS, Acquity UPLC/ TQD; Waters, Milford, MA, USA) using YMC-PACK C4 (Q2.0 3 100 mm, 3 mm, Waters). For reverse phase chromatography of RSLV-DNPs, the elution of the samples was carried out with 10% tetrahydrofuran (solvent A2) and acetonitrile (solvent B2), and the mobile phase was changed from 35% (v/v) B2–100% (vol/vol) at 2 and 21.5 min after the injection, respectively, at a flow rate of 0.3 mL min^{-1}. Elution was monitored by Photodiode and MS analysis with ES-negative mode. The column temperature was 40°C. MS/MS analysis conditions were as follows: Declustering potential, 40; collision energy, 40 V; and parent ion (m/z), 249 for (2*E*)-butenal-DNP.

Protein analysis

Protein was extracted with 5 volumes of 50 mM HEPES-NaOH, pH 7.0. Proteins were separated by sodium dodecyl sulfate-polyacrylamide gel electrophoresis (SDS-PAGE) in 10%

(HSP101) or 12% polyacrylamide gels (HSP17.6). The proteins were electroblotted onto polyvinylidene difluoride (PVDF) membranes (ATTO, Tokyo, Japan) according to the manufacturer's instructions, and anti-HSP101 and anti-HSP17.6 antibodies (Agrisera, Vännäs, Sweden) were used for immunochemical detection. Alkaline phosphatase–conjugated secondary antibody was used for visualizing signals with 5-bromo-4-chloro-3-indolyl phosphate and nitro blue tetrazolium as substrates. The bands were quantified by densitometric analysis using ImageJ software after scanning the blotted membrane.

Measurement of chlorophyll fluorescence

The maximum quantum yield of PSII was estimated from chlorophyll fluorescence measurements by pulse-amplitude– modulated (PAM) fluorometer (Junior-PAM; Walz, Effeltrich, Germany). Plants were dark-adapted at room temperature for 5 min before measuring. The yield of PSII was calculated as the ratio of *Fv/Fm*.

Thermotolerance test

For a hypocotyl elongation test (Hong and Vierling 2000), seeds planted on MS plates were wrapped in foil and incubated at 4ºC for 3 day, then at 23ºC for 2.5 days (Col-0) or 5 days (QK). After length of cotyledons was measured, they were separately treated as follows. i) For 45ºC treatment, seedlings were incubated at 45ºC for 2 h. ii) For acquired thermotolerance treatment, seedlings were incubated at 38ºC for 90 min followed by 2 h at 23ºC and then 2 h at 45ºC. ii) For volatile treatment, seedlings were treated with 10 nmol cm^{-3} of (2*E*)-butenal, (2*E*)-hexenal or 3-hepten-2-one for 2 h at 23ºC and then 2 h at 45ºC. After treatment, seedlings were incubated an additional 2.5 days in the dark, then length of seedlings was measured. For survival test, seeds (at least 30 plants) planted on MS plates were wrapped in foil and incubated at 4ºC for 3 day, then at 23ºC for 2.5 days. After the seedlings were subjected to the same treatments as elongation test, seedlings were additionally incubated under standard conditions of a 14-h–light (80 mmol photonsm^{-2} s^{-1})/10- h–dark cycle at 23ºC. The percentage of survival plants was calculated by counting the continuously developing plants per total plants after 3 days. Survival enhancement was determined by calculation using survival rate of RSLV treatment sample against that of 45ºC sample.

Statistical analysis

Data were analyzed by using the programs of Statistical analysis program (StatPlus, AnalystSoft). Data were subject to ANOVA with post hoc analysis, and means were compared by Tukey-Kramer test ($P<0.05$).

Results and discussion

RSLVs induced various abiotic-related transcription factors

(2*E*)-hexenal was selected as a model RSLV because (2*E*)-hexenal is a widely distributed C6 RSLV known as a green leaf volatile (GLV). An overview of the whole gene expression pattern obtained by a comprehensive microarray analysis showed that vaporized (2*E*)-hexenal treatment (10 nmol cm^{-3} for 30 min, Fig. 2-1A) induced genes upregulated in various abiotic stress responses (Fig. 2-1B, lane RSLV1). Comparing gene expression patterns under various abiotic stresses allowed us to classify up-regulated genes into the following 5 groups (Fig. 2-1B): heat, UV-B and oxidative stresses-responsive genes (Group A); various stresses-responsive genes (Group B); genes that respond to salt, oxidative, osmotic drought, cold and wounding (Group C); salt- and osmotic-responsive genes (Group D); and cold-responsive genes (Group E). Among these groups, gene expression of Groups A and B were stimulated by (2*E*)-hexenal treatment. Many of the 100 most highly up-regulated genes were abiotic stress-related genes (Fig. 2-1C, Table 2-1) as follows: genes encoding HSPs (21 genes); heat or oxidative stress related transcription factors (7 genes), including *HSFA2* (Nishizawa et al. 2006), *MBF1c* (Suzuki et al., 2005) and *ZAT*s (Kielbowicz-Matuk 2012); abiotic-related AP2/ERF transcription factors (10 genes), including *DREB2A* (Mizoi et al. 2012); and other transcription factors (5 genes).

RSLVs strongly and rapidly induced *HSFA2* gene expression

Because *HSFA2* and *HSP*s were prominently induced by (2*E*)-hexenal treatment, detailed biological activity of (2*E*)-hexenal was examined using the heat shock factor (HSF)-heat shock protein (HSP) system. Vaporized (2*E*)-hexenal rapidly and powerfully induced *HSFA2* expression within 30 min (Fig. 2-2A). This expression was transient and terminated after 2 h. These treatments increased the internal (2*E*)-hexenal concentration comparable to the intracellular concentration of intact higher plants (Mano et al. 2010, Matsui et al. 2012). At 10

min after applying (2*E*)-hexenal at 10 nmol cm^{-3} to Arabidopsis, the internal concentration of (2*E*)- hexenal exhibited a transient increase of up to 25 nmol g^{-1} fresh weight (FW) (Fig. 2-2B, Fig. 2-3). The effects of other GLVs on *HSFA2* expression were tested: (2*E*)-hexenol, (3*Z*)-hexenal, and n-hexanal did not induce *HSFA2* expression (Fig. 2-2D). Among ketones, (3*E*)-hepten-2-one but not 2-heptanone induced *HSFA2* expression, suggesting that the α, β-unsaturated carbonyl bond moiety was essential for *HSFA2* induction. Induction of *HSFA2* was dose-dependent above 2.5 nmol cm^{-3} and saturated at 25 nmol cm^{-3} (Fig. 2-2C).

RSLVs having longer hydrocarbon chains act as signal molecules with less cytotoxic effect

To determine the effect of carbon chain length on *HSFA2* induction, we compared the effects of a series of RSLVs with various carbon chain lengths, and found that RSLVs with chain lengths of C4 to C9 were effective with a slightly higher induction in the aldehyde form than in the ketone form (Fig. 2-4). Expression patterns obtained by microarray analyses using (2*E*)-butenal- or (3*E*)-hepten-2-one-treated Arabidopsis, were essentially homologous to that of (2*E*)-hexenal (Fig. 2-1B, lane RSLV2 and 3), suggesting that the RSLVs exhibit identical induction activity against abiotic stress-related genes. However, a member of RSLVs is potentially photosynthesis damaging agents, as shown by our previous in vitro study (Yamauchi and Sugimoto 2010). The ratio *Fv/Fm*, the maximum photochemical quantum efficiency of PSII, is used as a measure of stress response because PSII is one of the sites most sensitive to α, β-unsaturated carbonyls (Yamauchi and Sugimoto 2010; Almeras et al. 2003), thus we examined the photosynthesis damaging activity of RSLVs by measuring *Fv/Fm* in Arabidopsis at 23ºC. As a result, except vinyl group (H_2C=CH-) containing RSLVs such as 2-propenal, 1-buten-3-one, and 1-penten-3-one, RSLVs did not damage PSII (Fig. 2-4, right panel, Fig. 2-5). Therefore, the RSLVs with chain lengths of C4 to C9 having no vinyl group possibly act as signal molecules with less cytotoxic effect.

Evaluation of endogenous RSLVs on *HSFA2* expression

Production of (2*E*)-hexenal via an enzymatic pathway (Fig.2-8) is assumed to be activated when plant tissues are disintegrated by physical factors, such as pest invasion, wounding or freezing (Matsui 2006). In Arabidopsis ecotype No-0, which can produce (2*E*)-hexenal enzymatically, the (2*E*)-hexenal content in leaves reached 110 nmol g^{-1} FW when the leaf was disrupted

(Matsui 2012). However, in Arabidopsis ecotype Col-0 used in this study, (2*E*)-hexenal is undetectable because hydroperoxide lyase, which is necessary for producing C6 GLVs, is nonfunctional truncated protein due to 10-nucleotide deletion in its first exon (Duan et al. 2005). This difference allowed us to determine which RSLVs were produced by non-enzymatic peroxidation of PUFAs. Oxidative stress caused by treatment with 10 mM methylviologen (MV) under illumination resulted in an increase of (2*E*)-butenal (Fig. 2-6). Full-scan spectra of fragment ions (Fig.2-6B) and selected reaction monitoring using major fragment ions (Fig. 2-6C) confirmed the identity of this endogenous compound. Concomitant with increase in *HSFA2* mRNA expression (Fig. 2-7A, column Col-0), these results suggest that (2*E*)-butenal produced by non-enzymatic peroxidation of PUFAs (possible pathway is shown in Fig. 2-8B) can act as signaling chemicals that induce *HSFA2* expression. To assess the effect of endogenous RSLVs on *HSFA2* expression, *HSFA2* mRNA expression in *aor* mutants were analyzed. *aor* mutants are deficient in chloroplasticalkenal/one oxidoreductase (AOR) (Yamauchi et al. 2011), the enzyme that catalyzes the saturation of α, β-unsaturated carbonyl bonds in reactive carbonyls such as RSLVs (Fig. 2-7E). Previously, Yamauchi et al., 2012 found that *aor* exhibited high sensitivity to MV treatment concomitant with accumulation of reactive carbonyls including RSLVs. In this study, both *aor* and Col-0 showed similar levels of (2*E*)-butenal and *HSFA2* expression under normal condition, and MV treatment enhanced accumulation of (2*E*)-butenal and *HSFA2* expression in *aor* and Col-0 (Fig. 2-7A and 7B). The enhancement of *HSFA2* expression in the MV-treated *aor* was higher than that in MV-treated Col-0, corresponding to higher (2*E*)-butenal accumulation in *aor* (Fig. 2-7A and 7B). This result indicates that total of RSLVs including (2*E*)-butenal and minor RSLVs whose concentration is lower than detection-limit of our analysis might induce *HSFA2* higher in *aor* mutant than Col-0. Similar results were obtained from ultraviolet B (UV-B) stress treatment (Fig. 2-7C and 7D) that accompanies ROS production (AH-Mackerness et al. 2001) and lipid peroxidation (Takeuchi et al. 1995). These enhancements of *HSFA2* expression by stress treatments support the hypothesis that RSLVs are involved in the induction of *HSFA2* expression *in vivo*.

RSLV signaling is transmitted via both HSFA1-dependent and -independent pathways

In a heat-stress response, HSFA1s act as master regulators to drive the HSF-HSP system (Liu et al. 2011). To determine whether RSLV stimulates HSFA1-mediated HSP expression, an

HSFA1a/1b/1d/1e quadruple knockout mutant (QK) was used, which exhibited no *HSFA2* expression when exposed to heat conditions (Liu et al. 2011). In the genomic background ecotypes of QK, wild type Col-0 and Ws-0, *HSFA2* and *MBF1c* (belonging to group A, Fig. 2-9A), and *DREB2A*, *ZAT*10 and *ZAT*12 (belonging to group B, Fig. 2-9A) were induced by (2*E*)-hexenal treatment (Fig. 2-9B and 2C). In (2*E*)-hexenal–treated QK, *HSFA2* and *MBF1c* expression was almost eliminated (Fig. 2-9B), whereas expression of *DREB2A* and *ZAT10* remained at a similar level to that of Ws-0 (Fig. 2-9C). These results suggested that RSLV-mediated gene expression involves heterogeneous pathways, i.e. the HSFA1-dependent and HSFA1-independent pathways.

Tomato *HSFA2*s, and rice *HSFA2*s and *DREB2A* were also induced by (2*E*)-hexenal

(2*E*)-Hexenal is a common RSLV that is also detected in tomato (Buttery et al. 1987) and rice (Hernandez et al. 1989), thus might act as a signal chemical among various plant species. To explore this possibility, the induction of HSFs by (2*E*)-hexenal in a model tomato cultivar (*Solanum lycopersicum* 'Micro-Tom') and rice (*Oryza sativa* 'Nipponbare') were examined because these species in which the heat-stress response mechanism has been well-characterized. The results of tomato were similar to those described for Arabidopsis in that the tomato *HSFA2* genes were induced by (2*E*)-hexenal. The induction profiles of other classes of *HSFs—HSFA1* and *HSFB1* in tomato were similar to those in Arabidopsis (Fig. 2-10A and 10B). In the case of a monocotyledonous plant rice, (2*E*)-hexenal also upregulated heat-inducible *OsHSFA2*s and abiotic stress-inducible *OsDREB2A* (Fig. 2-10C). These similarities of gene expression profiles among species indicate that RSLVs might be common signal chemicals.

RSLV treatment could enhance abiotic stress tolerance

Because RSLVs induced *HSF* and *HSP* gene expression, protein expression enhancement by RSLV treatment was confirmed by detecting two HSPs: HSP101 (encoded by At1g74310) and HSP17.6 (encoded by At1g53540). As shown in Fig. 2-11A, HSP101 and HSP17.6 were induced by (2*E*)-hexenal, (2*E*)-butenal and (3*E*)-hepten-2-one treatment at 23ºC within 2 h, whereas the levels in acetonitrile (MeCN)-treated control plants remained low. Finally, an effect of RSLV treatment on abiotic stress tolerance was investigated. RSLV-induced thermotolerance was assessed by evaluating hypocotyl elongation (Hong and Vierling, 2000) and survival tests,

because RSLV treatment could enhance *HSFA2* expression and HSP17.6 production (Fig. 2-11) those confer acquired thermotolerance (Dafny-Yelin, 2008). After 2.5 days of growth on vertical plates in the dark, the seedlings were applied to the hypocotyl elongation test (Fig. 2-12A). After heat treatment at 45ºC for 2 h, the control and solvent-control seedlings stopped developing, whereas seedlings pretreated at 38ºC for 90 min (for gaining acquired thermotolerance) or RSLV-treated seedlings at 23ºC for 120 min continued hypocotyl elongation. The thermotolerance enhancing effect of (2*E*)-hexenal was not observed in HSFA1s-deficient QK mutants (Fig. 2-13), indicating that the physiological importance of HSFA1-dependent pathway in heat stress response. In the survival enhancement test, RSLV treatments enhanced thermotolerance similar level to that of acquired thermotolerance (Fig. 2-12C). In addition, RSLV treatments could enhance protection of PSII from heat- or UV-B-derived damages (Fig.2-14B and 14C).

Possible role of RSLVs in abiotic stress responses

RSLVs have been widely detected among plant species, and increased RSLV production has been observed under abiotic stresses (Mueller, 2009) including heat stress (Fig. 2-15). Production of (2*E*)-hexenal was detected in a photoinhibition sensitive Arabidopsis mutant (Col-0 background) npq1 by intense light conditions (Loreto et al., 2006), which could cause ROS to be overproduced from the loss of energy dissipation. Additionally, in tomato plants, production of (2*E*)-hexenal was enhanced under heat and cold stresses (Copolovici et al. 2012). Furthermore, increased levels of (2*E*)-pentenal and (2*E*)-hexenal were also detected in tobacco plants under photooxidative stress condition (Mano et al. 2010). Consequently, non-enzymatic pathway-derived small 2-alkenals, and both enzymatic and non-enzymatic pathways derived (2*E*)-hexenal can act as endogenous signal chemicals that respond to abiotic stresses. Volatiles such as isoprenoids play important roles in various stresses tolerance (Vickers et al. 2009). Also in the case of RSLVs, the results indicate that RSLVs stimulate heterogeneous signal transduction in response to abiotic stress (Fig. 2-16). One signal transduction pathway is an HSFA1-dependent pathway expressing proteotoxic stress-related genes that contribute to HSP production to maintain protein homeostasis. The other signal transduction pathway is mediated by HSFA1-independentpathway expressing various abiotic stress-response genes. RSLVs stimulate both pathways as oxidative stress signals to induce proteotoxic and abiotic

stress-response genes.

Table2-1. Descending order of gene expression ratio [(2*E*)-hexenal versus control] calculated from results of microarray. The "Ratio" values are the mean of 3 independent experiments,

TAIR_ID	Ratio	SD	DESCRIPTION
AT1G53540	117.26	21.24	HSP17.6C-CI
AT1G59860	91.02	10.82	HSP17.6A-CI
AT2G26150	80.58	10.75	ATHSFA2; DNA binding / transcription factor
AT4G08555	75.44	9.27	unknown protein
AT5G05410	73.62	14.17	DREB2A; DNA binding / transcription factor/ transcriptional activator
AT1G05575	69.62	6.34	unknown protein
AT5G27420	53.87	14.50	protein binding / ubiquitin-protein ligase/ zinc ion binding
AT3G29000	51.18	4.64	calcium ion binding
AT2G46240	44.81	3.64	protein binding
AT2G44840	43.08	14.95	ATERF13; DNA binding / transcription factor
AT5G47230	37.57	8.89	ATERF-5/ATERF5; DNA binding / transcription factor/ transcriptional activator
AT5G12020	35.85	6.22	HSP17.6II
AT4G25200	35.52	11.69	ATHSP23.6-MITO (MITOCHONDRION-LOCALIZED SMALL HEAT SHOCK PROTEIN 23.6)
AT5G12030	34.67	1.35	AT-HSP17.6A
AT2G32120	34.19	1.92	HSP70T-2; ATP binding
AT2G29500	33.98	2.73	HSP17.6B-CI
AT1G71000	33.91	27.28	heat shock protein binding / unfolded protein binding
AT5G14470	33.67	5.74	ATP binding / galactokinase/ kinase/ phosphotransferase, alcohol group as acceptor
AT1G22810	32.79	10.12	DNA binding / transcription factor
AT4G17500	28.60	10.25	ATERF-1 (ETHYLENE RESPONSIVE ELEMENT BINDING FACTOR 1); DNA binding / transcription factor/ transcriptional activator
AT1G03070	28.34	12.01	glutamate binding
AT5G48570	28.32	4.83	FK506 binding / calmodulin binding / peptidyl-prolyl cis-trans isomerase
AT4G27654	28.04	8.09	unknown protein
AT2G36800	26.91	3.27	DOGT1 (DON-GLUCOSYLTRANSFERASE); UDP-glycosyltransferase/ transferase, transferring glycosyl groups
AT5G51440	26.91	3.60	HSP23.5-M
AT2G20560	25.61	1.28	heat shock protein binding / unfolded protein binding

Table 2-1. (Continued)

AT1G02230	25.53	9.22	ANAC004; transcription factor
AT5G37670	25.24	5.28	HSP15.7CI
AT4G10250	24.28	14.07	ATHSP22.0
AT5G39670	22.16	2.08	calcium ion binding
AT3G09350	22.12	4.51	unknown protein
AT1G52560	22.11	3.25	HSP26.5-P
AT5G52760	21.62	7.15	metal ion binding
AT4G27670	21.22	16.48	HSP21 (HEAT SHOCK PROTEIN 21)
AT3G08970	21.04	5.19	heat shock protein binding / unfolded protein binding
AT4G17490	20.75	0.77	ATERF6 (ETHYLENE RESPONSIVE ELEMENT BINDING FACTOR 6); DNA binding / transcription factor
AT3G02800	20.44	1.81	phosphoprotein phosphatase
AT3G50260	20.30	1.45	ERF DNA binding / transcription factor
AT1G21550	20.11	3.32	calcium ion binding
AT2G32030	19.95	3.29	N-acetyltransferase
AT3G51910	19.49	2.17	AT-HSFA7A; DNA binding / transcription factor
AT5G54490	19.27	0.73	PBP1 (PINOID-BINDING PROTEIN 1); calcium ion binding
AT5G46295	19.10	6.63	unknown protein
AT5G59820	18.94	2.37	ZAT12 RHL41 (RESPONSIVE TO HIGH LIGHT 41); nucleic acid binding / transcription factor/ zinc ion binding
AT5G47220	18.79	14.31	ATERF-2/ATERF2/ERF2; DNA binding / transcription factor/ transcriptional activator
AT1G78410	18.33	3.40	unknown protein
AT1G61340	18.02	5.04	unknown protein
AT1G30370	17.51	7.34	triacylglycerol lipase
AT1G74930	17.49	9.35	ERF DNA binding / transcription factor
AT4G34131	17.46	2.43	UDP-glycosyltransferase/ transferase, transferring hexosyl groups
AT2G22880	17.45	7.62	unknown protein
AT1G56240	17.44	2.75	ATPP2-B13
AT5G45630	17.00	9.17	unknown protein
AT3G23230	17.00	4.79	ERF DNA binding / transcription factor
AT5G04340	16.97	0.57	ZAT6 C2H2; nucleic acid binding / transcription factor/ zinc ion binding
AT4G23493	16.76	4.41	unknown protein

Table 2-1. (Continued)

AT5G52640	16.19	0.16	HSP81-1 (HEAT SHOCK PROTEIN 81-1); ATP binding / unfolded protein binding
AT5G42380	15.85	2.66	calcium ion binding
AT5G64510	15.60	3.06	unknown protein
AT4G12400	15.56	1.06	unknown protein
AT3G10930	14.87	4.96	unknown protein
AT3G07150	14.69	3.05	unknown protein
AT1G70420	14.54	2.99	unknown protein
AT5G66650	14.30	1.51	unknown protein
AT3G49570	14.27	3.38	unknown protein
AT1G24140	13.77	1.09	metalloendopeptidase/ metallopeptidase/ zinc ion binding
AT2G37430	13.62	3.15	ZAT11nucleic acid binding / transcription factor/ zinc ion binding
AT3G25250	13.51	2.63	AGC2-1 (OXIDATIVE SIGNAL-INDUCIBLE1); kinase
AT4G28703	13.47	0.20	unknown protein
AT4G37290	13.46	0.47	unknown protein
AT5G63790	13.34	1.83	ANAC102; transcription factor
AT2G36750	13.14	4.54	UGT72C1; UDP-glycosyltransferase/ transferase, transferring glycosyl groups
AT3G54150	12.99	4.66	S-adenosylmethionine-dependent methyltransferase
AT5G22140	12.91	1.81	disulfide oxidoreductase/ electron carrier
AT3G17611	12.89	2.79	unknown protein
AT3G50800	12.84	3.53	unknown protein
AT4G21320	12.69	1.52	HSA32
AT3G11840	12.55	4.22	ubiquitin-protein ligase
AT5G16980	12.41	2.57	oxidoreductase/ zinc ion binding
AT2G26560	12.23	6.65	nutrient reservoir
AT2G29490	12.13	3.50	ATGSTU1 (GLUTATHIONE S-TRANSFERASE 19); glutathione transferase
AT5G24110	11.95	4.56	WRKY30; transcription factor
AT1G16030	11.69	2.99	HSP70B; ATP binding
AT1G79410	11.68	0.78	carbohydrate transporter/ sugar porter
AT3G14660	11.42	5.25	CYP72A13; heme binding / iron ion binding / monooxygenase/ oxygen binding
AT3G61190	11.34	4.23	BAP1 (BON ASSOCIATION PROTEIN 1)

Table 2-1. (Continued)

AT5G57220	11.21	2.91	CYP81F2; heme binding / iron ion binding / monooxygenase/ oxygen binding
AT2G29060	11.06	1.60	transcription factor
AT3G23170	11.00	4.14	unknown protein
AT2G46400	10.97	3.82	WRKY46; transcription factor
AT1G63820	10.74	0.38	unknown protein
AT4G15975	10.70	3.28	protein binding / ubiquitin-protein ligase/ zinc ion binding
AT1G27730	10.49	0.56	ZAT10; nucleic acid binding / transcription factor/ zinc ion binding
AT1G54050	10.45	1.07	HSP17.4-CIII
AT5G59720	10.32	3.75	HSP18.2 (HEAT SHOCK PROTEIN 18.2)
AT1G50750	10.31	2.17	unknown protein
AT4G34135	10.22	1.68	UDP-glycosyltransferase/ transferase, transferring hexosyl groups
AT1G56060	10.14	2.44	unknown protein
AT3G50770	9.96	1.39	calcium ion binding

Table 2-2

Primer sequences used in this study.

Target gene	Forward	Reverse
Arabidopsis		
Actin2	ACC AGC TCT TCC ATC GAG AA	GAA CCA CCG ATC CAG ACA CT
HSFA1a	GAC GGG TTC TCA TCT CCA AA	TCA TCA ATC TCG GGG TCT TC
HSFA1b	GAG GTG GGG AAG TTT GGA AT	TTG TGC TGC TTC GTT TAT CG
HSFA1d	TCA GAA GCA ACC GAG AAC TG	CCA TCC ATT TTG TTC CTG CT
HSFA1e	ATC GAT GAA CGA TGC AAC AA	CTG TCT CGC ATC CAA CAA GA
HSFA2	GCA AGG AAC GTC ATC ATC TG	ATC AGC AAG GAT CTG GGA TG
HSFB1	TTG GTT CGC CTT CTG AGT CT	CTT TCA ACC ACA CCC CAA AC
ZAT12	GGC GAA TTG TTT GAT GCT TT	CAA GCC ACT CTC TTC CCA CT
ZAT10	GCT TCT CCG ATT CCT CCT TT	GAC CAC CGA GAG CTT GGT AA
MBF1c	GAG CAG ATA CCC AGG AGC AG	TGA TCT GTT TCG CCA AAT CC
DREB2A	GTG GAG TGG AGC CGA TGT AT	ATC GTC GCC ATT TAG GTC AC
Tomato		
Actin	AGC AAT ACC AGG GAA CAT GG	GGA TCT TGC TGG TCG TGA TT
HSFA1	AGG AGG TCC CAC CAA CTT CT	TCC CAC TTT TCC CTC AAC TG
HSFA2	GAT CTG GTG CTT GCA TTG AA	TGG GGG TCA TCG TTA GTC TC
HSFB1	CAA AGG ATT TGC TTC CCA AA	CCG TGA ACT GGG ACA ACT TT

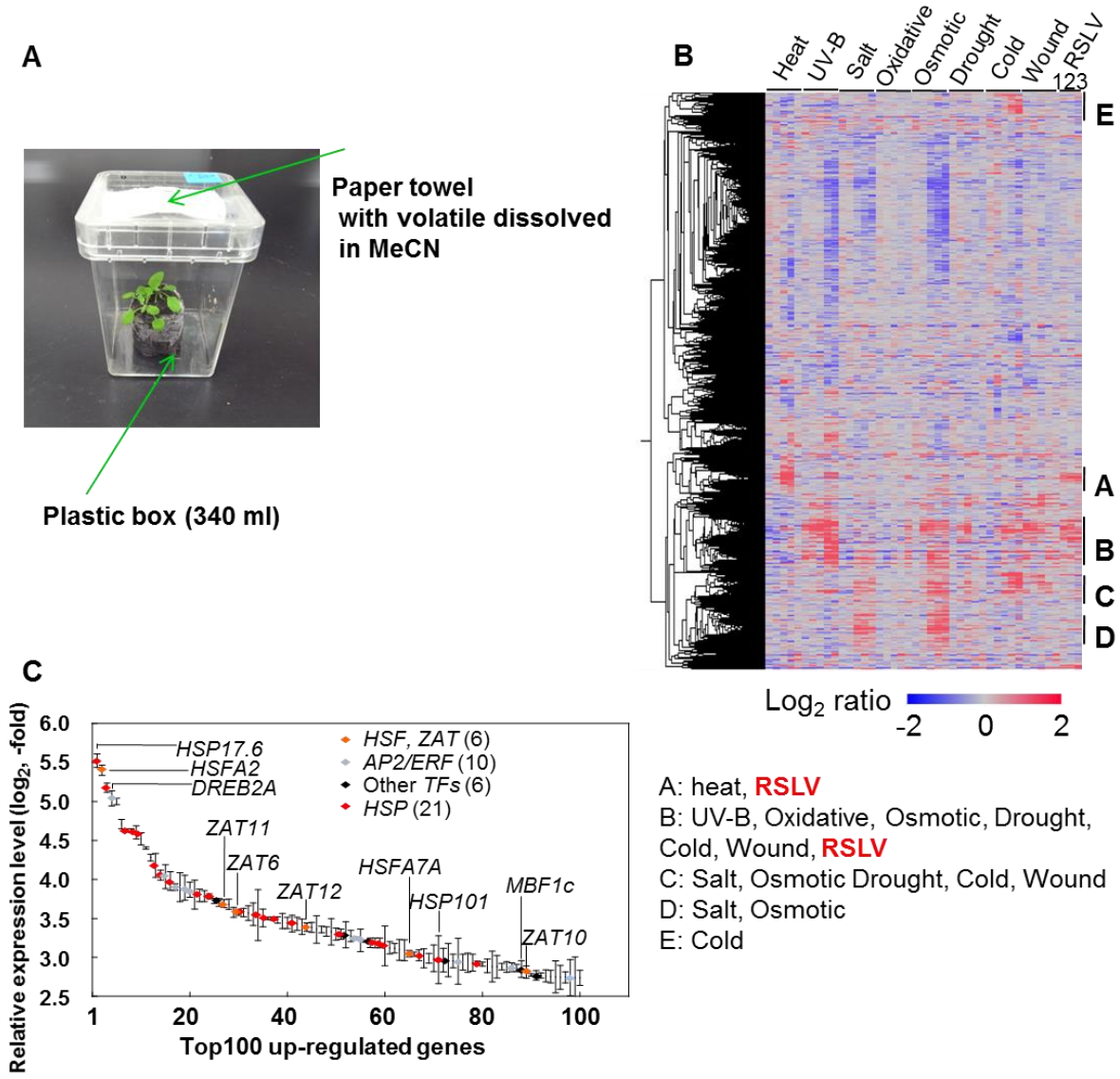

Figure 2-1. Abiotic stress-related genes were up-regulated by RSLV treatment in Arabidopsis.

A Arabidopsis plants vaporized (2*E*)-hexenal in plastic box. **B** Heat map constructed with the whole gene expression. Expression data used are data from shoots collected over the course (0.25, 0.5, 1, 3, 6 h of heat, UV-B, drought or wound stresses) and (0.5, 1, 3, 6, 12 h of oxidative, salt, osmotic or cold stresses) obtained from the AtGenExpress database. RSLVs used for obtaining expression data are (2*E*)-hexenal (lane 1), (2*E*)-butenal (lane 2) and 3-hepten-2-one (lane 3). Genes induced by heat and various stresses induced were classified into Groups A and B, respectively. In addition, responsive genes to salt, oxidative, osmotic drought, cold and wound (Group C), salt- and osmotic-responsive genes (Group D) and cold-responsive genes (Group E) are shown. **C** Transcription factors and HSPs in the 100 most highly up-regulated genes. Expressionwas induced by (2*E*)-hexenal treatment. Symbols indicate the HSF and ZAT genes (orange), AP2/ERF genes (blue), other transcription factor genes (black), and HSP genes (red). Symbols of other genes are omitted. Data are means±SE (n=3). Detailed list is shown in Table 2-1.

++++++++++

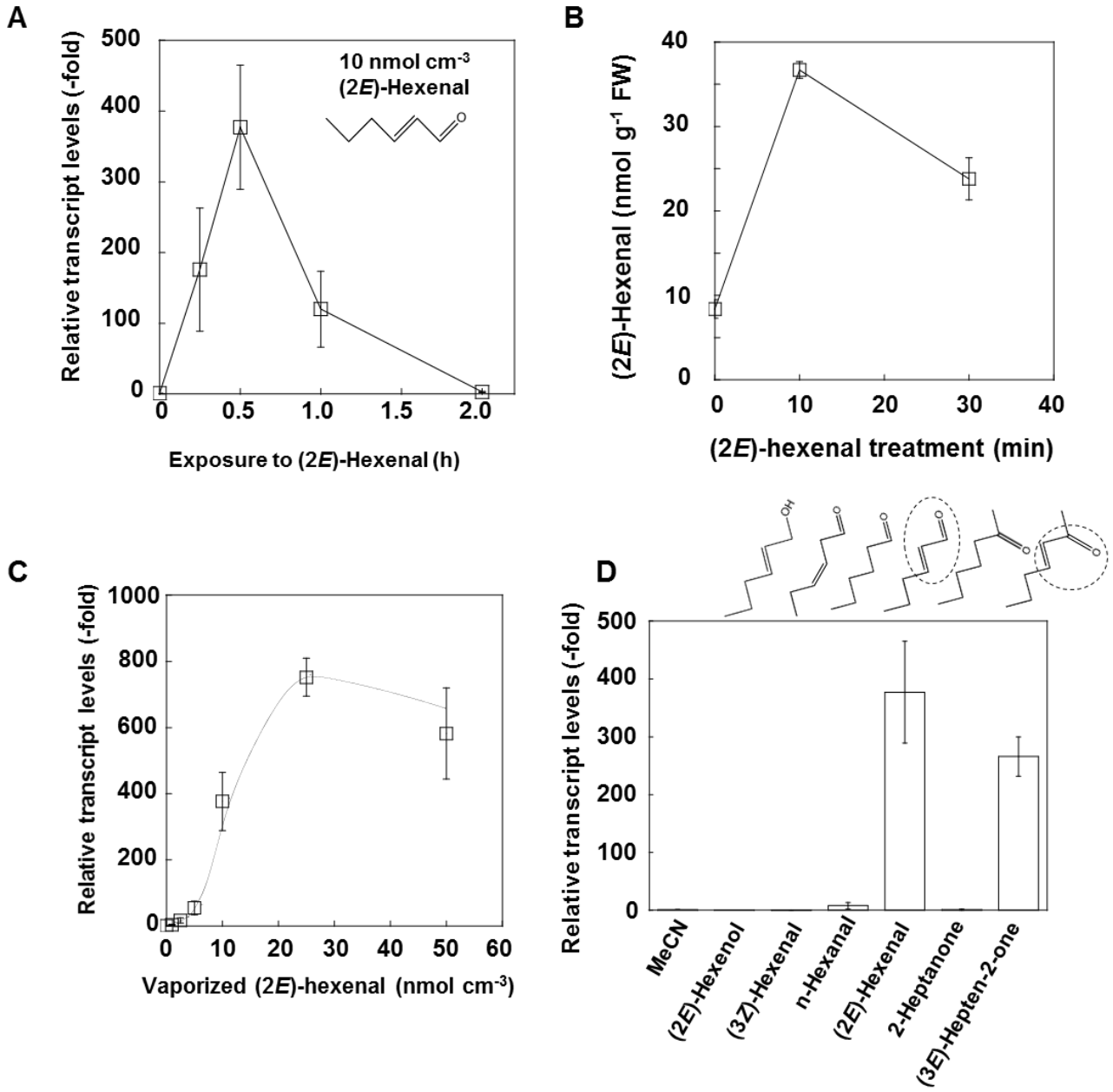

Figure 2-2. HSFA2 gene was specifically upregulated by (2*E*)-hexenal.

A Arabidopsis plants were exposed to (2*E*)-hexenal (10 nmol cm^{-3}) for various time periods (0 to 2 h). **B** Changes in (2*E*)-hexenal content. Data are means ± SD (*n* = 3). **C** Arabidopsis plants were exposed to various concentrations of (2*E*)-hexenal for 30 min to determine dose-dependence of HSFA2 expression. Expression of the HSFA2 gene was determined using qRT-PCR. Relative transcript levels were normalized to *ACTIN2* mRNA. Data are means ± SD

(n = 3). **D** Arabidopsis plants were exposed to series of C6 GLVs and their analogues (each 10 nmol cm^{-3}) for 30 min.

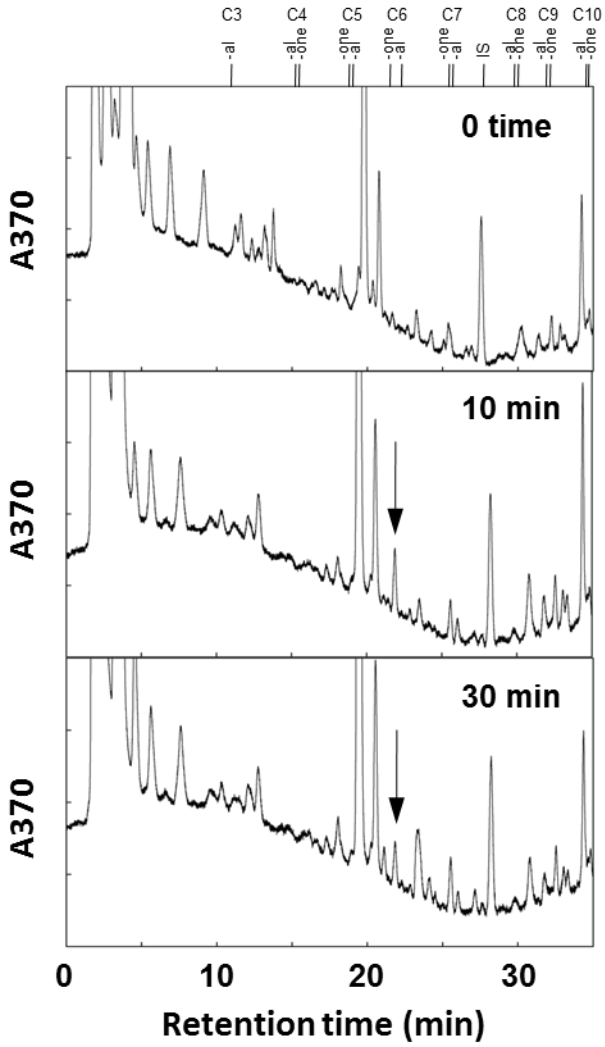

Figure 2-3. Transient increase in (2*E*)-hexenal in *Arabidopsis* treated at 10 nmol cm^{-3}. Typical HPLC chromatogram. Arrows indicate peaks of DNP-(2*E*)-hexenal. The retention times of authentic DNP-RSLVs and the internal standard (IS) are shown above the chromatogram.

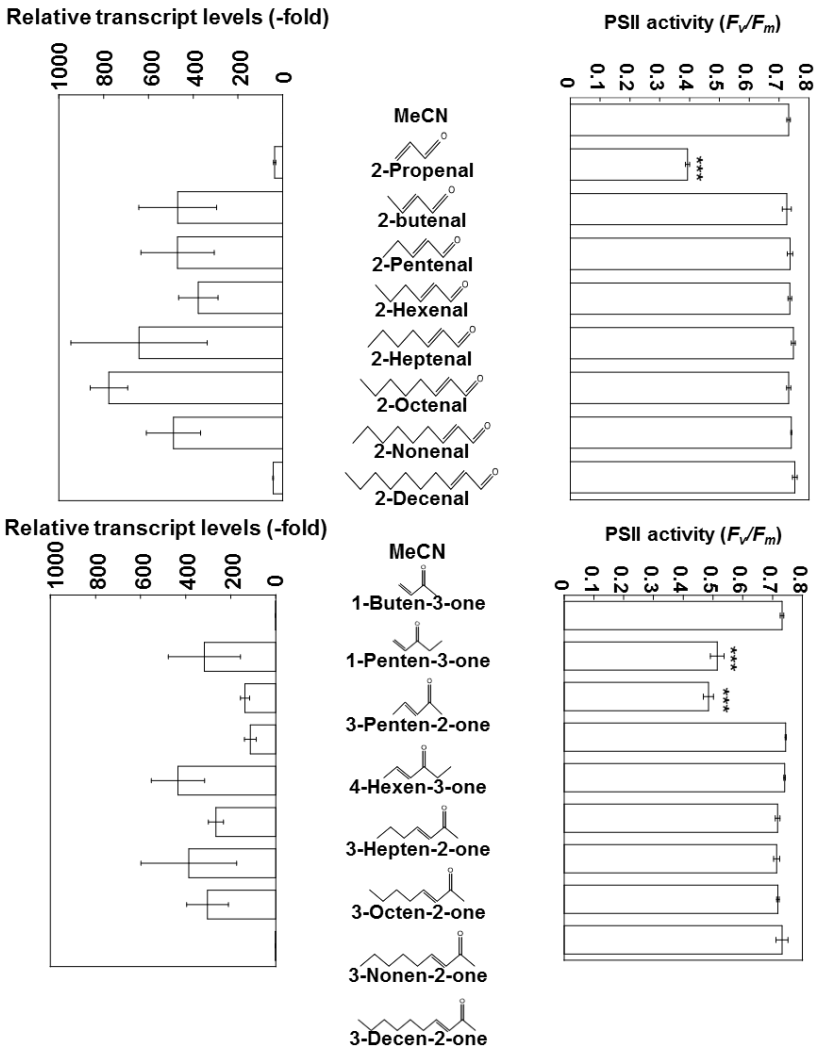

Figure 2-4. Effect of chain-length of RSLVs on Induction of HSFA2 expression and PSII activity. Arabidopsis plants were exposed to (2*E*)-hexenal (10 nmol cm^{-3}) a series of RSLVs of aldehyde form (each 10 nmol cm^{-3}) for 30 min, or a series of RSLVs of ketone form (each 10 nmol cm^{-3}) for 30 min (upper panel). Expression of the HSFA2 gene was determined using qRT-PCR. Relative transcript levels were normalized to ACTIN2 mRNA. The expression level of the 0 h exposure sample was set to 1. Effect of RSLVs on PSII activity was determined by treatment of the indicated a, b-unsaturated aldehydes or ketones (each 25 nmol cm^{-3}) for 90 min to Arabidopsis plants, and then PSII activity was measured (lower panel). The chemical structures of the RSLVs are shown above the graphs. Dotted and solid circles indicate the a, b-unsaturated carbonyl bond moieties and vinyl group, respectively. Data are means ± SE (n=3 in upper panel, n=5 in lower panel). Values followed by the same letter are not significantly different according to Tukey-Kramer ($P < 0.05$).

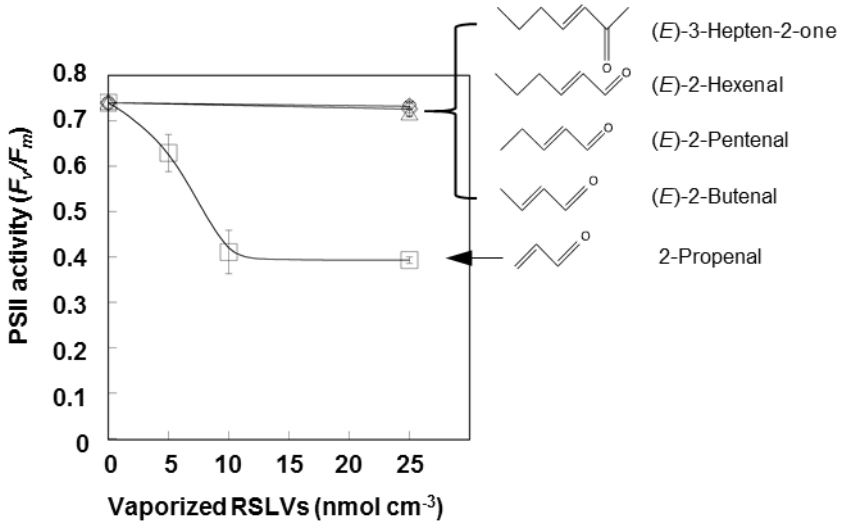

Figure 2-5. Effect of RSLVs on PSII activity

To determine toxicity of the RSLVs, Arabidopsis plants were exposed to various concentrations of 2-propenal (open square), (2*E*)-butenal (open diamond), (2*E*)-pentenal (open circle), (2*E*)-hexenal (open triangle), or (3*E*)-hepten-2-one. After 90 min, residual PSII activity (F_v/F_m) was measured. Data are means ± SE (n = 3).

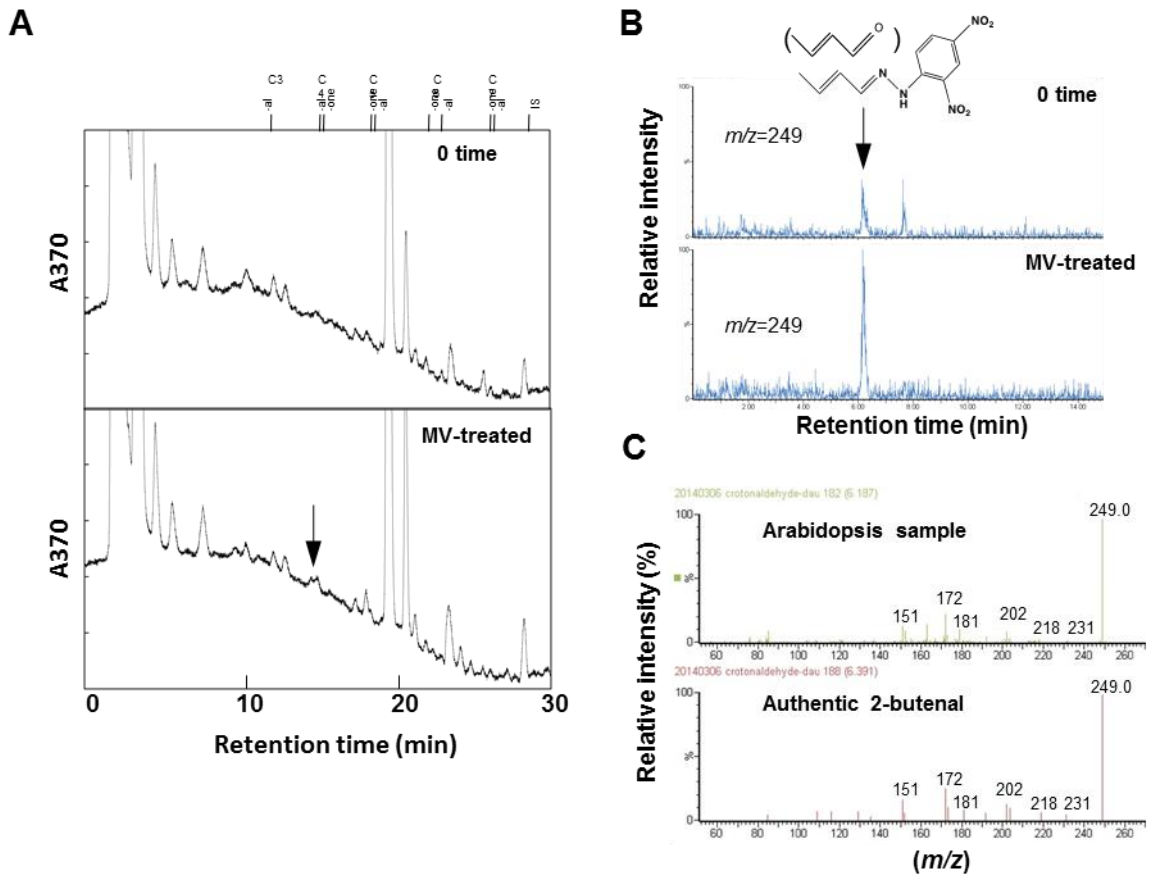

Figure 2-6. Determination of (2E)-butenal as endogeneous RSLV produced under oxidative stress.

Arabidopsis leaflets were treated with 10 µM MV in the presence of light (80 µmol m^{-2} s^{-1}) for an hour. **A** Typical chromatogram of HPLC analysis of DNP-carbonyls of MV-untreated (top) and MV-treated Arabidopsis (bottom). Arrow indicates peak of DNP-(2*E)*-butenal. The retention times of authentic DNP-RSLVs and the internal standard (IS) are shown above the chromatogram. **B** Typical chromatogram (selected reaction monitoring) of 2-butenal-DNP by LC-MS/MS analysis. Other RSLVs did not increase significantly after MV treatment. **C** Full-scan spectra of fragment ions of endogenous (top) and authentic 2-butenal (bottom).

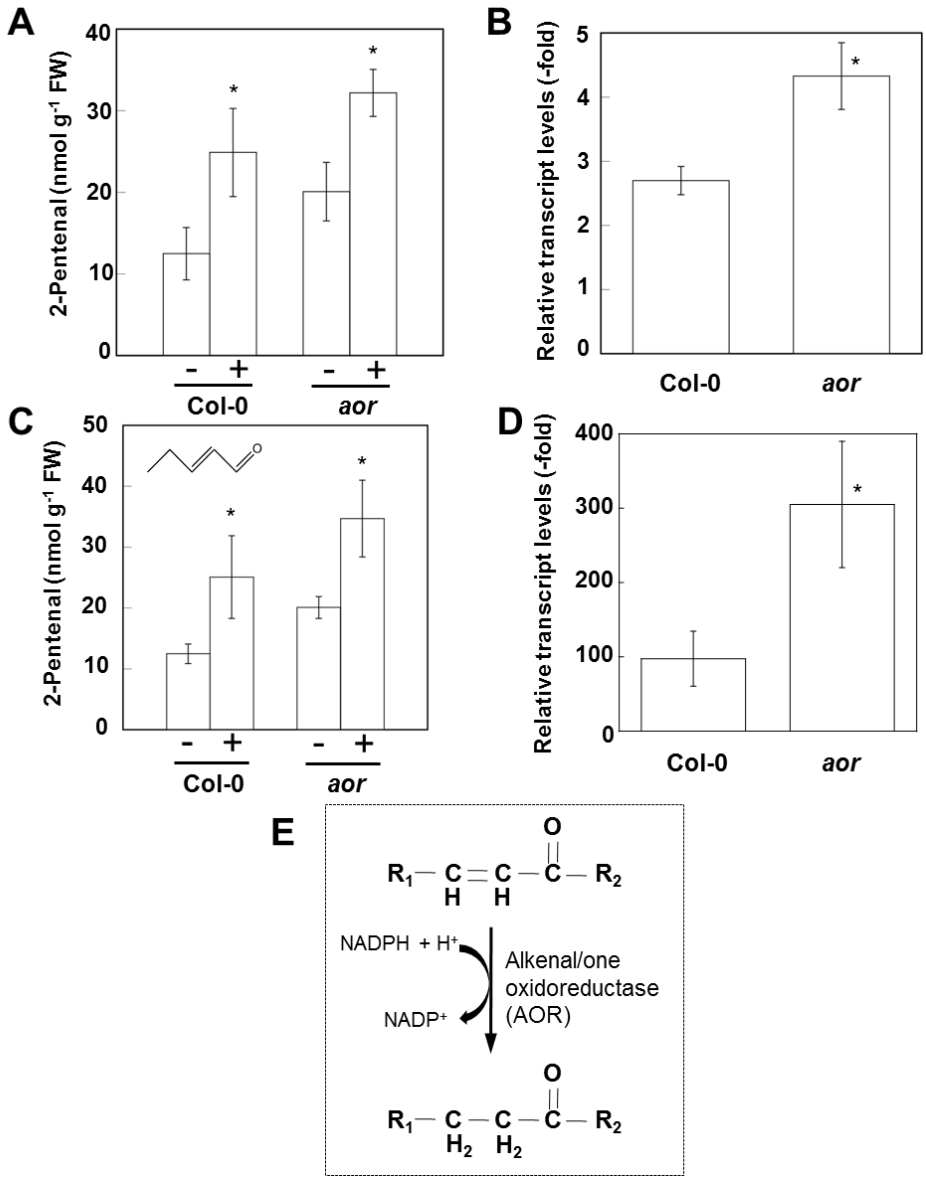

Figure 2-7. Estimation of (2*E*)-butenal contents and HSFA2 expression in MV-treated (A, B) or UVB-treated (C, D) Arabidopsis. A and **C** (2*E*)-butenal contents at 0 time (-) and after stress treatment **(+).** Data are means ± SD (*n* = 4). Values followed by the same letter are not significantly different according to Tukey-Kramer (P <0.05). **B** and **D** Expression of HSFA2 was enhanced in *aor* mutant under oxidative stress. HSFA2 mRNA expression in Col-0 and *aor* was determined by qRT-PCR. Relative transcript levels were normalized to *ACTIN2* mRNA. The expression level of the 0 time sample was set to1. Data are means ± SE (*n* = 3). (*, P < 0.05 vs Col-0, Student's *t*-test). Absolute HSFA2 transcripts were approximately 5 copies ng^{-1} RNA in both Col-0 and *aor*. **E** alkenal/one oxidoreductase (AOR) catalyzes saturation of α, β-unsaturated carbonyl bonds by using NADPH (shown in dotted box). RSLVs are food substrates for AOR (Yamauchi, 2011).

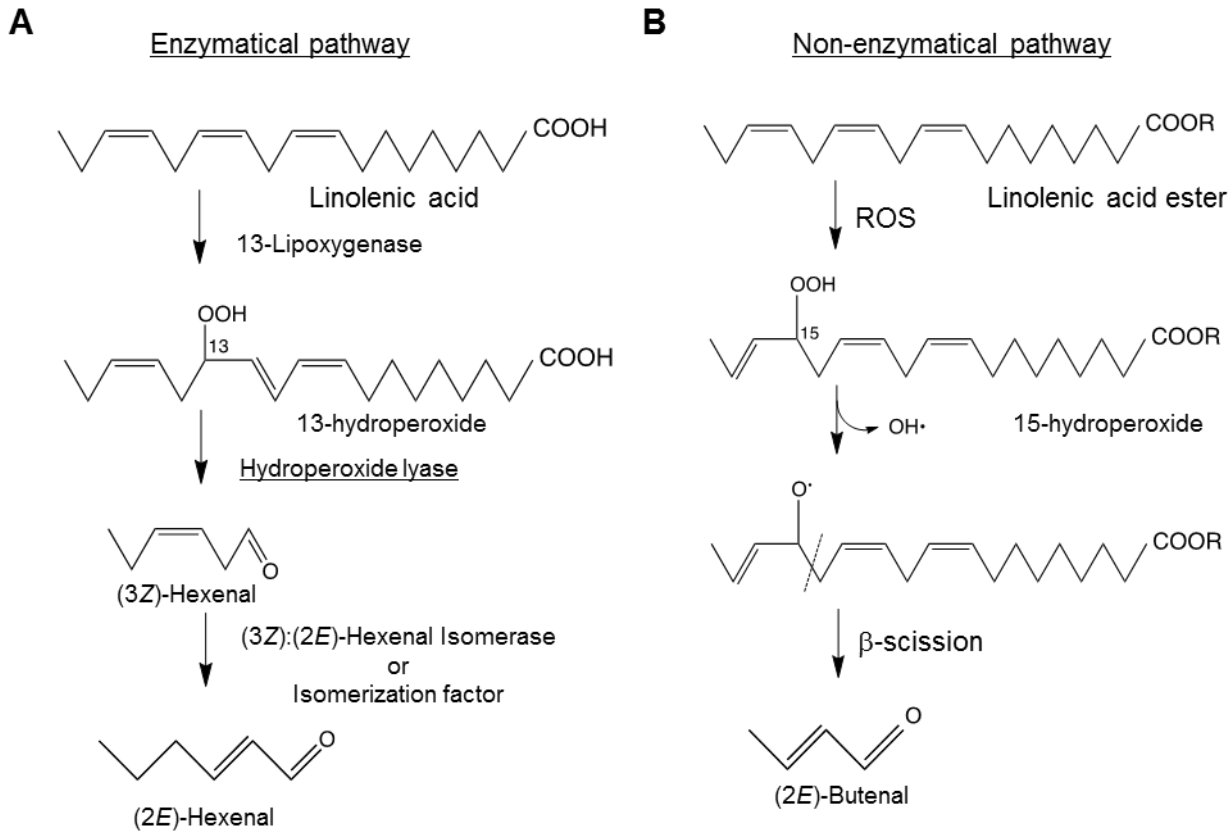

Figure 2-8. Pathways for production of RSLVs in plants. (2*E*)-Hexenal and (2*E*)-butenal are mainly produced via enzymatical A and non-enzymatical (**B**, referred from Frankel 1980) pathways, respectively.

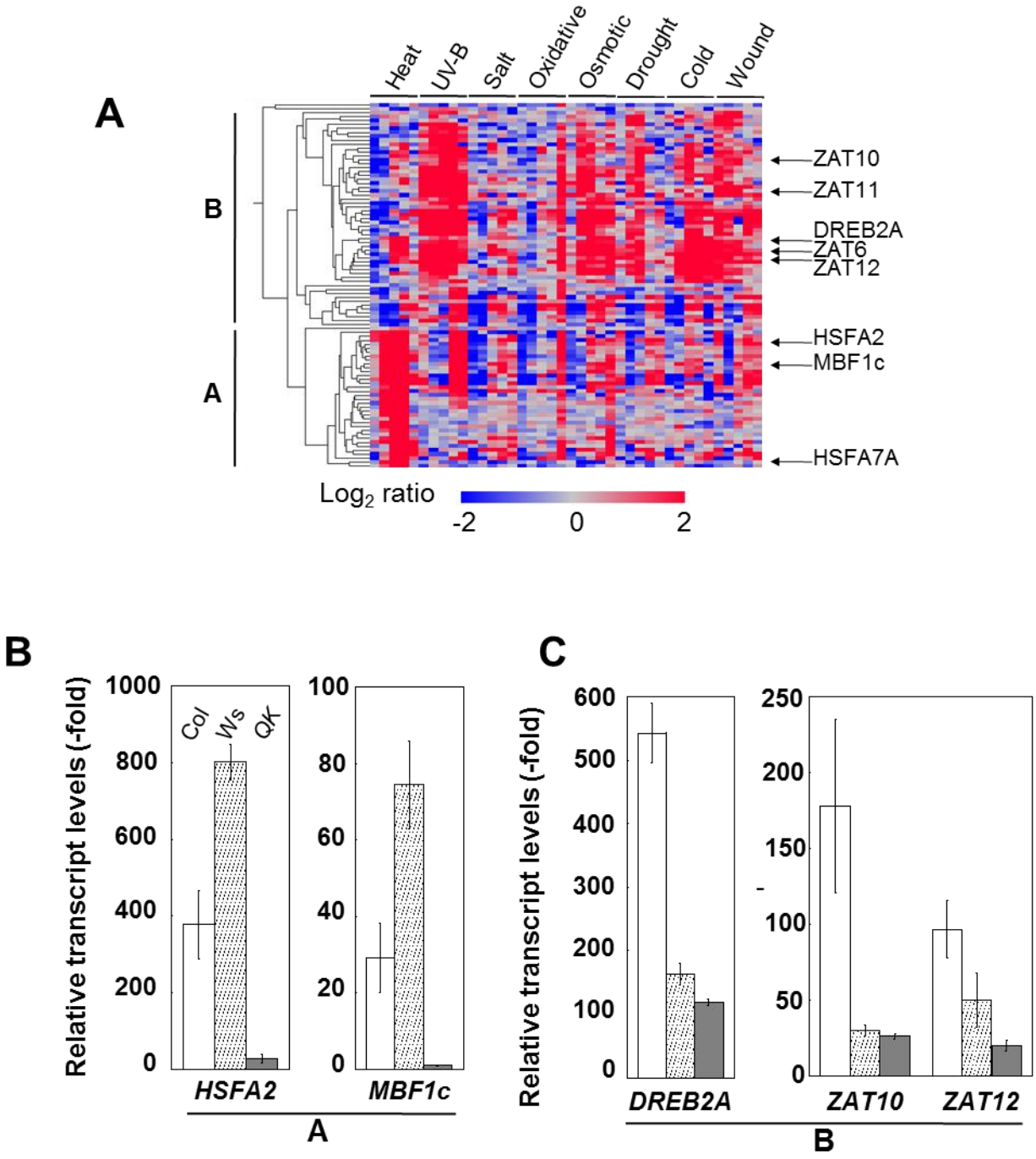

Figure 2-9. RSLV-induced genes are divided into HSFA1-dependent or –independent groups. A Heat map constructed with the 100 most highly upregulated genes by (2*E*)-hexenal treatment. **B** and **C** Expression of transcription factors in (2*E*)-hexenal treated Col-0 (Col, open column), Ws-0 (Ws, shaded column) and HSFA1quardruple knockout mutant (*QK*, gray column). A and B mean groups in panel a.

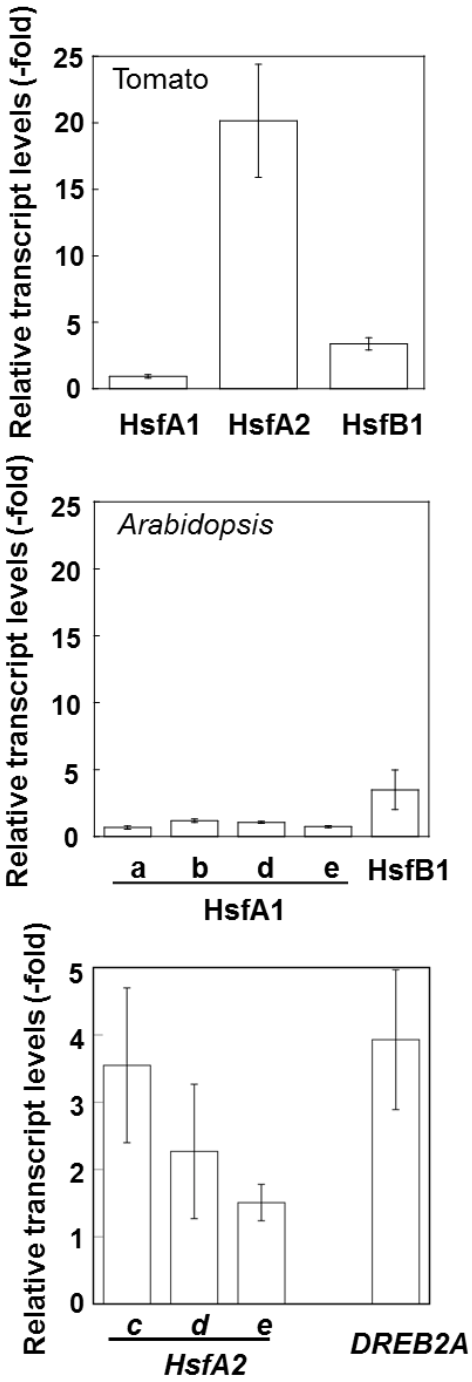

Figure 2-10. Expression of related transctiption factors by (2*E*)-hexenal treatment in *Arabidopsis* (a), tomato (b) and rice(c).

Tested plants were treated with (2*E*)-hexenal (10 nmol cm^{-3}) for 30 min, and then expression of each transcription factor gene was determined by qRT-PCR. Relative transcript levels were normalized ACTIN mRNA. For each gene examined, the expression level in the MeCN-treated control sample was set to 1. Data are means ± SD (n = 3).

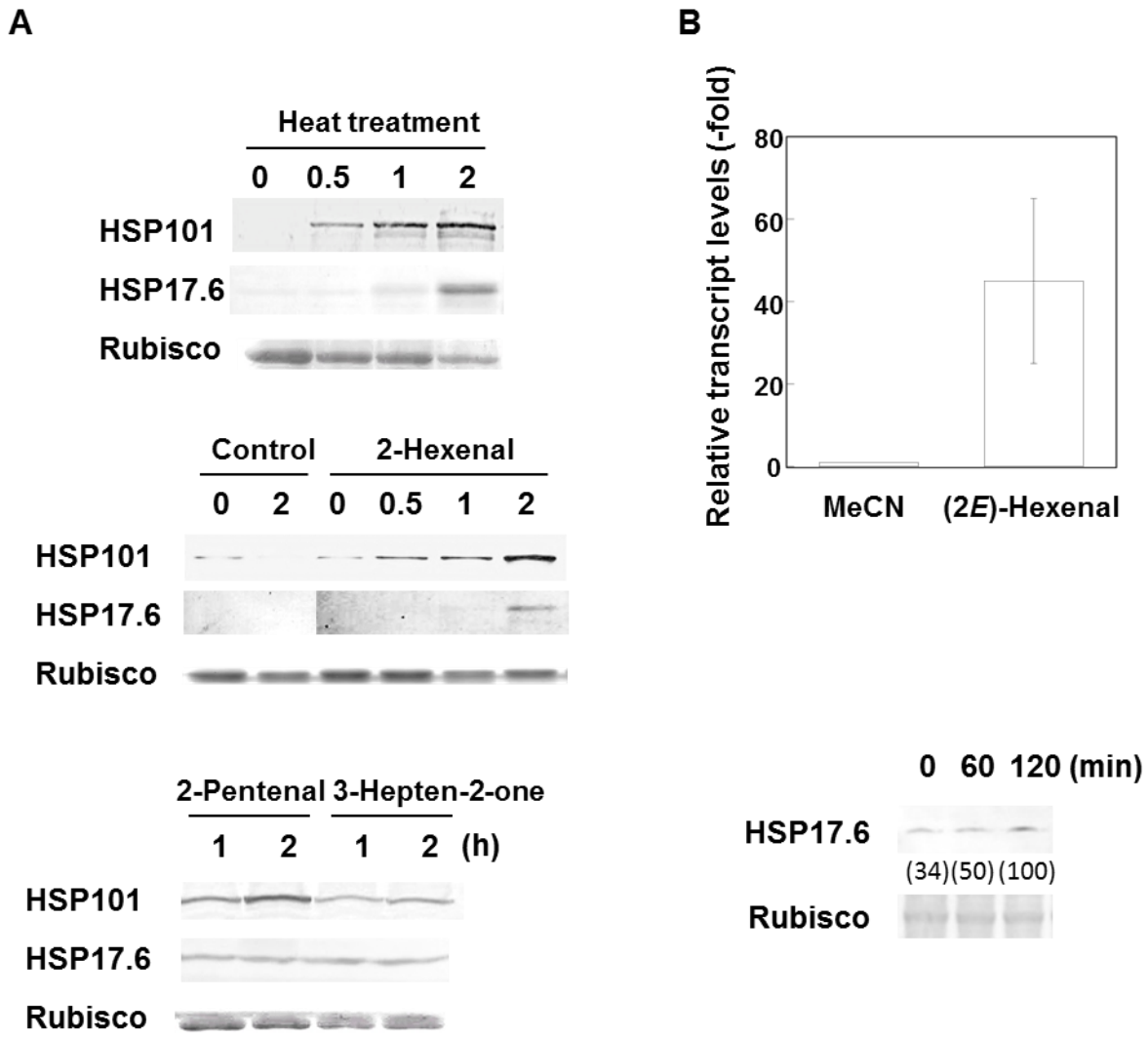

Figure 2-11. Biological effects of RSLV treatment of Arabidopsis.

A After the indicated RSLV treatment or heat treatment at 38ºC, expression of HSP101 and HSP17.6 proteins was detected by western blot analysis. Rubisco was stained using Coomassie Brilliant Blue R-250 as a loading control. **B** Induction of HSFA2 expression and HSP17.6 production by RSLVs in Arabidopsis seedlings. Quantified value of each band by densitometric analysis is indicated in parenthesis. Maximal intensity is set to 100. Rubisco was stained using Coomassie Brilliant Blue R-250 as a loading control.

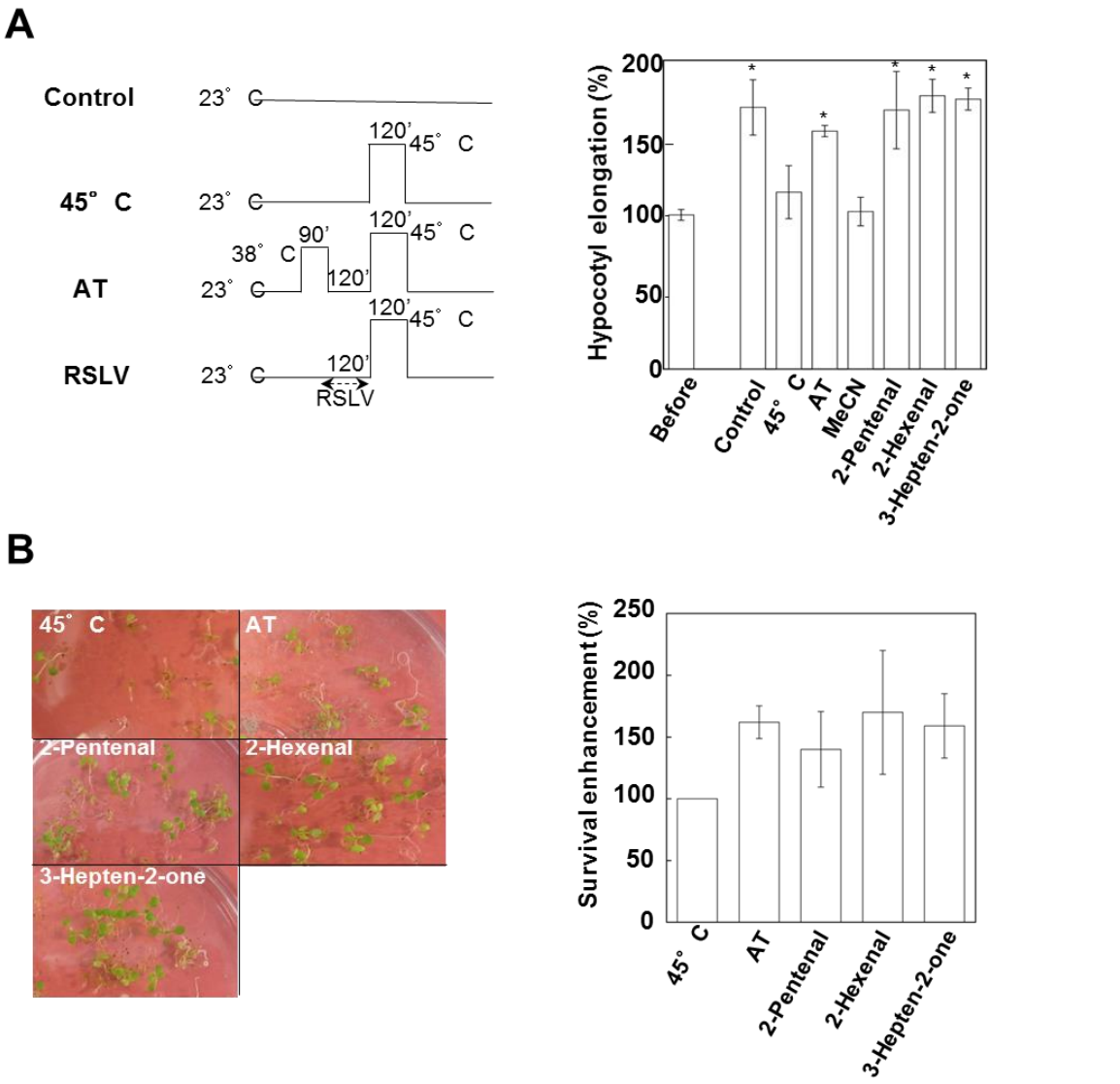

Figure 2-12. Biological effects of RSLV treatment of Arabidopsis

A The 2.5-day-old dark-grown seedlings (Before) were pretreated at 38ºC for 90 min to acquire thermotolerance (AT) or 10 mM indicated RSLVs or solvent control (MeCN) for 2 h and then heat-stressed at 45ºC for 2 h. Seedling were returned to 23ºC in the dark and length was measured after 2.5 days. Length of seedlings before treatment was set to 100%, and elongation of each treatment was calculated. Schemes of treatment are shown above the graph. **B** Survival enhancement was calculated by survival rate determined on 3 days after treatments with same scheme as shown in panel A. Left; Representative photographs of Arabidopsis plants on 7 days after heat stress treatments. Right; Survival enhancement by RSLV treatment calculated from 3 independent assays. Survival rate of 45ºC sample was set to 100%. Values followed by the same letter are not significantly different according to Tukey-Kramer (n = 4 or 5; $P < 0.05$).

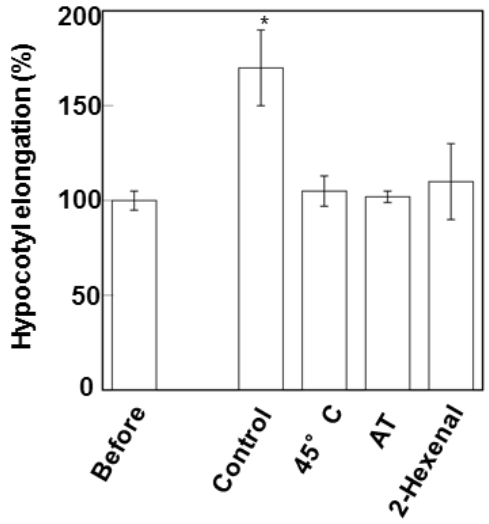

Figure 2-13. Effect of (2*E*)-hexenal treatment on thermotolerance of *QK*.

The 5-day-old dark-grown *QK* seedlings (Before) were pretreated at 38°C for 90 min to acquire thermotolerance (AT) or 10 µM (2*E*)-hexenal for 2 h and then heat-stressed at 45°C for 2 h. Seedling were returned to 23°C in the dark and length was measured after 2.5 days. Length of seedlings before treatment was set to 100%, and elongation of each treatment was calculated (n = 4 or 5; *, $P < 0.05$ *vs.* before treatment seedlings; Student's t-test). Schemes of treatment are shown in Fig. 2-12B.

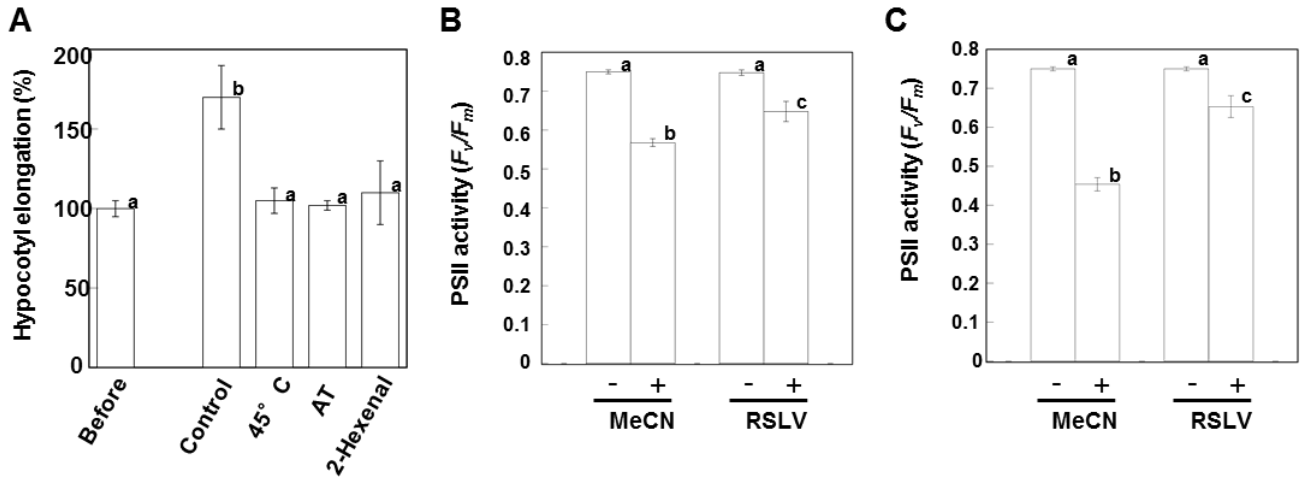

Figure 2-14. Effect of RSLV treatment on thermotolerance.

A The 5-day-old dark-grown *QK* seedlings (Before) were pretreated at 38°C for 90 min to acquire thermotolerance (AT) or 10 µM (2*E*)-hexenal for 2 h and then heat-stressed at 45°C for 2 h. Seedling were returned to 23°C in the dark and length was measured after 3 days. Length of seedlings before treatment was set to 100%, and elongation of each treatment was calculated. Schemes of treatment are shown in Fig. 2-12B. **B** and **C**, Effect of RSLVs on protection of PSII from heat **B** or UV-B treatment **C**. Two-week-old *Arabidopsis* (Col-0) were pretreated with 10 nmol cm^{-3} RGLV for an hour, and then treated with heat (45°C for 2h) or UV-B (1 mW cm^{-2} for 30 min). Data are means ± SE (n = 4 or 5). Values followed by the same letter are not significantly different according to Tukey-Kramer ($P < 0.05$).

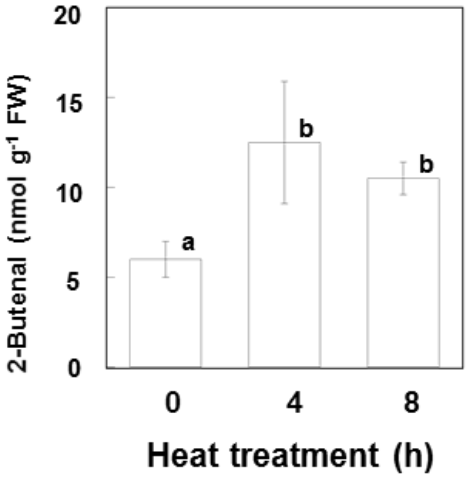

Figure 2-15. 2-Butenal contents in *Arabidopsis plants* under heat stress.

Data are means ± SE (n = 3). Values followed by the same letter are not significantly different according to Tukey-Kramer ($P < 0.05$).

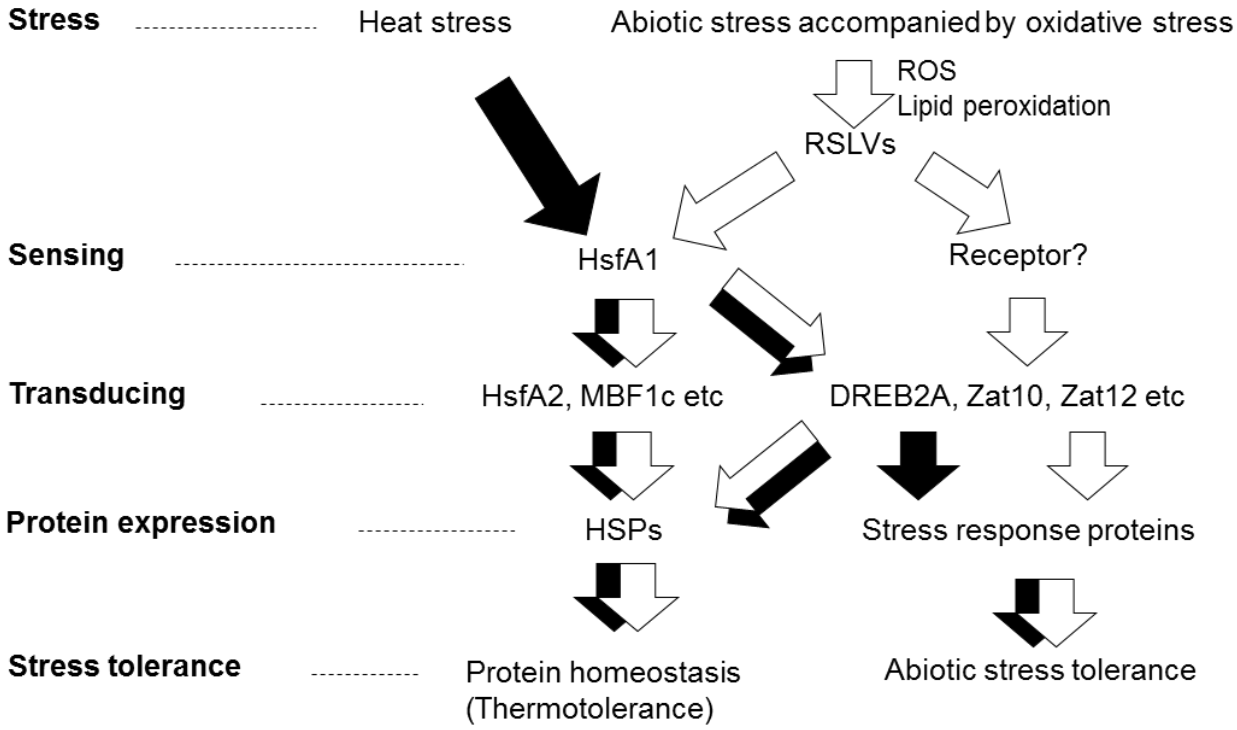

Figure 2-16. Hypothesized RSLVs-related signaling pathway in abiotic stress accompanied by oxidative stress. RSLV stimulates both HSFA1-dependent and independent pathways (white arrows). RSLVs are possibly involved in the upstream of signaling pathway triggered by abiotic stresses accompanied by oxidative stress. Proteotoxic stress such as heat and ROS are accepted by HSFA1s to drive HSFA1-denpendent pathway (black arrows).

Chapter III

Identification of hexenal isomerase and manipulation of RSLVs production

(2*E*)-Hexenal, a member of green leaf volatiles (GLVs), is a widely distributed RSLV in planta. GLVs act as semiochemicals involved in plant-insect and plant-plant interactions. In addition, as described in Chapter II, (2*E*)-hexenal induced expression of abiotic stress-responsive transcription factors such as *HSF*s, *DREB2A* and *ZAT*s, and Arabidopsis plants treated with (2*E*)-hexenal exhibited enhanced heat stress tolerance. Biosynthesis of (2*E*)-hexenal from (3*Z*)-hexenal had been proposed in plants although the enzyme hexenal isomerase (HI) responsible for the conversion remained unidentified. In this chapter, purification and characterization of HI was undertaken. HI from paprika fruits was purified to homogeneity. Based on internal amino acid sequences determined by Edman analysis, cDNA encoding the full length of the isomerase was cloned. The protein was heterologously expressed in *Escherichia coli* and the purified enzyme was characterized. Tomato, which produces (3*Z*)-hexenal as a major volatile with a negligible amount of (2*E*)-hexenal, was transformed by the HI gene to alter its RSLVs profile. (3*Z*)-Hexenal decreased to a negligible level and (2*E*)-hexenal significantly increased in some transgenic lines, thus verifying the *in vivo* involvement of HI in biological conversion of (3Z)-hexenal to (2E)-hexeanal in transgenic tomato.

Materials and methods

Materials

Paprika (*Capsicum annuum L.*), Arabidopsis (*Arabidopsis thaliana*, Columbia-0), tomato (*Solanum lycopersicum*, cv. Micro-Tom), potato (*Solanum tuberosum* cv. Sassy), tobacco (*Nicotianabenthamiana*), alfalfa (*Medicago sativa*), and rice (*Oryza sativa*, cv Nipponbare) were sown on Jiffy-7 peat pellets (Sakata Seed Co., Yokohama, Japan) and kept at 4°C for 3 days in the dark. The plants were then transferred to the conditions of a 14-h-light (80 µmol photons m^{-2} s^{-1})/10-h-dark cycle at 23°C (for Arabidopsis, tomato, potato, tobacco, alfalfa, and rice) or 28°C (for paprika). (3*Z*)-hexenal was obtained from Bedoukian Research Inc. (Danbury, CT, USA). Other chemicals of research grade were purchased from Wako Pure Chemicals (Osaka, Japan) or NacalaiTesque (Kyoto, Japan).

Crude extract preparation and HI activity measurement

Plant material was homogenized with two volumes of 50 mM Hepes-KOH, pH 7.0. After centrifugation at 10,000g for 10 min, the supernatant was used as a crude extract. Crude extract was incubated in 1 ml of reaction mixture containing 10 mM (3Z)-hexenal in 50 mM Hepes-NaOH, pH 7.0 for 30 min at 25°C. The reaction was stopped and derivatized with 2,4-dinitrophenylhydrazine (DNPH) by addition of 25 µl of 20 mM DNPH in acetonitrile and 20 µl of HCOOH. After 10 min, dinitrophenylhydrazine (DNP) derivatives were extracted with 300 µl of n-hexane. After centrifugation, 150 µl of the hexane layer was recovered and dried in vacuo. The residue was dissolved in 50 µl acetonitrile and filtered through a Cosmonice Filter (NacalaiTesque, Kyoto, Japan), after which 10 µl aliquots were subjected to HPLC as described previously (Yamauchi et al. 2012).

Purification of CaHI

Paprika pericarp (640 g) was homogenized with 1.5 volumes of 50 mM Hepes-NaOH, pH 7.0. Debris was removed by filtration through two layers of gauze, and the filtrate was centrifuged at 10,000g for 10 min. Ammonium sulfate was added to the supernatant to 30% saturation, followed by centrifugation at 10,000g for 10 min. After lipids floating on the supernatant were removed by filtration through two layers of gauze, the supernatant was applied to a phenyl-sepharose column (40 ml, GE Healthcare UK, Ltd., England) equilibrated with 30% saturated ammonium sulfate in 50 mM potassium phosphate buffer (K-PB), pH 7.0. Proteins were eluted with 50 mM K-PB, pH 7.0, and the eluent was applied directly to a hydroxyapatite (NacalaiTesque) column equilibrated with 50 mM K-PB, pH 7.0. After washing with 250 mM K-PB, pH 7.0, HI activity was eluted with 250 mM K-phosphate, pH 7.0, containing 1% Triton X-100. Nine volumes of 20 mM Hepes-NaOH, pH 7.0, containing 0.1% α-D-dodecyl maltoside (DDM) was added to the fraction containing activity, which was then applied to a Mono Q mini column (total volume 2 ml, GE Healthcare). After washing with 20 mM Hepes-NaOH, pH 7.0, containing 0.1% DDM, proteins were eluted with 20 mM Hepes-NaOH, pH 7.0, containing 0.1% DDM and 1 M NaCl. The enzyme solution was concentrated with Centricon-30 (Merck Millipore, Germany) and diluted by nine volumes of 20 mM Hepes-NaOH, pH 7.0, containing 0.1% DDM. The proteins were subjected to anion exchange column chromatography (Mono Q,

GE Healthcare) and fractionated with a gradient of 0–0.3 M NaCl. Protein concentration was determined by the method of Bradford.

Internal amino acid sequencing of purified enzyme

Purified paprika enzyme (2 μg) dissolved in 1 ml of 70% formic acid was chemically fragmented with BrCN at room temperature overnight in the dark. Fragmented peptides recovered by centrifugal evaporation were dissolved in SDS-sample buffer and then separated by Tricine-SDS-PAGE. After electrophoresis, the separated peptides were blotted onto a PVDF membrane with a semidry blotting system (Atto Corp., Tokyo, Japan), and peptides were visualized by CBB R-250 staining. Stained bands were excised from the membrane, and their amino acid sequences were determined with a protein sequencer (Procise Model 492, Applied Biosystems, Foster City, CA, USA).

Cloning of CaHI and quantitative RT-PCR (qRT-PCR)

Similarity search of internal amino acid sequences was performed against a Solanaceae-specific database (Solcyc.solgenomics.net). To confirm that Ca08g14620, including both internal amino acid sequences, was identical to CaHI, the open reading frame (ORF) of Ca08g14620 was cloned as follows. Total RNA was isolated from paprika fruits with an RNeasy Plant Mini Kit (QIAGEN), and cDNA was then synthesized with ReverTra Ace® qPCR RT Master Mix with gDNA Remover (TOYOBO, Osaka, Japan). To obtain the ORF of Ca08g14620, PCR was performed with ExTaq DNA polymerase (Takara Bio Inc., Shiga, Japan) using primers CaHIBamHI 5′ (5′-GGATCCATGGATTTAATATTGGCATCG-3′) and CaHISalI 3′ (5′-GTCGACTTAAGGTGGGGCAATGACTGC-3′). The PCR product was cloned into the TA Cloning vector pMD19 and then sequenced with a BigDye○R Terminator v3.1 Cycle Sequencing Kit for confirmation. Quantitative real-time RT-PCR (qRT-PCR) was performed with Thunderbird SYBR Green qPCR Mix (TOYOBO) and a Light Cycler Nano System (Roche, Basel, Switzerland) using template cDNA prepared as described above. Primers used for qRT-PCR are shown in Table S1. For analysis of relative transcript levels, internal standard mRNA was used in all qRT-PCR experiments, and the expression levels of genes of interest were normalized to that of the internal standard by subtraction of the cycle threshold (CT) value of the internal standard from the CT value of the gene of interest.

Heterogeneous expression of HIs

The ORF of HI was amplified by PCR using the primers shown in Table S2 and then subcloned into pMD19 (Takara Bio). After confirming DNA sequence, each HI gene was inserted into pColdProS2 vector (Takara Bio), and *Escherichia coli* was transformed with the resultant expression plasmid. *E. coli* harboring the expression vector was grown with shaking at 37ºC in LB broth with 50 μg/ml ampicillin to midlogarithmic phase. Expression was induced by addition of IPTG to 0.1 mM, and cultures were grown for a further 16 h at 15°C and harvested by centrifugation. The pellet was washed twice with phosphate-buffered saline (PBS) and then resuspended with 400 μl of PBS. After disruption of the cells by sonication, recombinant HI protein in the soluble fraction was purified on a His SpinTrap column (GE healthcare) according to the manufacturer's instructions. Electrophoretically homogenous HI fraction was used for enzyme assays. Point mutation of recombinant CaHI (rCaHI) was performed with a PrimeSTAR Mutagenesis Basal Kit (Takara Bio) using primers shown in Table S3.

3-Hexyn-1-al synthesis and measurement of its inhibitory activity against HI

3-Hexyn-1-al was chemically synthesized from 3-hexyn-1-ol (Tokyo Chemical Industry, Tokyo, Japan) by oxidation with the Dess–Martin periodinane (Wako Pure Chemical) reagent according to the method of Wavrin and Viala (2002). To confirm its purity, synthesized 3-hexyn-1-al was derivatized with DNPH as described above and then analyzed by LC–MS and NMR. Synthesized 3-hexyn-1-al was incubated with purified rCaHI for 4 h on ice, and free 3-hexyn-1-al was then removed by ultrafiltration using Vivaspin 500-30K (GE Healthcare). Residual HI activity was measured by standard assay as described above.

^{1}H-NMR analysis

All NMR experiments were performed on a JEOL JNM-AL300 (300 MHz at ^{1}H, JEOL Ltd., Tokyo, Japan), and chemical shifts were assigned relative to the solvent signal. Hexenal-DNP derivatives were dissolved in chloroform-d2, and the diameter of the tube was 5 mm.

Production of transgenic tomato overexpressing CaHI

A DNA fragment of CaHI amplified with primers (CaHINdeI 5′:

5′-CATATGGATTTAATATTGGCATCG-3′, CaHISalI 3′: 5′-GTCGACTTAAGGTGGGGCAATGACTGC-3′) was digested with NdeI and SalI and ligated into the pRI101-AN vector (Takara Bio Inc., Shiga, Japan) to construct a 35S promoter-driven expression plasmid. After *Agrobacterium tumefaciens* (strain C58C1Rifr) was transformed by pRI101-AN::35S::CaHI, cotyledons of tomato plants (cv Micro-Tom) were transformed by Agrobacterium-mediated transformation with kanamycin resistance as a selectable marker (Sun et al. 2006). For confirmation of insertion of CaHI and the neomycin phosphotransferase II gene in regenerated transgenic tomato plants, genome PCR was performed using the primers shown in Table 3-3. Candidates were further examined by qRT-PCR and volatile analysis to establish transgenic lines. Finally, transgenic lines showing stable seed production were used for analysis.

Volatile analysis

Harvested tomato materials were placed in a Falcon tube (15 ml) with three stainless steel beads (5 mm i.d.), and the tube was then sealed tightly with Parafilm. After samples were frozen in liquid N_2, the tissues were completely disrupted by vigorous vortexing. When volatiles in intact tissues were analyzed, 1 ml saturated $CaCl_2$ solution was added to inactivate enzymes. An SPME fiber (50/30 μm DVB/Carboxen/PDMS, Supelco, Bellefonte, PA, USA) was exposed to the headspace of the vial for 30 min (for leaf) or 60 min (for fruit) at 25°C. The fiber was inserted into the insertion port of a GC–MS (QP-5050, Shimadzu, Kyoto, Japan) equipped with a 0.25 μm × 30 m Stabiliwax column (Restek, Bellefonte, PA, USA). The column temperature was programmed as follows: 40°C for 1 min, increasing by 15°C min^{-1} to 180°C for 1 min. The carrier gas (He) was delivered at a flow rate of 1 ml min^{-1}. The glass insert was an SPME Sleeve (Supelco). Splitless injection with a sampling time of 1 min was used. The fiber was held in the injection port for 1 min to remove all compounds fully from the matrix. The temperatures of the injector and interface were 200°C and 230°C, respectively. The mass detector was operated in electron impact mode with ionization energy of 70 eV. To identify compounds, retention indices and MS profiles of corresponding authentic specimens were used.

Homology modeling

Three-dimensional structures of HI proteins were deduced by homology modeling using

SWISS-MODEL (Arnold et al. 2002; Bordoli et al. 2009; Biasini et al. 2014). The amino acid sequences of HIs were used to search for templates in the database. The templates were selected based on the Global Model Quality Estimation values and the QMEAN4 scores. Templates and the sequence identity between the HIs and their corresponding templates are shown in the figures. The protein structures were analyzed with Swiss PdbViewer (Guex et al. 1997).

Results

Purification of CaHI from red paprika

At the start of this study, plant materials for high HI activity were screened. First activity in red bell pepper (*Capsicum annuum L.*) fruits was assayed because bell pepper showed a large change in leaf aldehyde composition during ripening; (3*Z*)-hexenal was the predominant GLV in green bell pepper, whereas (2*E*)-hexenal became the predominant GLV during the change in fruit color from green to red (Luning et al. 1995). This phenomenon suggested that abundant HI activity occurs in ripening bell pepper. As expected, activity in red pepper fruits was detected, and another bell pepper variant, red paprika, showed the most abundant activity. No isomerase activities were detected in Arabidopsis leaves, tobacco leaves, or tomato fruits (Fig. 3-1). Accordingly, red paprika was used as a source for purification of HI. CaHI was purified from pericarp of red paprika fruits by successive column chromatography steps (Table 3-1). At the final step of purification, fractions containing activity matched elution peaks of proteins (Fig. 3-2A). SDS-PAGE analysis showed that each fraction contained a single protein of 35 kDa (Fig. 3-2B), suggesting that CaHI was purified to homogeneity. Native CaHI is a trimetric protein, given that the molecular mass of nondenatured isomerase was estimated by BN-PAGE to be 110 kDa (Fig. 3-2C). Isomerization of hexenal by purified CaHI is unidirectional, given that CaHI did not convert (2*E*)-hexenal to (3*Z*)-hexenal (Fig. 3-3). Kinetic parameters are shown in Table 3-2. CaHI showed high activity at acidic to neutral pH (Fig. 3-4).

Cloning of CaHI

To clone the cDNA encoding CaHI, the internal amino acid sequences were determined. After the purified protein was chemically cleaved by BrCN, polypeptide fragments were separated by Tricine-SDS-PAGE and blotted onto PVDF membrane (Fig. 3-5A). Among the blotted peptides, amino acid sequences of two major polypeptides could be determined (Fig. 3-5B). Homology

search of these sequences using a Solanaceae-specific database (Sol Genomics Network) indicated that the amino acid sequence of an unknown protein encoded by Ca08g14620 contained both sequences. To confirm that this unknown protein was identical to CaHI, the ORF of the unknown protein was cloned into pColdProS2 plasmid and then produced as a recombinant protein (Fig. 3-6A). The purified recombinant protein in soluble form showed high HI activity (Fig. 3-6B), indicating that Ca08g14620 encoded CaHI.

HI belongs to the cupin superfamily

BLAST search using the amino acid sequence of CaHI indicated that it is a member of the cupin superfamily. This superfamily is a large protein family containing diverse functional proteins such as storage proteins and various enzymes (Dunwell et al. 2004). A subfamily including CaHI is located near those of various seed storage protein families such as 11S globulin and vicilin (Fig. 3-7). CaHI and highly homologous proteins in Solanaceae species such as tomato and potato are included in a clade named Solanaceae HI, and another clade closely related to HI is named Solanaceae HI-like. Proteins belonging to clade HI and HI-like were produced as recombinant proteins and assayed their activity. Proteins belonging to clade HI showed activity, but those belonging to clade HI-like did not (Fig. 3-6C). To investigate the physiological role of HIs, their gene expression levels at different developmental stages were analyzed. Expression levels of HIs in paprika and potato showed developmental stage-specific expression, being extremely high in ripe fruits and sprouts, respectively (Fig. 3-8A and 8B). In contrast, expression levels of tomato HIs were consistently low (Fig. 3-8C), consistent with our inability to detect HI activity in tomato tissues (data not shown).

Determination of amino acid residues essential for enzymatic activity

To identify amino acid residues essential for the isomerization reaction, the action mode of bacterial β-hydroxydecanoylthiolester dehydrase (Leesong et al. 1996) was considered in which a His residue plays a critical role in the isomerization reaction. Among 357 amino acid residues, 38 differed among proteins belonging to Solanaceae HI and HI-like clades, and only His54 was conserved in all proteins in the HI clade but not in the HI-like clade, suggesting this His as a candidate catalytic amino acid in HIs. To test this hypothesis, point-mutated rCaHI (H54A) was produced. As expected, rCaHI (H54A) showed no activity (Fig. 3-9A), indicating that His54

plays a critical role in enzymatic reaction. By homology modeling to deduce other catalytic amino acids, K60 and Y128 were found to be candidates owing to their locations near H54 (Fig. 3-9B). Accordingly, rCaHI (K60A) and rCaHI (Y128A) were produced and found that these point mutations caused loss of isomerase activity (Fig. 3-9A). These results suggested that these three amino acid residues (named catalytic HKY) form a catalytic site in HI.

HIs are distributed among various plant species

Given that (2*E*)-hexenal has been detected in various plant species other than Solanaceae (Hatanaka et al. 1987), the presence of other types of HI was expected. To identify other HIs, proteins showing lower similarity but conserving the catalytic HKY were searched. As a result, candidates were formed in alfalfa, cucumber, and rice sequences (alignment is shown in Fig. 3-10). Recombinant HIs were produced and assayed their activity. All recombinant proteins having catalytic HKY showed HI activity (Fig. 3-11), confirming that HIs are widely distributed among various plant species. Phylogenetic tree analysis showed that these miscellaneous HIs form a branched clade from Solanaceae HI, and HI-like proteins having no HKY catalytic amino acids are present as in the case of Solanaceae HI (Fig. 3-7). HIs of monocotyledonous plants (OsHIs) are located far from those of dicotyledonous plants.

Catalysis mode of HI

To investigate the catalytic mechanism of HI, (3*Z*)-hexenal was incubated with rCaHI in the presence of D_2O as a solvent, and the enzymatic product was analyzed by ^{1}H-NMR to identify the positions and geometry of the C–C double bond in 2-hexenal. ^{1}H-NMR spectra of authentic (2*E*)-hexenal-DNP and enzymatic D-labeled 2-hexenal are shown in Fig. 3-12. The signals H-2 (6.35 ppm, *m*, 1H) and H-3 (6.27 ppm, *m*, 1H) were identified as the protons on the double bond, and the coupling constants between H-2 and H-3 (J=15.6 Hz) were determined to be E. By comparison of the authentic and enzymatic products, deuterium was introduced mainly at the C4 position (H-4) given that the integrated area of H-4 in enzymatically produced hexenal-DNP was half that in authentic 2-hexenal-DNP. These results indicate that rCaHI isomerized (3*Z*)-hexenal to (2*E*)-hexenal by abstraction of H^+ at the C2 position and subsequent H^+ donation at the C4 position in a keto–enol tautomerism reaction mode (a plausible catalytic mechanism is shown in Fig. 3-13A).

3-Hexyn-1-al acts as a suicidal substrate for HI

As suggested by studies of bacterial isomerases (Endo et al. 1970; Leesong 1996), an analogous compound having a C–C triple bond can behave as a suicidal substrate in an isomerization reaction by binding irreversibly to the catalytic His. Accordingly, 3-hexyn-1-al, a triple bond-containing analog of (3*Z*)-hexenal, was prepared and tested its inhibitory activity. As shown in Figure 3-13C, 3-hexyn-1-al inhibited rCaHI stoichiometrically. Ultracentrifugation after HI and 3-hexyn-1-al incubation did not restore activity, showing that inhibition by 3-hexyn-1-al was irreversible. This finding showed that plant HI shares a similar enzymatic property with bacterial isomerases that are irreversibly inhibited by suicidal substrates (a plausible inhibitory mechanism is shown in Fig. 3-13B).

Wounding treatment induced HI gene expression

(2*E*)-hexenal is assumed to play a protective role in wounding response because it shows antifungal activity (Croft et al. 1993; Kishimoto et al. 2006), leading to a hypothesis that HI genes are induced by wound treatment. To test this hypothesis, induction of HI gene expression in wounded paprika and tomato leaves was investigated. Expression of SlHI1, CaHI, and PINII genes, known as typical wound-inducible genes, was enhanced by wounding treatment (Fig. 3-14), suggesting that HIs may be regulated at the transcriptional level in response to wounding, leading to enhanced (2*E*)-hexenal production.

Overexpression of CaHI in transgenic tomatoes drastically changes the (3*Z*)-hexenal versus (2*E*)-hexenal proportion in planta

(3*Z*)-hexenal is known to be the most abundant volatile in tomato fruits and is thus recognized as a tomato-like flavor (Tandon et al. 2000). To assess the biological impact of HI on hexenal composition, transgenic tomato plants overexpressing CaHI was produced and their hexenal composition was assayed. In both leaves and fruits of wild-type tomatoes, (3*Z*)-hexenal was detected as the main hexenal, as reported by previous authors (Fig. 3-15), suggesting that the very low expression of inherited tomato HI genes does not contribute to production of (2*E*)-hexenal. In contrast, overexpression of CaHI in transgenic tomato plants resulted in a drastic change in (3*Z*)/(2*E*)-hexenal proportion in leaves (Fig. 3-15A), corresponding to the

much higher expression of CaHI introduced exogenously (Fig. 3-15A, inset). In fruits, the wild type contained (3*Z*)-hexenal as the main hexenal (85% ± 5.8%), but (2*E*)-hexenal occupied almost part of hexenals in transgenic plants (Fig. 3-15B). These results suggest that the CaHI transgene CaHI functions effectively and thus determines hexenal composition in planta.

Discussion

In this chapter, HIs responsible for (2*E*)-hexenal production was identified in various plant species and evidence was shown that plants produce (2*E*)-hexenal by enzymatic reaction. Expression analysis of HIs indicated that HI levels remained low except under several physiological conditions such as wounding and at specific developmental stages (Fig. 3-8), suggesting that the physiological roles of (2*E*)-hexenal are limited to certain conditions. Previous reports suggested that (2*E*)-hexenal as well as (3*Z*)-hexenal were wounding-responsive volatiles, given that they showed antibiotic and defense gene-inducing activities (Croft et al. 1993; Kishimoto et al., 2005, 2006). In response to wounding, the production of GLVs including both (3*Z*)- and (2*E*)-hexenals is an early event, a reflexive response that starts within a few minutes after wounding and leads to the presence of large amounts of detectable GLVs after 10 min (Fall et al. 1999). (3*Z*)- and (2*E*)-hexenal production is mediated by a series of enzymes including lipase, 13-LOX, HPL, and HI (Fig. 1-2), and these enzymes need no cofactors for their reactions. This biochemical property would facilitate the rapid hexenal burst after wounding. At the transcriptional level, expression of HIs was low except a specific developmental stage (Fig. 3-8) and was induced by wounding treatment over a period of hours (Fig. 3-14). Given that emission of (2*E*)-hexenal continues for hours after wounding (Fall et al. 1999), this transcriptional regulation of HIs in wounding response supports this long-term emission.

HIs showed characteristic expression at specific developmental stages. In the case of paprika, higher expression of CaHI was observed in ripe fruits (Fig. 3-8A). This expression might contribute to producing (2*E*)-hexenal as an antifungal volatile as in strawberry (Myung et al. 2006). In potato, higher expression of StHI1 and StHI2 was observed in sprouts (Fig. 3-8B). Because in transgenic potato, depletion of HPL to decrease GLV contents caused an increase in aphid performance (Vancanneyt 2001), higher expression of StHIs may promote the production of (2*E*)-hexenal as an insect repellent to protect sprouts from pests (De Moraes et al. 2001).

The isomerization mechanism of HI is likely to be the keto–enol tautomerism reaction mode (Fig. 3-13A), similar to that of the keto–enol tautomerism-mediated isomerization of the double bond of fatty acid derivatives, which has been well studied in bacterial fatty acid metabolism. β-Hydroxydecanoyl thioester dehydrase, which catalyzes the reaction of double bond isomerization on 10-carbon thioesters of acyl carrier protein in the biosynthesis of unsaturated fatty acids under anaerobic conditions (Bloch 1971). The catalytic mode of the dehydrase is the keto–enol tautomerism mediated by a catalytic His, and a specific suicidal substrate, 3-decynoyl-N-acetylcysteamine, inactivated the enzyme by irreversible binding to the catalytic His (Leesong et al. 1996). Also in HIs, a specific suicidal substrate, 3-hexyn-1-al, completely inhibited HI activities irreversibly (Fig. 3-13B), suggesting that the His residue plays a critical role in catalytic function, plausibly the immigration of H^+. The importance of two other catalytic amino acids (Lys and Tyr) was also shown by complete loss of HI activity of point-mutated HIs (Fig. 3-9), thus detailed property of the catalytic amino acids to be elucidated.

Identification of quantitative trait loci that affect the volatile emissions of tomato fruits has been studied, because tomato breeders wish to combine good flavor with high fruit firmness, long shelf life, and high disease resistance (Mathieu et al. 2009). However, conventional breeding for sensory quality has been severely limited (Alonso et al. 2009). For this reason, genetic manipulation is applied for improvement of tomato flavor. Changes in expression level of alcohol dehydrogenase (Speirs et al 1998), fatty acid desaturase (Wang et al. 2001), and linalool synthase (Lewinsohn et al. 2001) resulted in changes in composition of volatiles. Among tomato volatiles, (3*Z*)-hexenal is the main flavor volatile determining tomato flavor, thus that (3*Z*)-hexenal is assigned as tomato-like flavor (Tandon et al. 2000). As shown in this study (Fig. 3-15), both leaves and fruits of transgenic tomatoes overexpressing CaHI contained (2*E*)-hexenal as the main green odor but not (3*Z*)-hexenal. Alonso et al. (2009) found that (2*E*)-hexenal is one of the major contributors determining differences among conventional and hybrid tomato types, suggesting that gene manipulation of HI is a candidate approach with high potential in molecular breeding for tomato flavor.

In conclusion, HIs were identified in various plant species, and the identification of HIs allows the completion of the scheme of GLV biosynthesis in plants. HIs share a small number of catalytic amino acids, and catalytic His is plausibly responsible for the keto–enol tautomerism involved in isomerization of (3*Z*)-hexenal to (2*E*)-hexenal. Higher expression of the gene

encoding HI in transgenic tomatoes led to enhanced (2*E*)-hexenal production, suggesting that HI plays a key role in the production of (2*E*)-hexenal in planta.

Table 3-1. Summary of purification of CaHI from red paprika

	Total protein (mg)	Total activity (nmol/min)	Specific activity (nmol/min mg)	Purification (fold)	Yield (%)
Crude extract[a]	16,800	647,000	38.3	1.0	100
Phenyl-sepharose	866	130,000	150	3.92	20.1
Hydroxyapatite	153	98,700	646	16.9	15.3
Mono Q5/5	0.80[b]	10,000	12,600	328	1.56
Mono Q1.6/5	0.012[b]	3,840	320,000	8,350	0.59

[a]Prepared from 640 g of red paprika pericarp.

[b]Protein concentration was estimated using E_{A280} (0.1% protein) = 1.

Table 3-2. Kinetic parameters of purified CaHI and recombinant HIs

	k_{cat} (s^{-1})	K_m(mM)	k_{cat}/K_m ($s^{-1}mM^{-1}$)
CaHI	760	0.73	1040
rCaHI	521 ± 13.0	1.78 ± 0.06	293 ± 2.60
rSlHI1	264 ± 18.1	0.20 ± 0.04	1349 ± 126
rStHI1	27.7 ± 13.9	0.33 ± 0.03	83.7 ± 1.08
rStHI2	159 ± 13.9	0.72 ± 0.10	224 ± 13.7
rMsHI	308 ± 13.9	0.32 ± 0.04	990 ± 79.1
rCsHI	951 ± 66.2	0.56 ± 0.08	1749 ± 172
rOsHI	43.5 ± 2.23	1.23 ± 0.12	35.8 ± 1.61

HI, (3*Z*):(2*E*)-hexenal isomerase.

Table 3-3. Primers used for point-muted recombinant CaHI.

Mutated codons are underlined.

	Forward primer	Reverse primer
CaHI H54A	TTTACCTGCCTATGCTGATTCCTCAAA	AGCATAGGCAGGTAAAGCAAATCCACG
CaHI D57A	TATGCTGCTTCCTCAAAAATTGCTTAT	TGAGGAAGCAGCATAGTGAGGTAAAGC
CaHI K60A	TCCTCAGCCATTGCTTATGTTATTGAA	AGCAATGGCTGAGGAATCAGCATAGTG
CaHI K60R	TCCTCAAGAATTGCTTATGTTATTGAA	AGCAATTCTTGAGGAATCAGCATAGTG
CaHI S100A	AGCAACGGCATGGTGGTACAATGGAGG	CACCATGCCGTTGCTCCTATTGGAACT
CaHI S118A	GGAGAAGCTGGTGAATACACACCTGGT	TTCACCAGCTTCTCCCAAAAAAATTAT
CaHI Y128A	TTTTGCGCATTCTTTTTAACTGGAGCT	AAAGAATGCGCAAAATTCACCAGGTGT
CaHI Y128F	TTTTGCTTTTTCTTTTTAACTGGAGCT	AAAGAAAAAGCAAAATTCACCAGGTGT
CaHI K304A	TCTGTGGCAACATCGTCAAAGCAAATA	CGATGTTGCCACAGAGAAGAATTCAAT
CaHI K342A	TTTACCGCGTCCTTCAAGTCCAAGATT	GAAGGACGCGGTAAAATCTGGAGTCAT

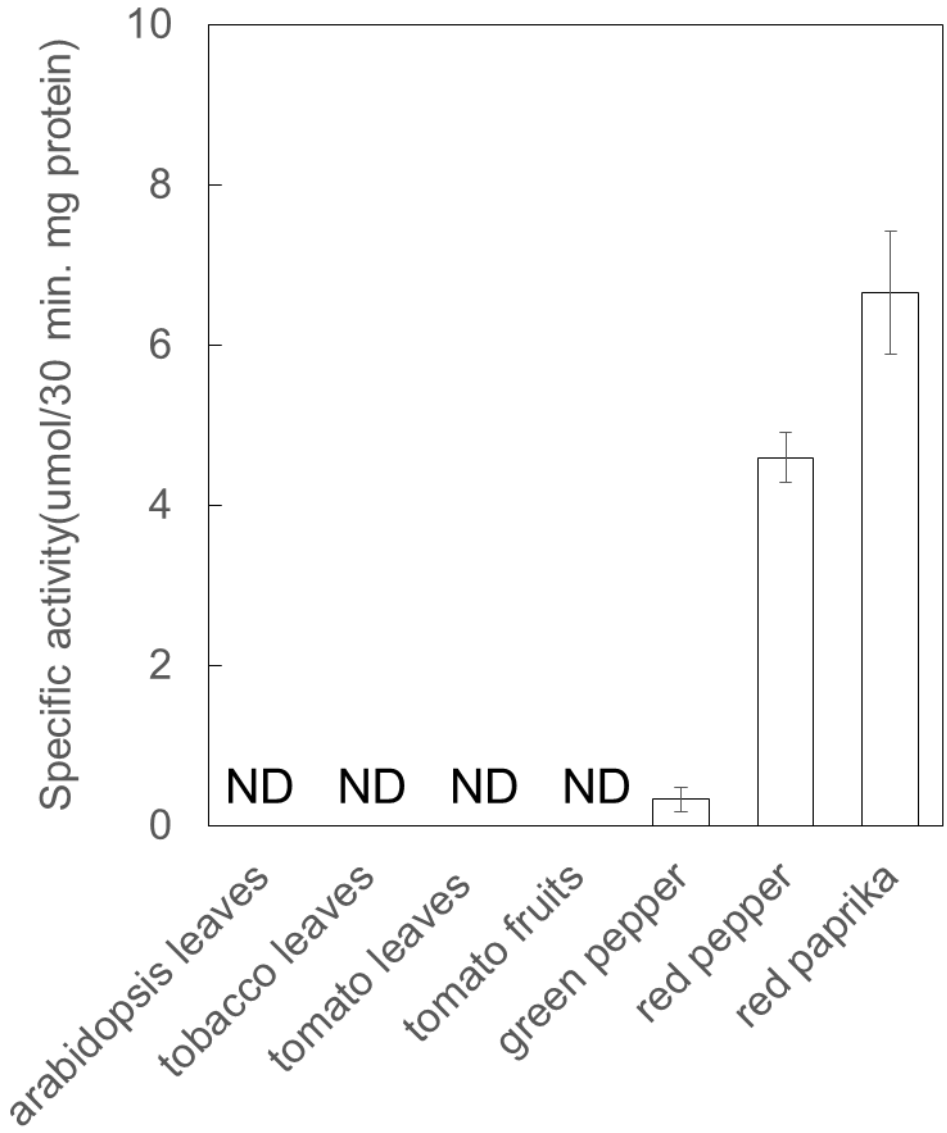

Figure 3-1. Screening of plant materials.

HI activity in crude extract prepared from each plant material was determined by standard assay. Data are means ± SE (n=3). ND, not detected.

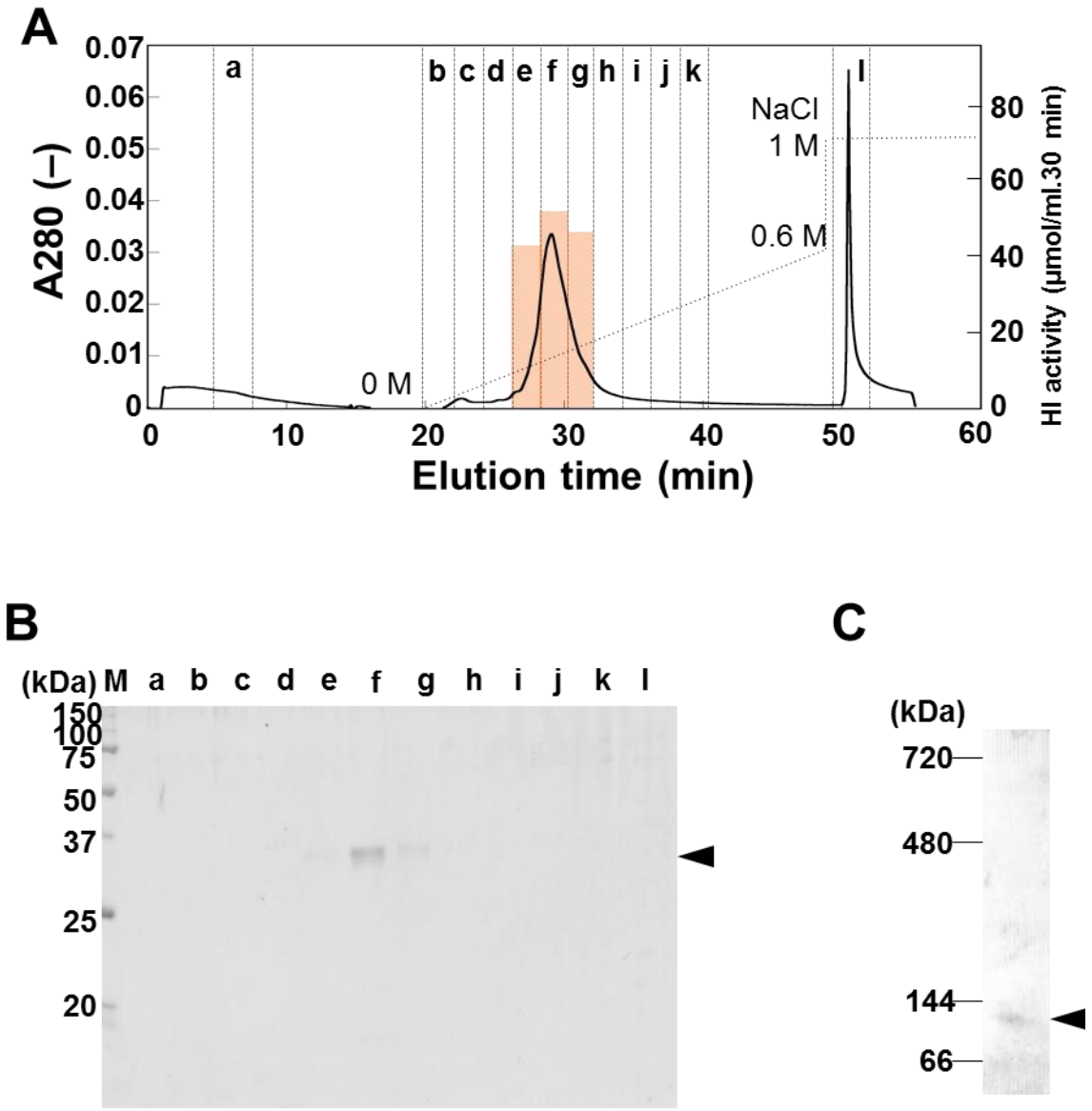

Figure 3-2. Purification of CaHI from paprika pericarp.

A Elution profile of CaHI in the final step of purification. HI activity in fractions containing proteins was measured by standard assay. Activity is shown by gray bar. **B** Protein profile in each fraction (alphabets in small letter are same as panel A; M, molecular marker) was analyzed by SDS-PAGE. **C** Molecular mass of native HI was determined by BN-PAGE. Arrowheads indicate bands of purified CaHI.

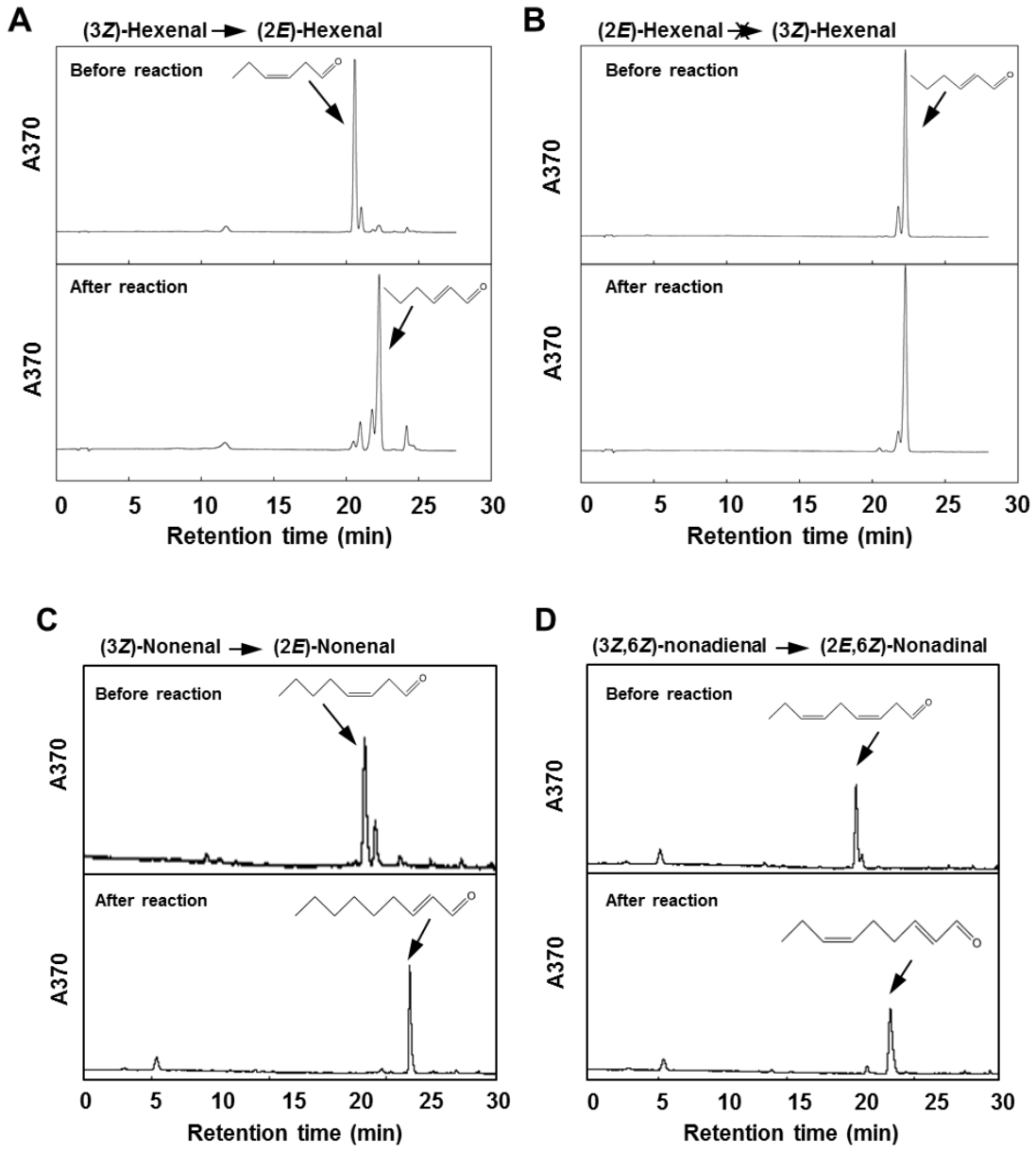

Figure 3-3. Detection of HI activity by HPLC.

Typical chromatograms of DNP-derivatized samples prepared from reaction mixtures before and after reaction are shown. Arrows indicate peaks of which retention time were identical to those of authentic compound-DNPs, respectively. Substrates are (3*Z*)-hexenal **A**, (2*E*)-hexenal **B**, (2*E*)-nonenal **C**, and (3*Z*, 6*Z*)-nonadienal **D**. (2*E*)-Hexenal was not isomerized **B**.

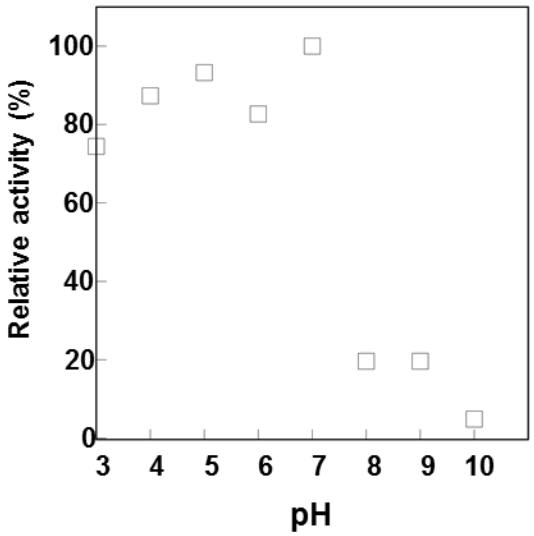

Figure 3-4. pH dependence of activities of native CaHI.

Enzyme activity was determined by standard assay in 50 mM Na-acetate buffer (pH 3.0-7.0) or 50 mM Tris-HCl buffer (pH 8.0-10.0). Data of native CaHI and rCaHI are from single assay and triplicate assays (means ±SE), respectively. Maximum activity was set to 100%.

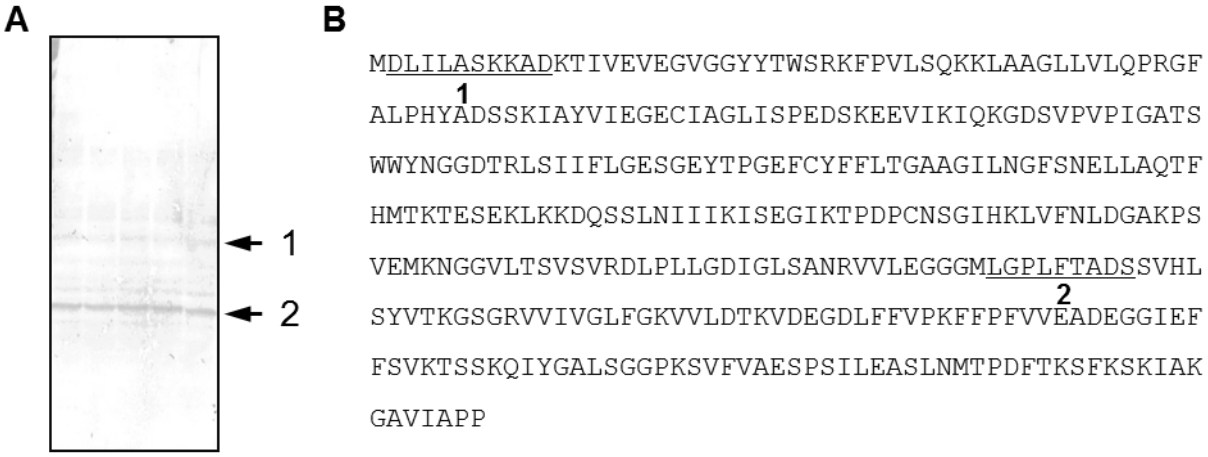

Figure 3-5. Determination of internal amino acid sequence of CaHI.

A Purified CaHI was cleaved by BrCN and then the resultant peptide fragments were separated with Tricine-SDS-PAGE. Peptides blotted onto PVDF membrane were stained by CBB R-250. Arrows indicate peptides of which sequences could be determined. **B** Determined internal amino acid sequences are underlined on the whole amino acid sequence of CaHI.

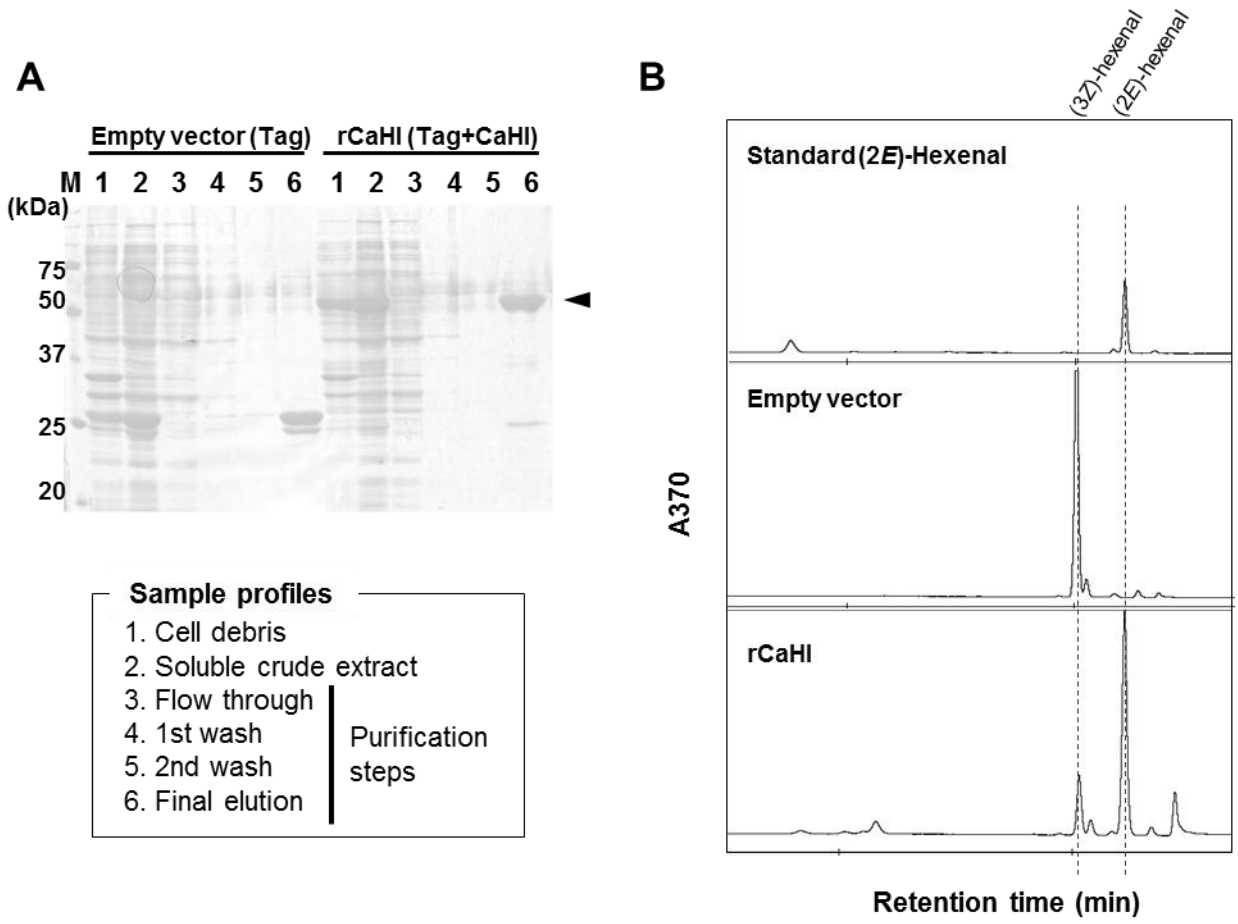

Figure 3-6. Production of recombinant HI by heterogeneous expression in *E. coli*

A Purification of recombinant CaHI (rCaHI). Proteins in each fraction were electrophoresed by SDS-PAGE. Purified rCaHI is indicated by an arrowhead (60 kD = 35 kD(CaHI) + 25kD (Tag)).

B Activity of the purified rCaHI was confirmed by the production of (2*E*)-hexenal.

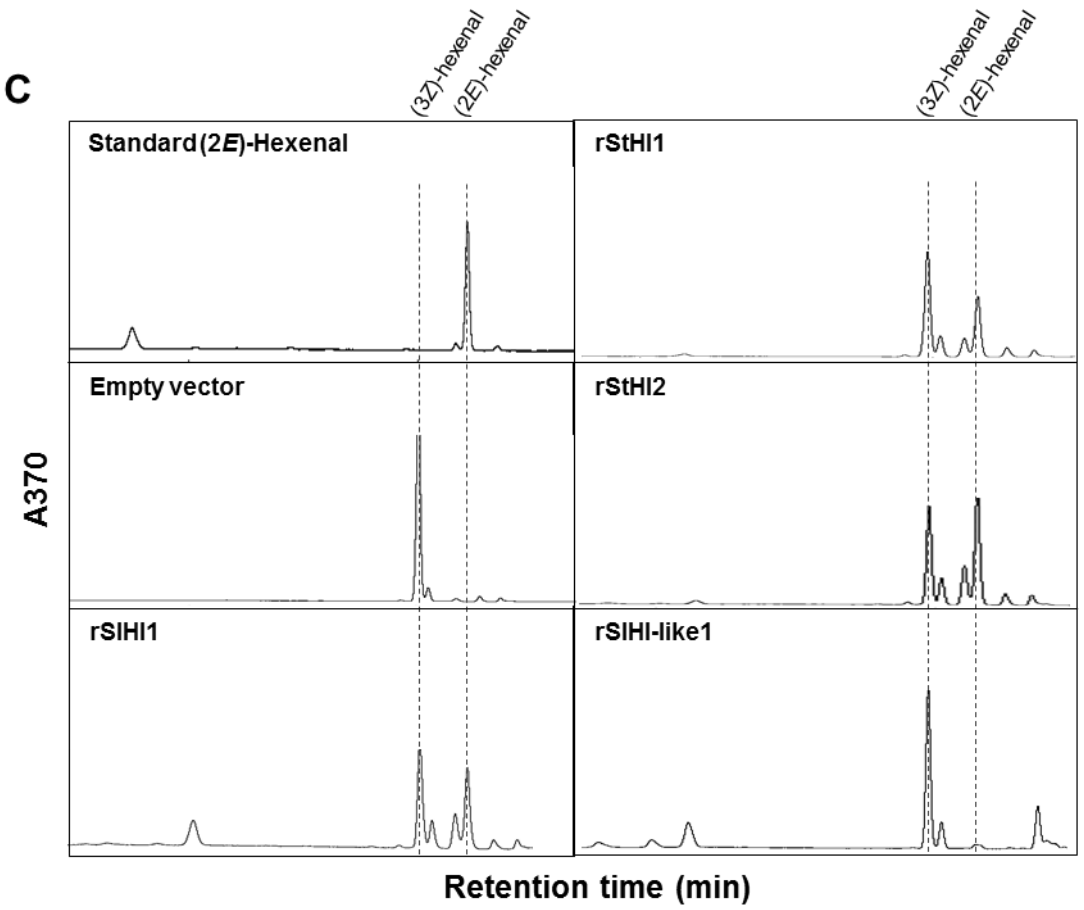

Figure 3-6(Continued). C By same strategy, activities of recombinant HIs from tomato (rSlHI1) and potato (rStHI1 and 2) were confirmed, on the contrary, recombinant HI-like protein from tomato (rSlHI-like1) did not show activity.

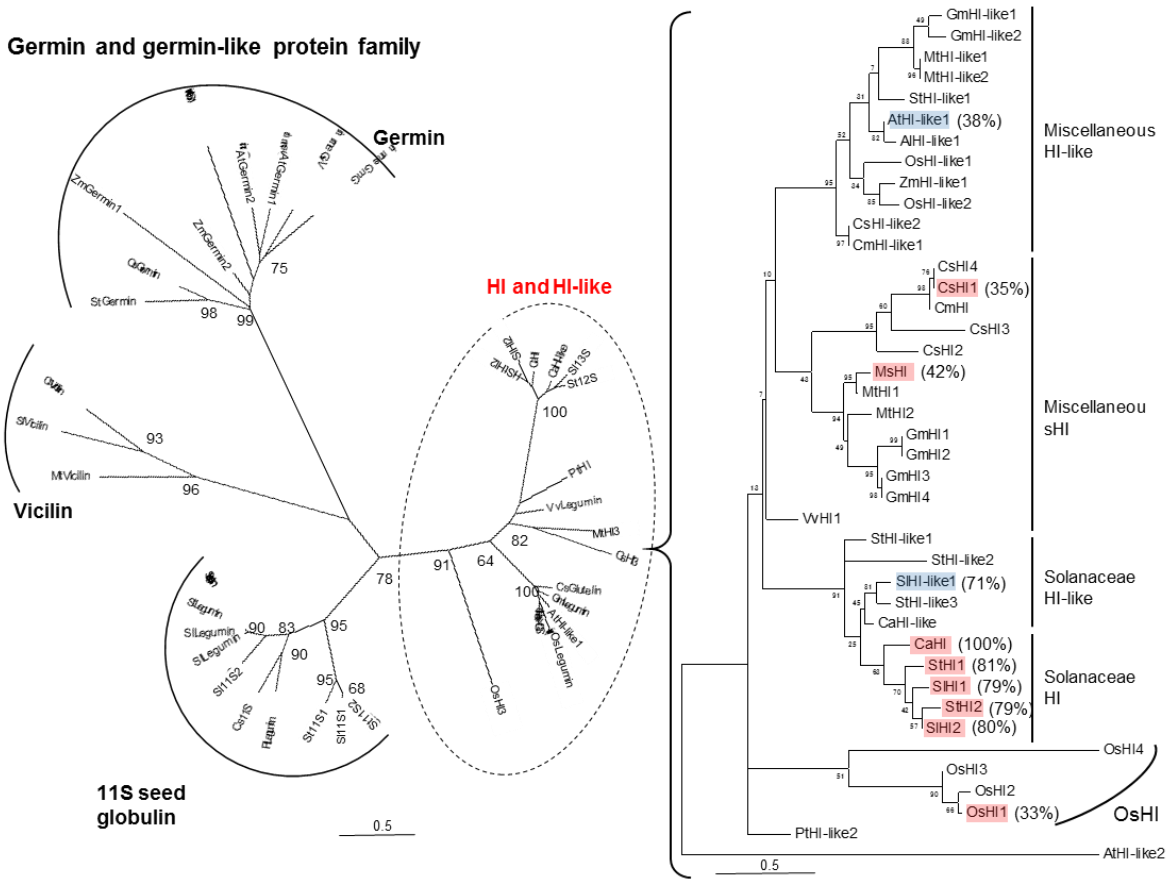

Figure 3-7. Phylogenic tree of HIs.

Proteins having catalytic HKY and homologous proteins but not having catalytic HKY are named as HI and HI-like, respectively. *Left*, HI and HI-like clades (shown by a dotted circle) belong to germin and germin-like protein family in the cupin superfamily. *Right*, Enlarged view of HI and HI-like clades. Recombinant proteins showing HI activity or no activity are marked with “o” or “-“, respectively. Numbers in parentheses indicate identity against CaHI. Values at the nodes indicate percentage of bootstrap support (of 1,000 bootstrap replicates).

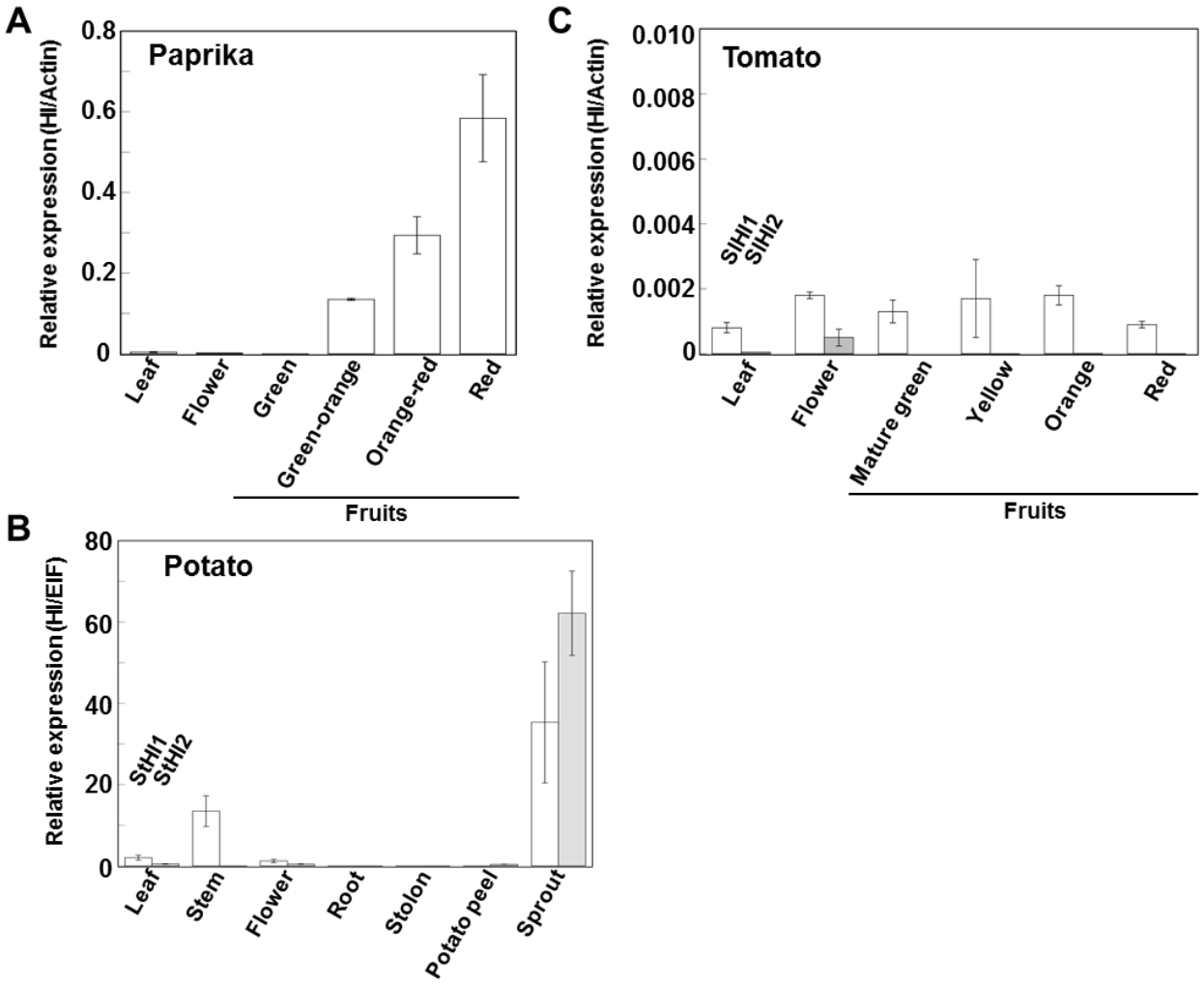

Figure 3-8. HI gene expression analysis of different tissues.

Paprika **A**, potato **B**, and Tomato **C**. Data are means ± SE (n = 3). Internal standard genes were elongation factor 1 for potato (*StEF1*), and actins for paprika (*CaACT*) and tomato (*SlACT*).

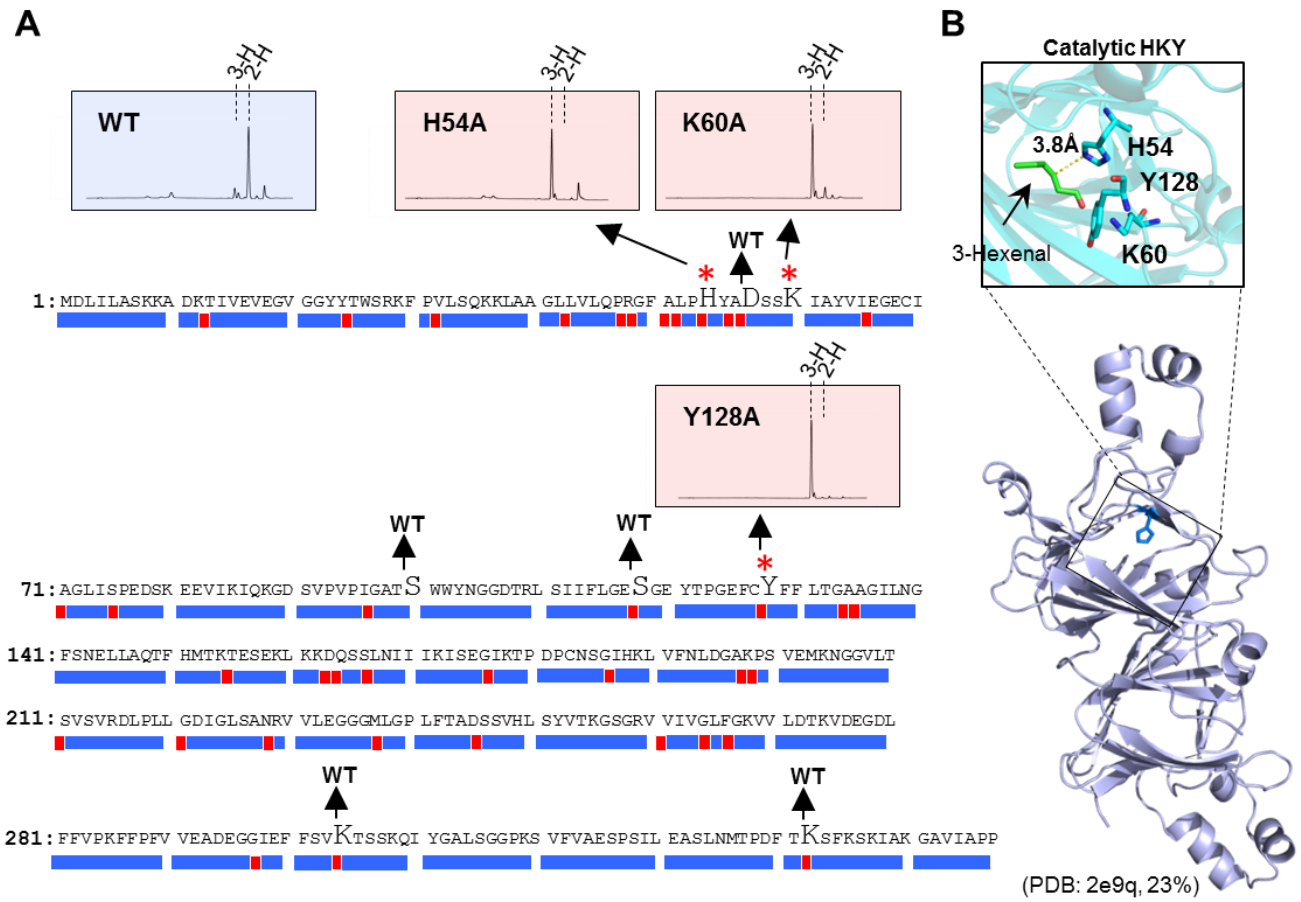

Figure 3-9. Determination of catalytic amino acids of HI.

A Effect of point mutation on HI activity. Amino acids written by large size indicate point-muted amino acids, and chromatograms of the point-muted proteins completely losing activity are shown. Asterisks suggest essential amino acids to show the HI activity, and point-mutated amino acids with no effect on the HI activity are indicated by "WT". Black boxes under amino acid sequence of CaHI indicate amino acids conserved in all proteins belonging to HI clade but not in HI-like clade. Gray boxes show amino acids not conserved in HI clade, or conserved both HI and HI-like clades. 3-H and 2-H in chromatograms indicate (3*Z*)- and (2*E*)-hexenal-DNPs, respectively. **B** Homology modeling of CaHI to deduce catalytic amino acids. Catalytic amino acids locate in the same pocket and near substrate (3*Z*)-hexenal. PDB ID of template protein, identity between CaHI and template protein, and QMEAN score are 2e9q, 23%, and 0.62, respectively.

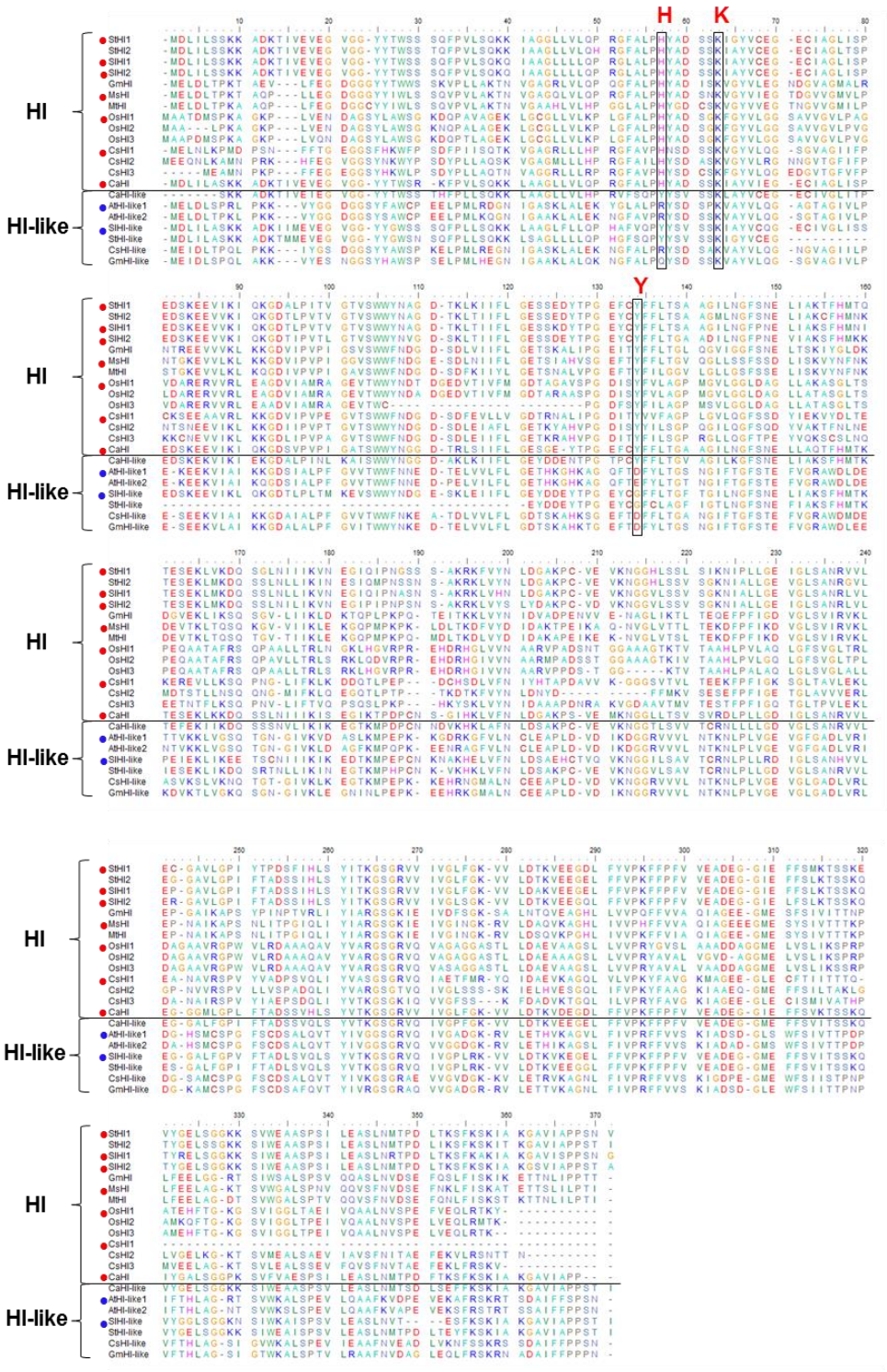

Figure 3-10. Alignment of HI and HI-like proteins. Positions of catalytic HKY are boxed. Red and blue dots indicate that their recombinant proteins showed activities and not, respectively.

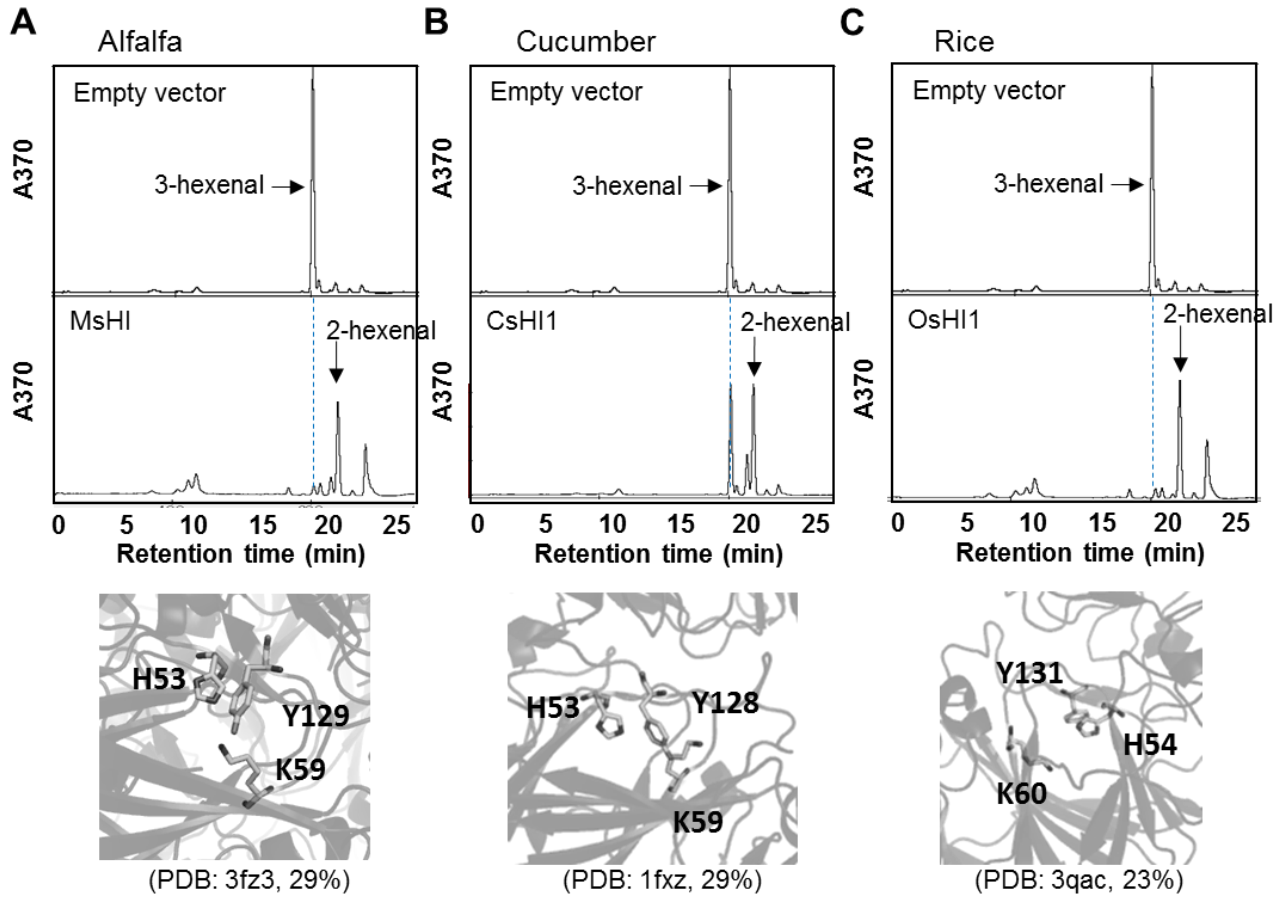

Figure 3-11. HI homologs of alfalfa **A**, cucumber **B**, and rice **C** showed HI activity. Catalytic pocket of each HI by homology modeling is shown in lower panel. Catalytic HKY locate in the same pocket. PDB ID of template protein and homology between CaHI and template protein are shown in parentheses.

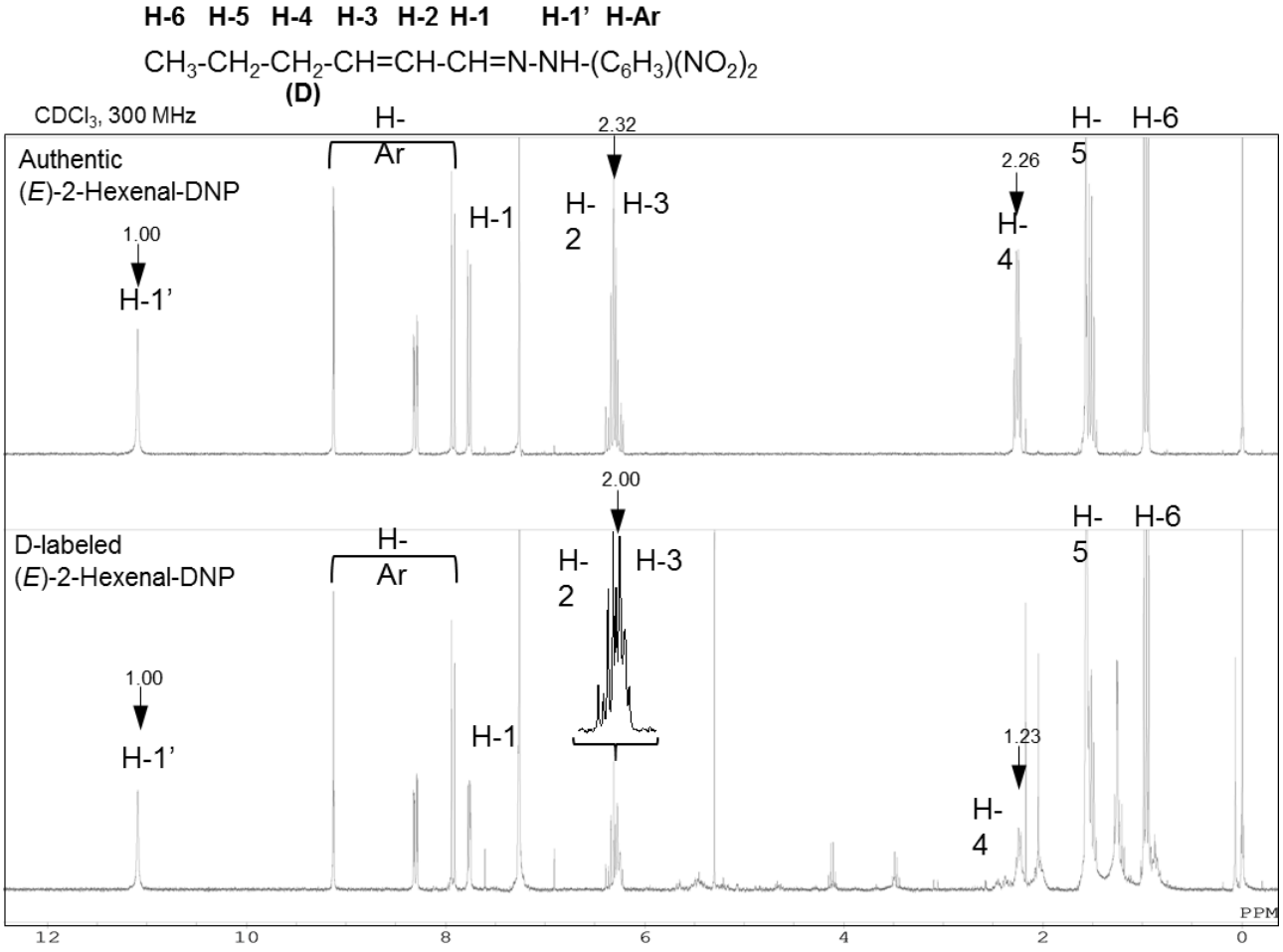

Figure 3-12.^{1}H-NMR spectra of authentic (*upper*) and D-labeled (*lower*) (2*E*)-hexenal-DNPs.

The letters indicate the position of protons and their corresponding signals. Arrows indicate integrated values of signals (that of H-1' is set to 1).

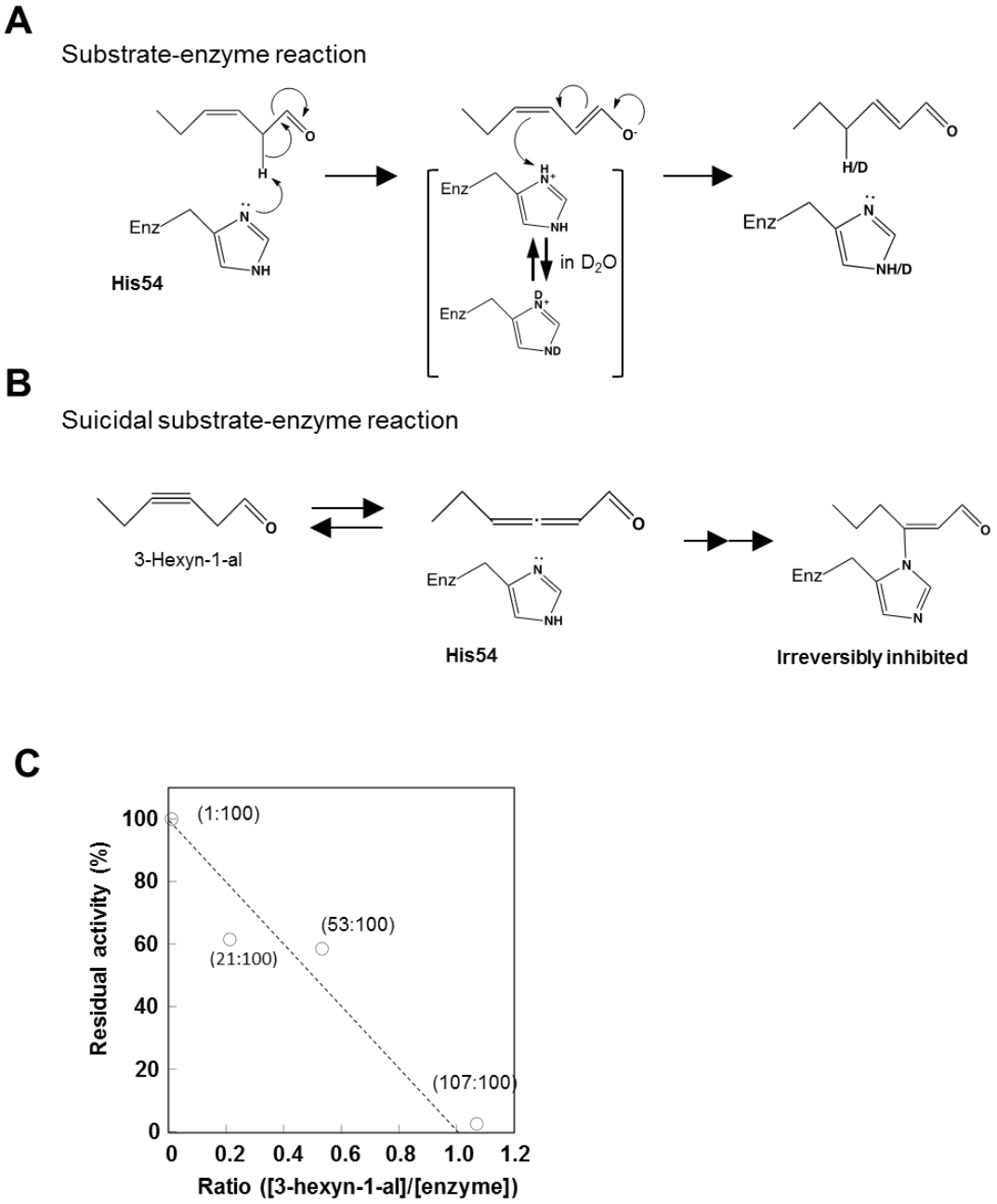

Figure 3-13. Hypothetical catalytic mechanism of HI.

A His-mediated isomerization from (3*Z*)-hexenal to (2*E*)-hexenal catalyzed by HI. In this scheme, γ-nitrogen of His is depicted as a representative example of the catalyst. **B** Inhibition of rCaHI activity by suicidal substrate, 3-hexyn-1-al. Numbers in parentheses indicate pmol of 3-hexyn-1-al and enzyme used for analysis, respectively. Activity without 3-hexyn-1-al was defined as 100% activity. Theoretically stoichiometrical relationship between enzyme and suicidal substrate is indicated by a dotted line. **C** Suicidal substrate inhibitory mechanism of HI. Also in this scheme, γ-nitrogen of His is depicted as a representative example.

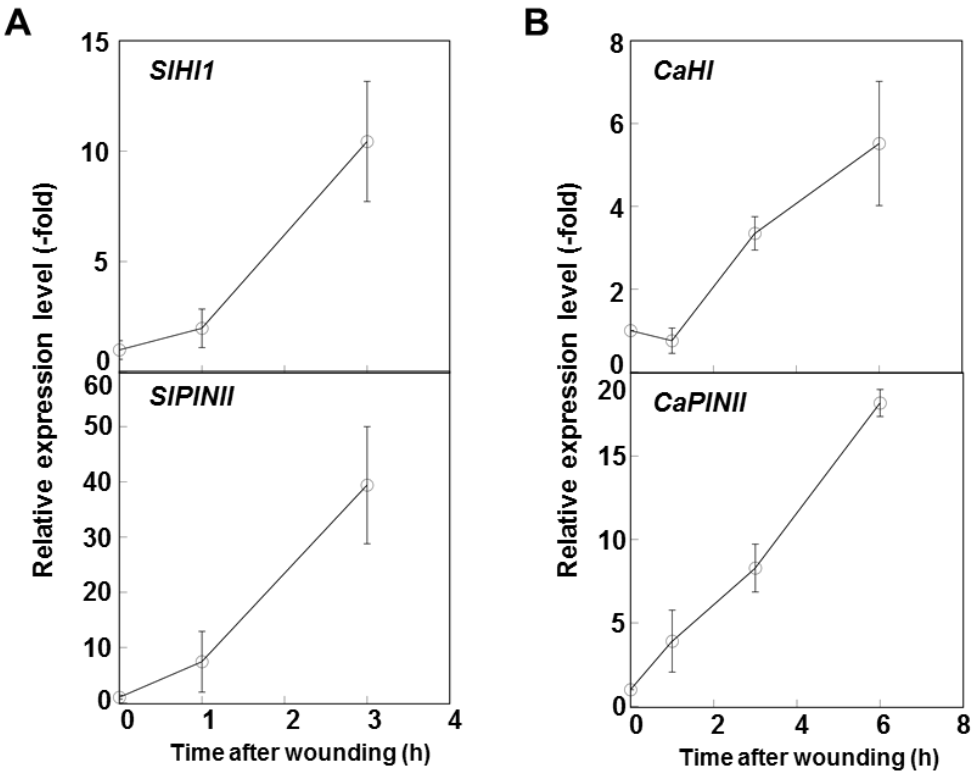

Figure 3-14. Induction of HIs and PINII by wounding treatment.

After leaves of tomato **A** and paprika **B** were wounded by tweezers, expressed genes were quantified by qRT-PCR. Relative expression level of 0 time sample against internal standard gene (the actin genes SlACT and *CaACT* for tomato and paprika samples, respectively) was set to 1. Data are means ± SE (n = 3).

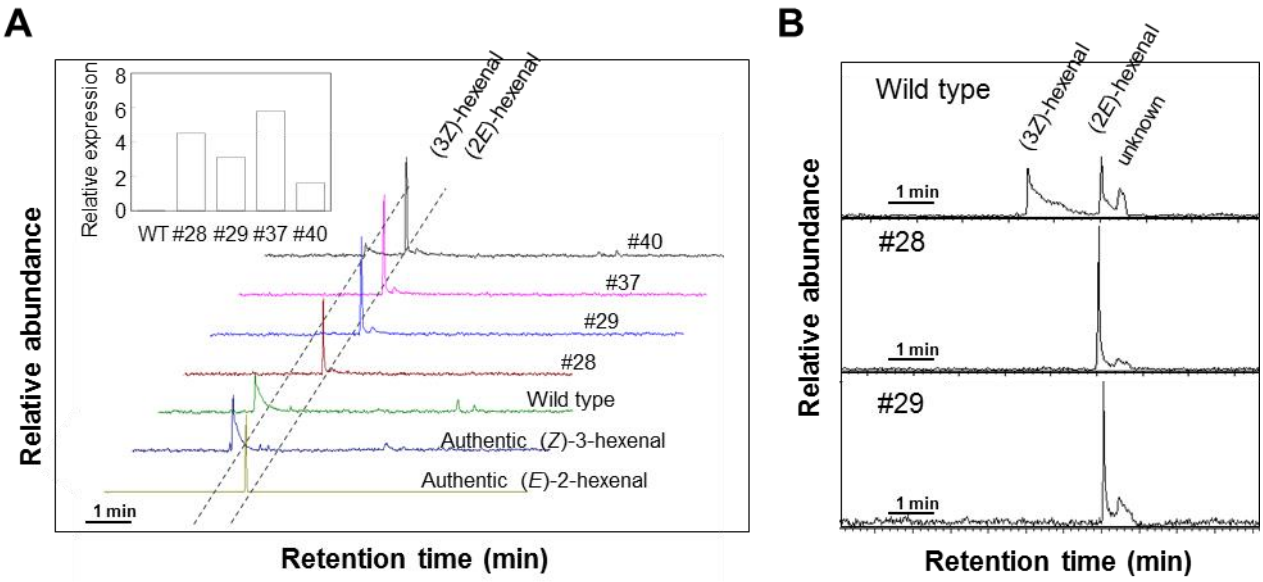

Figure 3-15. Overexpression of CaHI drastically changed (3*Z*)-hexenal and (2*E*)-hexenal composition in transgenic tomatoes.

A (3*Z*)- and (2*E*)-Hexenal analysis in wild-type and CaHI-overexpressing tomato (oxCaHI) leaves. Volatiles were collected by SPME, and then analyzed by GC-MS. SIM (m/z=98) chromatograms to detect (3*Z*)- and (2*E*)-hexenals are shown. Inset, confirmation of enhanced expression of CaHI in transgenic tomatoes by qRT-PCR (the actin gene SlACT was used as an internal standard). Numbers indicate transgenic tomato lines showing high CaHI expression. **B** SIM chromatogram (m/z=98) of volatiles from ripe tomato fruits.

Chapter IV

General discussion

Reactive carbonyl species (RCS) having α, β-unsaturated carbonyl group are generated by lipid peroxidation in plants under stress. The signaling functions of RCS under biotic stress have been reported (Famer, 2007; Mueller, 2009). Among RCS, reactive short-chain leaf volatiles (RSLVs) are reported to accumulate in plants subjected to abiotic stresses. However, there has been little information about their functions. This study was designed and implemented with the primary objective of getting more insight into the physiological functions of RSLVs in plants under abiotic stress.

In Chapter II, a comprehensive DNA microarray analysis was performed using *Arabidopsis thaliana* exposed to RSLVs (Fig. 2-1B). Up-regulated genes included those renowned for modulating responses to heat, UV-B, oxidative, salt, osmotic, drought, cold and wounding stresses. The 100 most highly up-regulated genes include those encoding HSPs and heat or oxidative stress related transcription factors. (2*E*)-Hexenal, vapour, rapidly and powerfully induced HSFA2 expression within 30 min (Fig. 2-2A). RSLVs with carbon chain length of 4 to 9 were effective in induction of HSFA2 gene expression, with a slightly higher efficacy out turn in aldehydes than in ketones (Fig. 2-4). Among the compounds, those having the vinyl ketone group adversely affected PSII activity. The RSLVs with chain length of C4 to C9 having no vinyl group possibly act as signal molecules with less cytotoxic effects. RSLVs have been widely distributed among plant species, and their increased production has been observed under abiotic stress conditions (Mueller, 2009) including oxidative, UV-B and heat stress (Figs. 2-7 and 2-15). *aor* knockout mutant accumulated more RSLVs than the wild type Col-0. *HSFA2* expression was enhanced in *aor* mutant than in Col-0(Fig. 2-7). In *hsfa1* knock out mutant, expression of *HSFA2* significantly decreased, whereas expression of *DREB2A*, *ZAT10* and *ZAT12* (Fig. 2-9B and 9C) was comparable to that in Col-0. These results support the hypothesis that RSLVs are involved in the induction of *HSFA2* expression *in vivo* and RSLV-mediated gene expression involves HSFA1-dependent and HSFA1-independent pathways.

(2*E*)-hexenal knows as the leaf aldehyde is a representative member of RSLVs. Although (2*E*)-hexenal is emitted immediately after wounding, enzymes involved in the

synthesis had not been identified. Therefore, in Chapter III, hexenal isomerase (HI) responsible for the conversion of (3*Z*)-hexenal to (2*E*)-hexenal was isolated from Paprika fruit (Fig. 3-2), the highest producer of (2*E*)-hexenal among tested plants (Fig. 3-1), and subsequently purified, identified and characterized. Based on partial amino acid sequences, full length DNA encoding the protein was obtained (Fig. 3-5). The protein was heterologously expressed in *E. coli* and the purified enzyme was characterized (Fig. 3-6). Phylogenetic analysis revealed that HI belongs to the Cupin super family and is widely distributed in plants (Fig. 3-7). Expression analysis of the HI genes in various plants, at different developmental stages, revealed that HIs showed characteristic expression in each plant (Fig. 3-8). Analysis, using point mutated recombinant CaHI, showed that H54, K60 and 128Y are necessary for HI activity (Fig. 3-9). To investigate the catalytic mechanism of HI, (3*Z*)-hexenal was incubated with recombinant CaHI in D_2O and the (2*E*)-hexenal formed was analyzed by ^{1}H-NMR. The spectrum revealed that deuterium was introduced, predominantly, at the C4 position of (2*E*)-hexenal (Fig. 3-13). Based on the effects of HI obtained in this study and those reported elsewhere on bacterial isomerase, a catalytic mechanism was proposed (Fig. 3-13). To give an experimental proof to the proposal, a suicidal substrate 3-hexynal was designed and prepared. Efficient inhibition of HI activity with the suicidal substrate supported the proposed catalytic mechanism. To elucidate physiological roles of HI, gene expression level of the enzyme was analyzed in wounded tomato leaves. As a result, induction of *HI* genes was observed within 3h (Fig. 3-14). Transgenic plants overexpressing HI displayed a drastic increase in (2*E*)-hexenal production with decreased (3*Z*)-hexenal production (Fig. 3-15).

In conclusion, this study revealed that RSLVs act as efficient inducers of abiotic stress-related gene expression, HI is a member of the Cupin superfamily, HI gene expression was induced by wound treatment, and GLVs profile can be altered by manipulating the HI gene. It has been reported that (2*E*)-hexenal is involved in plant-pathogen, plant-insect and plant-plant interactions. However, detailed studies including functional analysis of (2*E*)-hexenal under biotic stress conditions have not been reported because, in part, the knowledge about the biochemical and molecular mechanisms pertaining to (2*E*)-hexenal biosynthesis are not available. It is noteworthy that HI, identified for the first time in this study, shed light on a hidden mechanism of (2*E*)-hexenal formation. HI protein and HI gene elucidated in this study bridged the only missing link and completed the overall biosynthetic pathway of GLVs. In

addition, an HI inhibitor was developed based on the catalytic mechanism of the enzyme. These molecular and chemical findings are useful to alter RSLVs profile of plants. The author wishes the results obtained in this study, provide an additional intellectual basis for the formation of GLVs and make a significant contribution to deepen understanding of the physiological roles of this important class of plant volatiles.

Acknowledgement

Firstly, I would like to express my deepest appreciation to Professor Yukihiro Sugimoto, Laboratory of Functional Phytochemistry, Graduate School of Agricultural Science, Kobe University, for excellent guidance and sincere encouragement. He also gave me the chance to interact with researchers at national and international academic societies.

I am indebted to Associate Professor Masaharu Mizutani for valuable suggestions, constructive advice and constant encouragement. My heartfelt appreciation goes to Assistant Professor Yasuo Yamauchi for mentoring my study, long-term support, enormous help and patience.

I would also like to express my sincere appreciation to Professor Kaoru Maeto, Laboratory of Insect Biodiversity and Ecosystem Science, Graduate School of Agricultural Science, Kobe University, Associate Professor Chikahiro Miyake, Laboratory of Plant Nutrition, and Prof. Abdel Gabar Babiker, National Center for Research, Sudan, for reviewing the manuscript of this dissertation.

I express profound gratitude to Professor Hirosato Takikawa, Laboratory of Natural Products Chemistry, Graduate School of Agricultural Science, Kobe University for helpful discussions about catalytic mechanisms of hexenal isomerase, and Associate Professor Masaki Kuse for instructing me on purification of the enzyme reaction products and NMR analysis.

I am thankful to Ms. Aya Matsuda for her sincere fruitful collaboration, and to all members of the Laboratory of Functional Phytochemistry for encouragement during the course of this study.

Finally, I would like to express special thanks to my parents for continuous support and encouragement.

Reference

Alme´ras, E., Stolz, S., Vollenweider, S., Reymond, P., Mène-Saffrané, L., and Farmer, E. E. (2003). Reactive electrophile species activate defense gene expression in Arabidopsis. Plant J. 34, 205–216.

Alonso, A., García-Aliaga, R., García-Martínez, S., Ruiz, J. J., and Carbonell-Barrachina, A. A. (2009). Characterization of Spanish tomatoes using aroma composition and discriminant analysis. Food Sci. Tech. Int. 15, 47-55.

Arnold, K., Bordoli, L., Kopp, J., and Schwede, T. (2006). The SWISS-MODEL workspace: a web-based environment for protein structure homology modelling. Bioinformatics 22, 195–201.

AH-Mackerness, S., John, C. F., Jordan, B. & Thomas, B. (2001). Early signaling components in ultraviolet-B responses: distinct roles for different reactive oxygen species and nitric oxide. FEBS Lett. 489, 237–242.

Bahmani, M. and Maali-Amiri, R. (2015). Genetic regulation of cross tolerance in plants under biotic and abiotic stresses. Genetics in the 3rd Millennium, 13(3), 4076-4083.

Bate, N. J., Riley, J. C. M., Thompson, J. E., and Rothstein, S. J. (1998). Quantitative and qualitative difference in C6-volatile production from the lipoxygenase pathway in an alcohol dehydrogenase mutant of Arabidopsis thaliana. Physiol. Plant. 104, 97-104.

Benkert, P., Kunzli, M., and Schwede, T. (2009). QMEAN server for protein model quality. Nucleic Acids Res.37, W510-W514.

Biasini, M., Bienert, S., Waterhouse, A., Arnold, K., Studer, G., Schmidt, T., Kiefer, F., Cassarino, T. G., Bertoni, M., Bordoli, L., and Schwede, T. (2014). SWISS-MODEL: modelling protein tertiary and quaternary structure using evolutionary information. Nucleic Acids Res.42, W252–258.

Bloch, K. (1971). β -Hydroxydecanoyl thioester dehydrase: The Enzymes, 3rd Ed, Vol. 5, p. 441-464, Academic Press, NY

Block, A., Schmelz, E., Jones, J. B. & Klee, H. J. (2005). Coronatine and salicylic acid: the battle between *Arabidopsis* and *Pseudomonas* for phytohormone control. Molecular Plant Pathology, 6(1), 79-83.

Bordoli, L., Kiefer, F., Arnold, K., Benkert, P., Battey, J., and Schwede, T. (2009). Protein structure homology modeling using SWISS-MODEL workspace. Nat. Protocols 4, 1-13.

Boyer, J. S. (1984). Plant productivity and environment. Science 218, 443–448.

Bradford, M. M. (1976). A rapid and sensitive method for the quantitation of microgram quantities of protein utilizing the principle of protein-dye binding. Anal. Biochem. 72, 248-254

Buttery, R. G., Ling, L. C. and Light, D. M. (1987). Tomato leaf volatile aroma components. J. Agric. Food Chem. 35, 1039–1042.

Chen, L., Song, Y., Li, S., Zhang, L., Zou, C. and Yu, D. (2012). The role of WRKY transcription factors in plant abiotic stresses. Biochimica et Biophysica Acta (BBA)-Gene Regulatory Mechanisms,

1819(2), 120-128.

Chen, G., Hackett, R., Walker, D., Taylor, A., Lin, Z., and Grierson, D. (2004). Identification of a specific isoform of tomato lipoxygenase (TomloxC) involved in the generation of fatty acid-derived flavor compounds. Plant Physiol. 136, 2641-2651

Copolovici, L., Ka¨nnaste, A., Pazouki, L. and Niinemets, U. (2012). Emissions of green leaf volatiles and terpenoids from Solanum lycopersicum are quantitatively related to the severity of cold and heat shock treatments. J. Plant Physiol. 169, 664–672.

Croft, K. P. C., Juttner, F., and Slusarenko, A. J. (1993). Volatile products of the lipoxygenase pathway evolved from Phaseolus vulgaris (L.) leaves inoculated with Pseudomonas syringae pv phaseolicola. Plant Physiol. 101, 13-24.

Cruz de Carvalho, M. H. (2008). Drought stress and reactive oxygen species: production, scavenging and signaling. Plant Signaling & Behavior, 3(3), 156-165.

Curtius, T., and Franzen, H. (1912) Über die chemischen Bestandteile grüner Pflanzen. Über den Blätteraldehyd. Ann. Chem. 390, 89-121.

D'Auria, J. C., Pichersky, E., Schaub, A., Hansel, A., and Gershenzon, J. (2007). Characterization of a BAHD acyltransferase responsible for producing the green leaf volatile (Z)-3-hexen-1-yl acetate in Arabidopsis thaliana. Plant J. 49, 194-207

Dafny-Yelin, M., Tzfira, T., Vainstein, A. and Adam, Z. (2008). Non-redundant functions of sHSP-CIs in acquired thermotolerance and their role in early seed development in Arabidopsis. Plant Mol. Biol. 67, 363–373.

De Moraes, C. M., Mescher, M. C., and Tumlinson, J. H. (2001). Caterpillar-induced nocturnal plant volatiles repel conspecific females. Nature 410, 577-580.

Duan, H., Huang, M. Y., Palacio, K. and Schuler, M. A. (2005). Variations in CYP74B2 (hydroperoxide lyase) gene expression differentially affect hexenal signaling in the Columbia and Landsberg erecta ecotypes of Arabidopsis. Plant Physiol. 139, 1529–1544.

Dunwell, J. M., Purvis, A., and Khuri, S. (2004). Cupins: the most functionally diverse protein superfamily? Phytochem.65, 7-17 16.

Endo, K., Helmkamp, G. M. Jr., and Bloch, K. (1970). Mode of inhibition of ß-hydroxydecanoyl thioester dehydrase by 3-decynoyl-N- acetylcysteamine. J. Biol. Chem. 245, 4293–4296.

Eckardt, N. A. (2008). Oxylipin signaling in plant stress responses. The Plant Cell, 20(3), 495-497.

Fall, R., Karl, T., Hansel, A., Jordan, A., and Lindinger, W. (1999). Volatile organic compounds emitted after leaf wounding: on-line analysis by proton-transfer-reaction mass spectrometry. J. Geophys. Res. 104, 15963-15974.

Foyer, C. H. and Noctor, G. (2003). Redox sensing and signaling associated with reactive oxygen in chloroplasts, peroxisomes and mitochondria. Physiol. Plant 119, 355–364.

Frankel, E. N. (1980). Lipid oxidation. Prog. Lipid Res. 19, 1-22.

Gill, S. S. and Tuteja, N. (2010). Reactive oxygen species and antioxidant machinery in abiotic stress tolerance in crop plants. Plant Physiology and Biochemistry, 48(12), 909-930.

Guex, N., and Peitsch, M. C. (1997). SWISS-MODEL and the Swiss-PdbViewer: an environment for comparative protein modeling. Electrophoresis18, 2714–2723.

Hatanaka, A., Kajiwara, T., and Sekiya, J. (1987). Biosynthetic pathway for C6-aldehydes formation from linolenic acid in green leaves. Chem. Phys. Lipids 44, 341-361.

Han, C., Liu, Q. and Yang, Y. (2009). Short-term effects of experimental warming and enhanced ultraviolet-B radiation on photosynthesis and antioxidant defense of *Picea asperata* seedlings. Plant Growth Regulation, 58(2), 153-162.

Hassan, M. N., Zainal, Z. and Ismail, I. (2015). Green leaf volatiles: biosynthesis, biological functions and their applications in biotechnology. Plant Biotechnology Journal, 13(6), 727-739.

Hernandez, H. P., Hsieh, T. C. Y., Smith, C.M. and Fischer, N. H. (1989). Foliage volatiles of two rice cultivars. Phytochemistry 28, 2959–2962.

Hegedüs, A., Erdei, S., Janda, T., Tóth, E., Horváth, G. and Dudits, D. (2004). Transgenic tobacco plants overproducing alfalfa aldose/aldehyde reductase show higher tolerance to low temperature and cadmium stress. Plant Science, 166(5), 1329-1333.

Hong, S. W. and Vierling, E. (2000) Mutants of Arabidopsis thaliana defective in the acquisition of tolerance to high temperature stress. Proc. Natl. Acad. Sci. USA 97, 4392–4397.

Howe, G. A., Lee, G. I., Itoh, A., Li, L., and DeRocher, A. E. (2000). Cytochrome P450-dependent metabolism of oxylipins in tomato. Cloning and expression of allene oxide synthase and fatty acid hydroperoxide lyase. Plant Physiol. 123, 711-724.

Howe, G. A. and Schilmiller, A. L. (2002). Oxylipin metabolism in response to stress. Current Opinion in Plant Biology, 5(3), 230-236.

Kie bowicz-Matuk, A. (2012). Involvement of plant C2H2-type zinc finger transcription factors in stress responses. Plant Sci. 185–186, 78–85.

Kishimoto, K., Matsui, K., Ozawa, R., and Takabayashi, J. (2005). Volatile C6-aldehyde and allo-ocimene activate defense genes and induce resistance against Botrytis cinerea in Arabidopsis thaliana. Plant Cell Physiol. 46, 1093-1102.

Kishimoto, K., Matsui, K., Ozawa, R., and Takabayashi, J. (2006). Components of C6-aldehyde-induced resistance in Arabidopsis thaliana against a necrotrophic fungal pathogen, Botrytis cinerea. Plant Sci. 170, 715-723.

Leesong, M., Henderson, B. S., Gillig, J. R., Schwab, J. M., and Smith, J. L. (1996). Structure of a dehydratase–isomerase from the bacterial pathway for biosynthesis of unsaturated fatty acids: two catalytic activities in one active site. Structure4, 253-264.

Lewinsohn, E., Schalechet, F., Wilkinson, J., Matsui, K., Tadmor, Y., Nam, K.-H., Amar, O., Lastochkin, E., Larkov, O., Ravid, U. Hiatt, W., Gepstein, S., and Pichersky, E. (2001). Enhanced levels of

the aroma and flavor compound S-linalool by metabolic engineering of the terpenoid pathway in tomato fruits. Plant Physiol. 127, 1256-1265.

Liu, H. C., Liao, H. T. and Charng, Y. Y. (2011). The role of class A1 heat shock factors (HSFA1s) in response to heat and other stresses in Arabidopsis. Plant Cell Environ. 34, 738–751.

Loreto, F., Barta, C., Brilli, F. and Nogues, I. (2006). On the induction of volatile organic compound emissions by plants as consequence of wounding or fluctuations of light and temperature. Plant Cell Environ. 29, 1820–1828.

Luning, P. A., Carey, A. T., Roozen, J. P., and Wichers, H. J. (1995). Characterization and occurrence of lipoxygenase in bell peppers at different ripening stages in relation to the formation of volatile flavor compounds. J. Agric. Food Chem. 43, 1493-1500.

Mano, J., Torii, Y., Hayashi, S., Takimoto, K., Matsui, K., Nakamura, K., Inzé, D., Babiychuk, E., Kushnir, S., and Asada, K. (2002). The NADPH:quinone oxidoreductase P1-ζ-crystallin in Arabidopsis catalyzes the □□□-hydrogenation of 2-alkenals: Detoxication of the lipid peroxide-derived reactive aldehydes. Plant Cell Physiol.43, 1445-1455

Mano, J., Tokushige, K., Mizoguchi, H., Fujii, H. and Khorobrykh, S. (2010). Accumulation of lipid peroxide-derived, toxic a, b-unsaturated aldehydes (E)-2-pentenal, acrolein and (E)-2-hexenal in leaves under photoinhibitory illumination. Plant Biotech. 27, 193–197.

Mathieu, S., Cin, V. D., Fei, Z., Li, H., Bliss, P., Taylor, M. G., Klee, H. J., and Tieman, D. M. (2009) Flavour compounds in tomato fruits: identification of loci and potential pathways affecting volatile composition. J. Exp. Bot. 60, 325-337.

Matsui, K., Sugimoto, K., Kakumyan, P., Khorobrykh, S. A. and Mano, J. Volatile oxylipins and related compounds formed under stress in plants, Methods in Molecular Biology 'Lipidomics' Vol. 580 (Armstrong, D. ed.) 17–28.

Matsui, K., Sugimoto, K., Mano, J., Ozawa, R. and Takabayashi, J. (2012). Differential metabolisms of green leaf volatiles in injured and intact parts of a wounded leaf meet distinct ecophysiological requirements. PLoS ONE 7, e36433.

Matsui, K. (2006). Green leaf volatiles: hydroperoxide lyase pathway of oxylipin metabolism. Curr. Opin. Plant Biol. 9, 274–280.

Mano, J. (2012). Reactive carbonyl species: their production from lipid peroxides, action in environmental stress, and the detoxification mechanism. Plant Physiology and Biochemistry, 59, 90-97.

Mittler, R. (2002). Oxidative stress, antioxidants and stress tolerance. Trends Plant Sci. 7, 405–410.

Mizoi, J., Shinozaki, K. and Yamaguchi-Shinozaki, K. (2012). AP2/ERF family transcription factors in plant abiotic stress responses. Biochim. Biophys. Acta 1819, 86–96.

Mosblech, A., Feussner, I. and Heilmann, I. (2009). Oxylipins: structurally diverse metabolites from fatty acid oxidation. Plant Physiology and Biochemistry, 47(6), 511-517.

Mueller, M. J. and Berger, S. (2009). Reactive electrophilic oxylipins: Pattern recognition and signalling. Phytochemistry 70, 1511–1521.

Nishizawa, A. Yabuta, Y., Yoshida, E., Maruta, T., Yoshimura, K., and Shigeoka, S. (2006). Arabidopsis heat shock transcription factor A2 as a key regulator in response to several types of environmental stress. Plant J. 48, 535–547.

Noordermeer, M. A., Veldink, G. A., and Vliegenthart, F. G. (1999). Alfalfa contains substantial 9-hydroperoxide lyase activity and a 3Z:2E-enal isomerase. FEBS Lett. 443, 201-204.

Ogasawara, Y., Kaya, H., Hiraoka, G., Yumoto, F., Kimura, S., Kadota, Y. and Nara, M. (2008). Synergistic activation of the Arabidopsis NADPH oxidase AtrbohD by Ca^{2+} and phosphorylation. Journal of Biological Chemistry, 283(14), 8885-8892.

Oracz, K. and Karpiński, S. (2016). Phytohormones signaling pathways and ROS involvement in seed germination. Frontiers in Plant Science, 7, 864.

Phillips, D. R., Matthew, J. A., Reynolds, J., and Fenwick, G. R. (1979). Partial purification and properties of a *cis* -3: *trans* -2-enal isomerase from cucumber fruit. Phytochem. 18, 401-404.

Sagi, M. and Fluhr, R. (2006). Production of reactive oxygen species by plant NADPH oxidases. Plant physiology, 141(2), 336-340.

Sharma, P., Jha, A. B., Dubey, R. S. and Pessarakli, M. (2012). Reactive oxygen species, oxidative damage, and antioxidative defense mechanism in plants under stressful conditions. Journal of Botany.

Sharma, P. and Dubey, R. S. (2005). Lead toxicity in plants. Brazilian Journal of Plant Physiology, 17(1), 35-52.

Suzuki, N., Rizhsky, L., Liang, H., Shuman, J., Shulaev, V., and Mittler, R. (2005). Enhanced tolerance to environmental stress in transgenic plants expressing the transcriptional coactivator multiprotein bridging factor 1c. Plant Physiology, 139(3), 1313-1322.

Speirs, J., Lee, E., Holt, K., Yong-Duk, K., Scott, N. S., Loveys, B., and Schuch, W. (1998). Genetic manipulation of alcohol dehydrogenase levels in ripening tomato fruit affects the balance of some flavor aldehydes and alcohols. Plant Physiol. 117, 1047-1058.

Sun, H.-J., Uchii, S., Watanabe, S., and Ezura, H. (2006). A highly efficient transformation protocol for Micro-Tom, a model cultivar for tomato functional genomics. Plant Cell Physiol. 47, 426-431.

Takeuchi, Y., Fukumoto, R., Kasahara, H., Sakaki, T. and Kitao,M. (1995). Peroxidation of lipids and growth inhibition induced by UV-B irradiation. Plant Cell Rep. 14, 566–570.

Tamura, K., Peterson, D., Peterson, N., Stecher, G., Nei, M., and Kumar, S. (2011). MEGA5: molecular evolutionary genetics analysis using maximum likelihood, evolutionary distance, and maximum parsimony methods. Mol. Biol. Evol. 28, 2731–2739

Tandon, K. S., Baldwin, E. A., and Shewfelt, R. L. (2000). Aroma perception of individual volatile compounds in fresh tomatoes (*Lycopersicon esculentum*, Mill.) as affected by the medium of

evaluation. Postharv. Biol. Technol. 20, 261-268.

Torres, M. A. and Dangl, J. L. (2005). Functions of the respiratory burst oxidase in biotic interactions, abiotic stress and development. Current Opinion in Plant Biology, 8(4), 397-403.

Vancanneyt, G., Sanz, C., Farmaki, T., Paneque, M., Ortego, F., Castañera, P., and Sánchez-Serrano, J. J. (2001) Hydroperoxide lyase depletion in transgenic potato plants leads to an increase in aphid performance. Proc. Natl. Acad. Sci. USA 98, 8139-8144.

Vickers, C. E., Gershenzon, J., Lerdau, M. T. and Loreto, F. (2009). A unified mechanism of action for volatile isoprenoids in plant abiotic stress. Nature Chem. Biol. 5, 283–291.

Vollenweider, S., Weber, H., Stolz, S., Che´telat, A. and Farmer, E. E. (2000). Fatty acid ketodienes and fatty acid ketotrienes: Michael addition acceptors that accumulate in wounded and diseased Arabidopsis leaves. Plant J. 24, 467–476.

Wang, C., Xing, J., Chin, C.-K., Ho, C.-T., and Martin, C. E. (2001). Modification of fatty acids changes the flavor volatiles in tomato leaves. Phytochem. 58, 227-232

Wavrin, L., and Viala, J. (2002). Clean and efficient oxidation of homoallylic and homopropargylic alcohols into β, γ-unsaturated aldehydes by the Dess-Martin periodinane. Synthesis3, 326-330.

Yamauchi, Y. Furutera A, Seki K, Toyoda Y, Tanaka K and Sugimoto Y. (2008). Malondialdehyde generated from peroxidized linolenic acid causes protein modification in heat-stressed plants. Plant Physiol. Biochem. 46, 786–793.

Yamauchi, Y. and Sugimoto, Y. (2010). Effect of protein modification by malondialdehyde on the interaction between oxygen-evolving complex 33 kDa protein and photosystem II core proteins. Planta 231, 1077–1088.

Yamauchi, Y., Hasegawa, A., Taninaka, A., Mizutani, M. and Sugimoto, Y. (2011). NADPH dependent reductases involved in the detoxification of reactive carbonyls in plants. J. Biol. Chem. 286, 6999–7009.

Yamauchi, Y., Hasegawa, A., Mizutani, M. and Sugimoto, Y. (2012). Chroloplastic NADPH-dependent alkenal/one oxidoreductase contributes to the detoxification of reactive carbonyls produced under oxidative stress. FEBS Lett. 586, 1208–1213.

Yin, L., Mano, J., Wang, S., Tsuji, W. and Tanaka, K. (2009). The involvement of lipid peroxide-derived aldehydes in aluminum toxicity of tobacco roots. Plant Physiol. 152, 1406–1417.